BULLETIN OF RSMU

MAR-APR 2016 (2)
VESTNIKRGMU.RU

NEUROINTERFACES REVIEW

BULLETIN OF RUSSIAN STATE MEDICAL UNIVERSITY

Scientific Medical Journal of Pirogov Russian National Research Medical University

ВЕСТНИК РОССИЙСКОГО ГОСУДАРСТВЕННОГО МЕДИЦИНСКОГО УНИВЕРСИТЕТА

Научный медицинский журнал Российского национального исследовательского медицинского университета имени Н. И. Пирогова

The journal is included in the list of the leading peer-reviewed scientific journals and publications approved by the Higher Attestation Commission

The journal is available in Google Scholar.

IF RSCI 2014: 0,139.

Approved for print April 25, 2016

Address: ul. Ostrovityanova, d. 1, Moscow, Russia, 117997
For papers submission: editor@vestnikrgmu.ru
For collaboration: manager@vestnikrgmu.ru

The mass media registration certificate no. 012769 issued on July 29, 1994
Subscription index in the Rospechat catalog: 46826
Printed by Premium Print
www.premium-print.ru

BULLETIN OF RSMU 2, 2016
ВЕСТНИК РГМУ

CONTENTS
СОДЕРЖАНИЕ

BRAIN-COMPUTER INTERFACE: THE FUTURE IN THE PRESENT

Levitskaya OS[1]✉, Lebedev MA[2]

[1] Cyber Myonics, Moscow, Russia

[2] Department of Neurobiology,
Duke University, Durham, North Carolina, USA

Brain-computer interfaces (BCIs) are a promising technology intended for the treatment of diseases and trauma of the nervous system. BCIs establish a direct connection between the brain areas that remain functional and assistive devices, such as powered prostheses and orthoses for the arms and legs, motorized wheelchairs, artificial sensory organs and other technologies for restoration of motor and sensory functions. BCIs of various kinds are currently developing very rapidly, aided by the progress in computer science, robotic applications, neurophysiological techniques for recording brain activity and mathematical methods for decoding neural information. BCIs are often classified as motor BCIs (the ones that reproduce movements), sensory BCIs (the ones that evoke sensations), sensorimotor BCIs (the ones that simultaneously handle motor and sensory functions), and cognitive BCIs intended to regulate the higher brain functions. All these BCI classes can be either invasive (i. e. penetrating the body and/or the brain) or noninvasive (i.e. making no o little contact with the body surface). Noninvasive BCI are safe to use and easy to implement, but they suffer from signal attenuation by scalp and skin, its contamination with noise and artifacts, and an overall low information transfer rate. Invasive BCIs are potentially more powerful because they utilize implanted grids that can both record neural signals in high-resolution and apply stimulation to the nervous tissue locally to deliver information back to the brain. BCI technologies are being developed not only for individual use, but also for collective tasks performed by multiple interconnected brains.

Keywords: brain-computer interface, neuronal network, neuronal activity, neuronal decoding algorithm, neuronal plasticity of brain, encephalogram, functional electrical stimulation, cochlear implant, visual prosthesis

✉ **Correspondence should be addressed:** Olga Levitskaya
ul. Marshala Biryuzova, d. 30, kv. 45, Moscow, Russia, 123060; olia_levits@mail.ru

Recieved: 11.03.2016 **Accepted:** 25.03.2016

ИНТЕРФЕЙС МОЗГ–КОМПЬЮТЕР: БУДУЩЕЕ В НАСТОЯЩЕМ

О. С. Левицкая[1]✉, М. А. Лебедев[2]

[1] ООО Cyber Myonics, Москва

[2] Отдел нейробиологии,
Университет Дьюка, Дарем, Северная Каролина, США

Интерфейс мозг–компьютер (ИМК) — одна из самых многообещающих технологий в области лечения неврологических заболеваний и травм. ИМК позволяет установить связь между неповрежденными участками мозга и протезами отсутствующих конечностей, носимыми нейропротезами, инвалидными креслами, искусственными органами чувств и другими устройствами, компенсирующими утраченные функции. В настоящее время ИМК быстро развиваются благодаря бурному росту вычислительных мощностей, робототехники, методов записи сигналов мозга и математических алгоритмов для их декодирования. Принято классифицировать ИМК на моторные (воспроизводящие движения), сенсорные (чувствительные) и двунаправленные (сенсорномоторные). Существуют также интерфейсы, интерпретирующие или воздействующие на высшие нервные функции. По степени проникновения в биологические ткани организма выделяют инвазивные (глубоко проникающие) и неинвазивные (взаимодействующие лишь с поверхностью тела, но не проникающие) ИМК. Неинвазивные ИМК безопаснее и проще в использовании, но имеют ограничения по пропускной способности сигнала. Инвазивные же благодаря непосредственному контакту мультиэлектродных матриц с нейронными ансамблями без зашумления и дополнительных фильтрующих барьеров позволяют считывать сигналы в высоком разрешении и локально стимулировать нервную ткань для передачи сигналов обратной связи в мозг. Технологии ИМК разрабатываются не только для индивидуального пользования, но и для выполнения коллективных задач при помощи мозгосетей.

Ключевые слова: интерфейс мозг–компьютер, нейронная сеть, нейрональная активность, нейрональное декодирование, нейропластичность мозга, электроэнцефалограмма, функциональная электростимуляция, кохлеарный имплантат, зрительный протез

✉ **Для корреспонденции:** Ольга Сергеевна Левицкая
123060, г. Москва, ул. Маршала Бирюзова, д. 30, кв. 45; olia_levits@mail.ru

Статья получена: 11.03.2016 **Статья принята в печать:** 25.03.2016

Ultimately, any mental activity is expressed as muscle contractions and relaxations that allow us to interact with the external world and each other: muscles control limb and eye movements, facial expression, and speech production. Muscle contractions are involved in practically any sensation. For example, we scan visual scenes with eye movements and move our hands to obtain tactile sensations.

The movements of our body are monitored by a large number of sensory receptors. The continuous streams of incoming (sensory) and outgoing (motor) signals are processed

at multiple levels of the nervous system, from the lowest to the highest. This immense sensory and motor processing is largely subconscious, and we take it for granted that we can effortlessly perform very complex tasks, such as walking upright, maintaining balance, moving fingers and toes, speaking, etc.

Unfortunately, the ability to move and sense can be severely impaired if the nervous system is damaged. Millions of people around the world suffer from sensory and motor deficits caused by spinal cord injuries, stroke, Parkinson's disease, amyotrophic lateral sclerosis and other pathological conditions. Even in the cases of devastating deficits, very often higher brain regions retain their functionality but turn to be isolated from muscles, the result being the patient's paralysis and inability to speak or feel.

Currently, there is no effective treatment for many motor and sensory disorders. Patients are bed - or wheelchair bound till the end of their lives. Development of effective rehabilitation methods and devices that compensate for the lost functions is an extremely important issue faced by modern medicine.

Artificial components for nervous system

A brain-computer interface (BCI) is a promising tool for treating various neurological disorders. BCIs connect intact areas of the brain to assistive devices that can restore motor and sensory functions [1–5]. For example, patients paralyzed after a spinal cord injury could potentially restore mobility using a BCI that connects their intact motor cortex to robotic arms, exoskeletons or devices that apply functional electrical stimulation (FES) to the muscles. So far, there has been certain success in the development of such motor BCIs [6–9]. Moreover, patients can hope to restore sensitivity of paralyzed body parts with sensory BCIs that connect somatosensory areas of the nervous system to prostheses equipped with touch and position sensors. Such BCIs induce sensations by electrical stimulation of the somatosensory cortex.

Being of assistance to patients, BCIs can also be used by healthy individuals, for example, in computer games [10] or as an alarm clock for long-haul truck drivers [11]. In the latter case the drowsiness is detected using the encephalogram (EEG).

BCIs are often called brain-machine interfaces (BMIs). In general, these terms can be used interchangeably, but conventionally, noninvasive interfaces have been termed BCIs and invasive interfaces have been termed BMIs. "Neuroprosthesis" and "neuroimplant" are their synonyms. In this article the term BCI is used.

Brain-computer interfaces belong to that knowledge area where the gap between science fiction and its practical implementation does not exceed 50 years. However, despite the fact that the number of publications on this subject has increased over the past few years, many BCI technologies are still at experimental stage, not used in clinical practice and not available in retail. The exception to that are some FES-based systems [12] and cochlear implants [13, 14] that are successfully used for rehabilitation.

In this article we will cover motor and sensory BCIs. Classification of functions into sensory and motor is, however, oversimplistic. The brain of any organism does not have areas solely responsible for movements or sensations [15, 16]. That is why recently developed sensorimotor interfaces are the most ergonomic ones [17].

The history of research and BCI development

The initial experiments in monkeys date back to the mid-1960s. The monkeys were implanted with multi-electrode arrays for electrical stimulation and recording of cortical potentials [15, 18]. It was shown that the sensorimotor cortex was activated when monkeys performed movements; the electrical stimulation of the sensorimotor cortex, in turn, caused muscle contractions.

In 1963 Walter carried out an experiment in which the first BCI as we understand it now was implemented [19]. To assist clinical diagnosis, patients were implanted with electrodes in different cortical areas. They were asked to advance carousel projector slides by pressing a button. After discovering the cortex area responsible for reproducing that muscle pattern, the researcher connected it straight to the projector. The button was disconnected, but the slides kept on moving: the brain controlled slide advance and did it even before the subject pushed the disconnected button.

An idea similar to the concept of modern BCIs was formulated by American researchers from the National Institute of Health in the late 1960s. They announced that they would focus on the development of principles and methods of controlling external devices by brain signals [20]. The researchers implanted electrodes to the motor cortex area of monkeys. The electrodes recorded action potentials of a few neurons while the animals were moving their hands [21]. The recorded neuronal discharges were transformed into the trajectory of movement of a hand using linear regression. It took another 10 years of effort to implement such transform in real time: the monkeys had learned to control the cursor on a LED display by activating their motor cortex neurons [22].

At that time a similar study was carried out under Fetz's supervision [23], but the focus was on studying the biological feedback; the scientists faced the question: could a monkey control its neuronal discharges volitionally? It was found that volitional control of neurons responsible for movement was possible without performing the actual movement. That result is important for understanding the mechanisms of mirror neurons and even neurons involved in empathy.

Parallel to the development of motor BCIs, sensory interfaces were emerging [14]. In 1957 French scientists Djourno and Eyriès succeded in inducing auditory sensations in deaf individuals using a single-channel electrode that stimulated the auditory nerve. In 1964 Simmons proposed a multi-channel upgrade for the device. In the 1970s House and Urban developed the device that consisted of an acoustic signal converter and a multi-channel cochlear implant. The device was approved by the US Food and Drug Administration. After further improvements, the device was introduced into clinical practice.

In the 1980s a possibility of vision restoration using BCIs became the subject of the research. An electrode array was implanted over the visual cortex of totally blind individuals. Visual sensations induced during the experiment were termed phosphenes. People who had never seen light (or had not seen it for a long time) learned to identify simple phosphene patterns [24, 25]. At present electrically stimulated vision continues to be tested in clinical trials, where a complex image from a video camera is transmitted to the stimulating implants located in the eye or visual cortex.

A tremendous advance in BCI research took place in the 1990-2000s. Nicolelis and Chapin constructed the first BCI for controlling a robotic device [26]. The recorded activity of the cortex and basal ganglia neurons of awake rats was transmitted to a robot that fetched water to animals. Then Nicolelis continued his research with primates. Primates were used in a number of research projects, such as a robotic arm controlled by cortical neuronal ensembles [27–29], a BCI establishing an artificial

tactile feedback [17], a BCI for decoding leg movements [30], BMI for bimanual movements [31], and others.

Also in the 1990s, experiments on implanting electrodes into human brain were launched. Kennedy, who implanted electrodes into his own brain in 2015, worked with a patient with amyotrophic lateral sclerosis. The patient was implanted with an electrode that contained myelinated fibers growth factor in the tip. As a result, the patient was able to issue a binary neural command [32].

In the early 2000s several laboratories began to compete in the area of invasive BCI development. A group headed by Donoghue worked with monkeys and humans; the researchers implanted multi-electrode arrays into human motor cortex, which allowed paralyzed individuals to control the cursor [8] and robotic manipulators [9]. Schwartz et al. studied movement control in three-dimensional space [33]. Eventually, success was achieved in the experiments with people controlling anthropomorphic robotic arm [7]; it is currently one of the most impressive achievements of BCI technology.

In the process of BCI development, many laboratories including those of Andersen, Shenoy and Vaadia, studied various cortical areas as signal sources for BCI and created new and original algorithms of decoding brain signals.

Parallel to that, studies on noninvasive neurointerfaces were carried out. They were based on EEG recording, near-infrared brain imaging and FES. Birbaumer, Pfurtscheller, Walpaw, Müller, Schalk, Neuper, Kübler, Millan, and other researchers offered a number of practical solutions for wheelchair operation and limb mobility restoration after traumas and strokes [12].

Neuronal decoding and neuronal tuning

How do motor BCIs manage to decode motor parameters from neuronal recordings? Many neurophysiological studies have shown that discharge rates of single cortical neurons are correlated to behaviors. For example, discharge rates of motor cortical neurons are correlated to the position, acceleration and the joint torques of the arm. Developers use such correlations for decoding neuronal signals. Reproducibility and recognizability of neural patterns, the so-called neuronal tuning, are a key factor for successful decoding. Neurons can be badly tuned or noise-contaminated, which impedes the decoding process.

Investigations of encoding of various parameters by single neurons began in the 1950-1960s. Those studies utilized a single sharp-tipped electrode to record the extracellular activity of neurons in different brain areas. Somatosensory [34], motor [16] and visual [35] systems were studied using this approach. It became clear that even single neurons demonstrate repeatable activity patterns that encode a number of sensory and motor phenomena.

Extracellular recording from single neurons in awake behaving animals continued in many laboratories around the world. Wise et al. discovered that cortical neurons modulate their rates several seconds before the actual movement. In their experiments, the monkeys knew what movement they had to make, but were trained not to make it before the trigger stimulus [36]. To study the transformation of visual stimuli on movement direction, Kalaska et al. recorded single neuron activity and employed a task in which a movement had to be executed after a delay [37]. Those experiments demonstrated that neuronal discharges contain information about the movements that are executed and those that are planned by the brain, but not initiated.

Georgopoulos and his colleagues recorded activity patterns of single motor cortical neurons while monkeys made arm movements in different directions [38]. The researchers found the dependency between the signal intensity and movement direction that could be described by a cosine function, meaning that discharge frequency of neurons was maximal for a certain direction, called preferred direction, and reduced gradually when movements deviated from it. To explain how neuronal discharges transform into arm movement in a given direction, Georgopoulos suggested the concept of the population vector. Such vector is a vector sum of contributions from multiple neurons that has been shown to match the movement direction. Interestingly, even imagery of arm movement without its execution, such as imaginary 90° rotation in space, can be well described by a population vector [39].

Owing to these studies, it became clear that the activity of individual neurons carries information on behavior parameters and these parameters can be decoded. Neurophysiologists often use an audio speaker to monitor discharges of single neurons. An experienced neurophysiologist can tell what his monkey is doing by listening to the sound of discharges. Similarly, a BCI decoder "listens" to neurons and tries to infer what movement or intent underlies this "neuronal sound". The more neurons are "heard" by the decoder, the more accurate is the decoding.

What do neuron ensembles sing about?

The more "musicians" a neuronal ensemble consists of, the higher is the accuracy of decoding: increased neuronal sample enables to exclude occasional noisy fluctuations of single neurons [1, 2]. This does not mean that small neuronal populations are useless for BCIs. Sometimes a few neurons are enough for the interface to work [33, 40], particularly if those neurons are highly tuned to the parameter of interest. Highly tuned neurons are sometimes called grandmother cells or Jennifer Aniston neurons, because they are selectively activated by specific stimuli: grandmother's or Jennifer Aniston's photographs. [41]. If a BCI task is to identify the presence of a grandmother or Jennifer Aniston, such neurons come handy. However, they are quite rare, and in real life the brain processes information using highly distributed neuronal representations. The melody of single neurons gives the main idea of a behavior pattern, but its symphony is played by many instruments. The more neurons are recorded simultaneously, the more accurate is the encoding [2]. Because of that, multielectrode recording of neuronal activity from a large number of neurons is most effective for BCI decoding. It is especially important to record the signals of large neuronal ensembles if the task is to decode several behavioral parameters simultaneously [30]. Such ensemble recording improves decoding and maintains its stability [1].

Decoding algorithms

BCI decoders use statistical and machine-learning methods to reconstruct behaviors from neuronal activity. Initial decoder settings are based on a training set. In experiments with monkeys a 5-10-minute recording is necessary to obtain the training set. During this time interval, the animal performs the task manually, for example, moves the joystick with its hand [17, 28, 29], and the decoder "learns" to detect movement parameters (position, acceleration, force). Then the mode is changed to brain control, and the monkey performs the task (moves the cursor and places it over the target) using the decoder and not its own hands.

A training set can be obtained without moving the hand. Instead, a subject observes a cursor movement or — in experiments with humans — we ask him to imagine the movement. The latter approach is especially important if the participant of the study is paralyzed.

The choice of a decoding algorithm is dictated by the behavioral parameters that need to be extracted from neuronal activity and neural signal features used for decoding (single neuron activity, field potentials, etc.), the number of recording channels, the specifics of the behavioral task (for example, a continuous control of cursor position or, in contrast, making discrete decisions).

If decoding is based on population vectors, a training set often consists of movements from the center to different directions along the radius. Then a population vector is computed; it is a weighted vector sum of contributions from single neurons. Each neuron contributes a vector pointing in that neuron's preferred direction, and the vector length is proportional to the neuron's discharge frequency [39]. Despite some advantages, a clear conceptual framework being one of them, this method is not optimal because it is not based on statistical procedures that would optimize decoding accuracy.

Wiener filter is a linear decoder which is very similar to the population vector, but it is much more accurate, since it minimizes the mean square error. Wiener filter output for time *t* is a weighted sum of neuron rates measured at different time points in the past (usually, 5-10 time points within a 1-second time window preceding *t*) [42]. Weights are computed for each neuron using standard linear regression methods based on matrix algebra.

In many cases, for example, in the presence of stereotype movement patterns, another filter — Kalman filter — demonstrates better performance. Kalman filter separates variables into the sets of state variables (limb position or velocity) and observable variables (relation of neuronal discharge to movement direction). During the decoding process, the state vector is updated for discrete time steps (usually 50–100 ms). During each update, two computations are performed: prediction of the next state and its correction based on neuronal activity data. Correction uses the model that compares an expectation of neuronal rates and the actually observed rates.

Unscented Kalman filter improves estimation made with a classic Kalman filter by taking into account non-linear dependencies between neuronal activity and movements.

Interestingly, research on neuronal decoding facilitates the development of new analytical mathematical methods of physiological interaction between the neurons. For example, artificial neural networks were both inspired by the organization of a nervous system and can be used for the interpretation of the activity of brain circuitry. Some laboratories use recurrent neural networks for decoding [43].

When solving tasks that imply a number of discrete solutions, discrete classifiers are used. EEG decoding of letters and numbers based on cortical potentials is one example [44, 45]. In BCI decoding, the following methods of machine learning have also found their application: Gaussian classifier, probabilistic classifier structures (Bayesian networks), hidden Markov models, k-nearest neighbour algorithm, artificial neural networks, multilayer perceptron, elements of fuzzy logic.

Theories of movement control and motor BCIs

To explain neuronal mechanisms of movements, several theories of movement control have been elaborated; they are also influential for BCI design.

A classical scheme of movement control includes a set of hierarchically organized regions of nervous system. As suggested by this scheme, cortical structures are at the top of this hierarchy. They control the most complex movements, such as finger movements. Brain stem and spinal cord supervise simpler functions: postural automatisms and spinal reflexes [46]. The spinal cord of quadrupeds is known to contain central pattern generators that control rhythmic movements of the limbs during walking [47].

Historically, motor control has been described as a set of reflexes for a long time. The concept of a reflex arch was proposed by Sherrington [46]. Currently, reflexes are acknowledged, but the emphasis has shifted to the top-down control exerted by the brain higher centers during volitional movements. Typical motor activity contains both voluntary and reflex components [48]. Some BCIs, called shared control BCIs, imitate these two components: they give the control over higher-level components (the onset and the end of movements, target choice) to the subject and delegate low-level tasks, such as maintaining balance, to a robotic controller.

Many modern theories of motor control are based on the idea that the brain forms an internal model of the body that is used for both perception of the body configuration and planning and executing movements. Such an internal model was first described by Head and Holmes as "body schema", which the brain uses to monitor and update information of multiple signals from the body sensory receptors [49]. Currently, BCI developers strive to construct neurally controlled limb that can be finally incorporated into the brain body schema [1]. It is important to distinguish between the body schema and the body image. The body schema is a model constructed by the brain that reflects the structural and dynamic organization of the body, while the image is a conscious esthetic and sexual perception of one's own body.

From the concept of body schema the researchers moved on towards the modern internal model theory [50]. This theory describes two parts of the control loop: the controlled object (for example, an arm with muscles and joints) and the controller (a neuronal network that controls arm movements). The controller uses an internal model to generate an expectation of the object position, as well as an expectation of sensory feedback. The controller then compares these expectations with the actual sensory feedback and, if a discrepancy is found, introduces corrections to the object state. The equilibrium point hypothesis describes one implementation of this view [51]. According to it, higher motor centers set an equilibrium point for the controlled object, and servo-mechanisms of the spinal cord transfer the object there.

Arm BCI

Arm movements constitute the major part of motor repertoire of our everyday lives. That is why many BCI developers focus on the task of arm control. Besides, arm movements have a substantial cortical component to them, which is convenient for the developers, because it is easier to record the signals of the cortex than those of subcortical structures.

Figure 1 shows the interface that reproduced arm movements. It was an invasive BCI that monkeys used to control a robotic arm performing reaching and grasping movements. For decoding, multiple Wiener filters running in parallel were used.

In another experiment with monkeys, stereoscopic glasses were used to enable BCI control in a three-dimensional space [33]. Motor cortical activity was translated into cursor

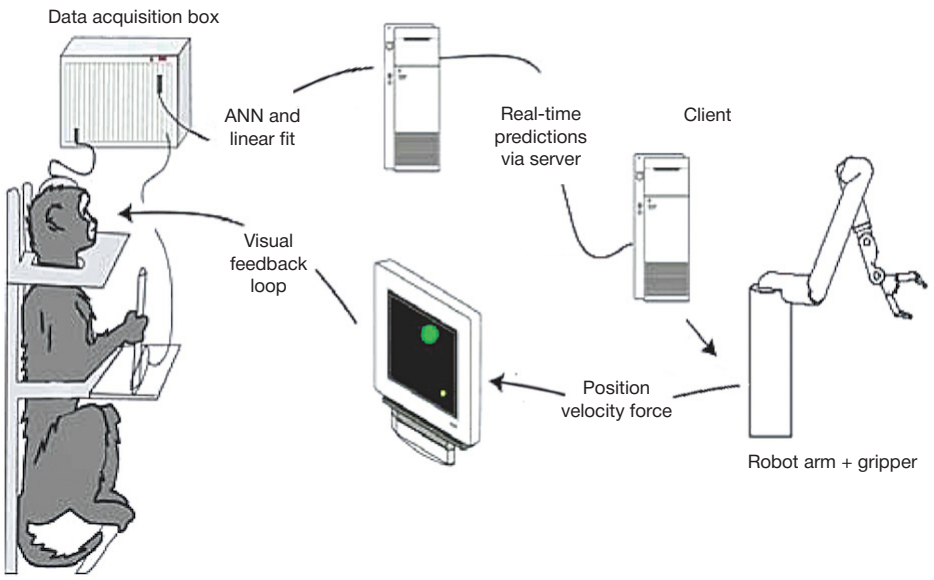

Fig. 1. A BCI-based robotic arm capable of grasping objects

Extracellular activity of cortical neurons was recorded by a multi-electrode array implanted into several cortical areas of the monkey. Signals were decoded using Wiener filters and then transmitted to the robotic arm controller. On the screen, the monkey was presented with a cursor that changed its size depending on the gripping force the animal applied. The task was to reach toward a virtual object after it appeared on the screen and to grasp it. In one task the monkey controlled the robot using a hand-held joystick with two degrees of freedom, and the gripping force was determined by how strongly the joystick was gripped. In another task the joystick was not connected to the robot, and the robot was controlled directly by the commands issued by the motor cortex (Carmena et al., [28]).

position in space. Decoding was initially performed using the above mentioned method of population vectors. In further experiments, system accuracy was improved by applying the adaptive algorithm that minimized trajectory errors. Later, the same group of researchers demonstrated a BCI which monkeys used to feed themselves with the robotic arm [52]. Similar technologies involving robotic arms are currently used to improve the quality of life of paralyzed patients [7, 9].

Also, virtual technologies have been developed, such as a pair of virtual arms moving on the computer screen and a BCI for their control [31]. In those experiments several hundreds of electrodes recorded neuronal activity in both cortical hemispheres, which enabled monkeys to control two arms simultaneously.

Functional electrical stimulation

Robotic BCIs are necessary in case of limb loss, but if limbs are paralyzed but not lost, it is possible to use FES. This technology utilizes electrode arrays for electrical stimulation of muscles with a set of impulses that imitate nervous system signals. Muscles activation by stimulation, in turn, produces limb movements. For surface stimulation, a multi-electrode array is placed on patient's skin. Such contact electrodes can be sewn into clothes turning them into wearable electronic devices (gloves, trousers, etc.) [53]. Control over BCI can be performed by EEG beta oscillations, and that is how the movements of a paralyzed hand have been reproduced [54].

Using invasive BCIs, a paralyzed monkey hand was moved by FES, the movements being quite precise [40]. In the experiments involving FES for a larger number of muscles and decoding over a hundred of neurons, monkeys with paralyzed arms could perform grasping [55, 56]. Recently, such invasive BCI–based control has been demonstrated by a paralyzed human [6].

According to the experimental data, a part of lower-level functions, such as adjusting the limb position in the external force field, can be handed over to the local self-control. In this case, feedback systems are used, such as position sensors [57]. FES-based BCIs can take into account the specifics of muscle contractile properties. For feedback, vision can be used [53], as well as sensory substitution with vibrostimulation.

BCIs for bipedal locomotion

A possibility of reproducing kinematic parameters of bipedal walking based on brain cortical activity recording was first tested by Fitzsimmons, Lebedev and their colleagues [30]. The schematics of this experiment are presented in figure 2. Monkeys were trained to walk on a treadmill. During this task, neuronal activity of sensorimotor cortex representation of lower limbs was recorded while the movements of the monkey's legs were video tracked. The BCI decoder was trained to decode monkey lower limb kinematics. The decoder performed well for both forward and backward walking directions.

Based on those results, the Walk Again Project was founded, an international consortium, the goal of which is to develop an exoskeleton driven by the brain [2]. Nicolelis demonstrated the EEG-controlled exoskeleton built by Gordon Cheng at the opening of World Football Cup in 2014. A similar project, the Mindwalker, emerged in Europe [58]. In parallel, Contreras Vidal and his colleagues proposed an idea of developing a leg exoskeleton controlled by slow EEG rhythms; in 2012 they decoded gait kinematics of a human walking on the treadmill [59]. In Russia, ExoAtlet, a very practical leg exoskeleton, was developed [60].

As an alternative to EEG, a possibility of reactivating the spinal central pattern generator is studied. It was demonstrated in the experiments on rat models of complete spinal cord injury that locomotion can be restored using epidural electrical stimulation combined with treatment with serotonergic agonists [61].

Nueroplasticity and BCIs

Many studies have convincingly demonstrated that learning to

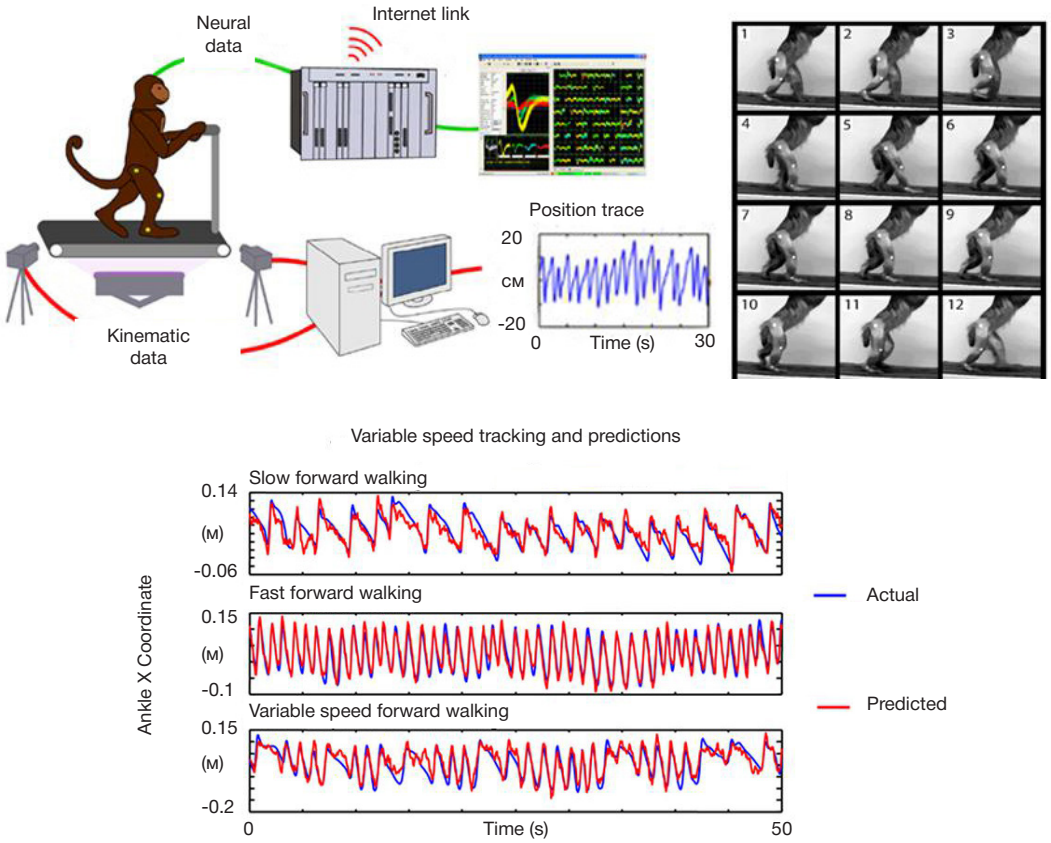

Fig. 2. Reproduction of kinematics of bipedal walking based on ensemble cortical activity

Activity of neuronal ensembles of monkey sensorimotor cortex was recorded while the animals were walking on a treadmill. Blue curves represent movements recorded by video tracking system; red curves represent decoded movement (Fitzsimmons et al., [30]).

use a BCI boosts the plasticity of the subject's brain. It was speculated that due to that phenomenon, artificial limbs could become incorporated into the brain representation of the body and eventually feel and act as normal limbs [1, 62].

Controlling external devices by BCIs has a lot in common with tool use. Thus, in a famous experiment with monkeys trained to use rakes to retrieve distant objects [63], it was shown that posterior parietal cortex neurons that normally respond to objects in the vicinity of the hand started to respond to objects in the vicinity of rakes. In other words, the brain incorporated the rakes into the body schema.

Long-term use of BCIs can lead to similar changes in the brain. Indeed, the neurons participating in BCI control change activity patterns [64]. Correlations between pairs of neurons also change [28, 31], as well as neuronal tuning to movement directions [29].

Noninvasive BCIs

An important requirement for BCIs is safety. Noninvasive BCIs are the safest, as they do not penetrate biological tissues to record neuronal activity. Numerous types of noninvasive BCIs have been developed so far, mainly for operating wheelchairs and restoring communicative function by using spelling systems [44, 45, 65–68].

EEG recording is the most popular method used for the development of noninvasive BCIs. EEG-based BCIs can be independent (based on endogenous activation by motor imagery) and dependent (based on exogenous activation by external stimuli). In the former case, slow cortical potentials, mu (8–12 Hz), beta (18–30 Hz) and gamma rhythms (30–70 Hz) are used to exert control [4]. The effectiveness of the method can be improved by using adaptive decoding algorithms [69]. With exogenous activation, the attention is focused on the external visual stimulus, which leads to a conspicuous cortical response, compared to the response to an ignored stimulus; the patient's intentions are decoded based on the previously recorded difference in the response to attended and ignored stimuli. Thus, during BCI control based on steady-state visually evoked potentials, a reaction to frequently presented stimuli is recorded [70]. The subject is presented with several objects on the screen. Each object appears and disappears at its own frequency. The subject focuses on each object, one by one. P300 potentials can be used in a similar way [71].

Artifacts of EEG recording process present a considerable problem. They can be taken for neural activity and even serve as controlling signals. Dependent BCIs are less sensitive to artifacts. A better signal quality, compared to EEG, a higher spatial and temporal resolution and a lower sensitivity to artifacts are demonstrated by electrocorticographic BCIs. However, they are invasive.

Apart from EEG, magnetic encephalography is used (MEG) [72]. To register weak magnetic field generated by the brain, a highly sensitive method is required. Such sensitivity can be provided by superconducting quantum magnetometers. As a result, MEG recording requires special equipment and special conditions, magnetic shielding in the first place. Still, MEG provides a better temporal and spatial resolution, compared to EEG.

Another method for brain activity recording is based on detecting the levels of oxyhemoglobin and deoxyhemoglobin in cerebral circulation by using near-infrared spectroscopy (NIRS) with temporal resolution of 100ms and spatial resolution of 1 cm. The major disadvantage of this technology is a considerable signal delay (up to several seconds). However, the BCIs based on NIRS are becoming popular [73].

A powerful tool for recording changes in cerebral circulation is functional magnetic resonance imaging. Its temporal resolution is limited to 1–2 s, signal delay is about several seconds, but it stands out in the line of noninvasive methods because of its unsurpassed spatial resolution that makes it possible to detect the activity of every brain area [73].

Sensory BCIs

Sensory BCIs can be used for restoring vision, hearing, the sense of taste, smell or balance, and tactile and proprioceptive sensitivity. Functions of sensory organs can be impaired as a result of peripheral nervous system damage leading to complete loss of senses (deafness, blindness) and as a result of damage to the organs that process sensory information of a higher level (thalamus, cerebellum, basal ganglia, brain cortex); the latter does not cause a complete loss of sensitivity, though. An interesting example is blindsight in patients with damaged visual cortex; they are blind but still can sense and process visual stimuli subconsciously [74].

At present, sensory BCIs cannot replace high-level components of a sensory system. For example, blindsight cannot be repaired. Currently, researchers focus on developing devices for repairing low-level damage associated with peripheral areas and receptors dysfunction. Such systems replace physiological sensors with artificial ones that are connected to undamaged sensory areas [17, 75, 76]. Signal transmission from artificial sensors to the nerve tissue is usually mediated by electrical stimulation, but recently optogenetic methods have gained popularity [77].

We should also mention sensory substitution, a method in which a signal flow from an artificial sensor is redirected to the undamaged sensors of other body parts or another sensory organ. With such sensory substitution, a switch from one sensor modality to another becomes possible. For example, artificial vision can be implemented by transmitting the signal from a video camera to a tactile matrix that stimulates the back [78].

Cochlear implants

Cochlear implants are the most successful devices among sensory BCIs [13, 14]. Patients with such implants can detect speech, tell female voices from male voices and even perceive melodies. Bilateral implantation restores spatial hearing. The implant consists of six components: (1) an external microphone, (2) a speech processor that transforms the signal from the microphone to a stimulation sequence, (3) a transmitter placed on the skin, (4) a receiver and a stimulator implanted into the bone under the skin (5), a cable connecting stimulators with the electrodes, and (6) an array of stimulation electrodes implanted into the cochlea.

A sequence of impulses is applied to undamaged areas of the auditory nerve. The use of several electrodes enables to stimulate various areas of the nerve; the number of electrodes usually varies from 4 to 22. Several different methods of signal formation by multichannel stimulation were developed. In continuous interleaved sampling, a signal from a microphone is transformed into a frequency spectrum and the intensity of the signal in each band is transformed into the intensity of a stimulus. Compression of a wide dynamic range of signals into a narrow range of stimuli is performed using non-linear transform. Also, there are systems based on the continuous analysis of a signal from a microphone where an electrode is selected for signal transmission in a recurrent cycle.

For patients with severely damaged cochlear, brain stem implants have been developed [13]. These devices stimulate the cochlear nucleus of the brainstem by means of surface or penetrating electrodes. Some patients who tested such implants reported a low quality of sound recognition, while in the others the device performance was comparable to cochlear implant performance.

Visual prosthesis

Visual prostheses are currently capable of restoring simple visual sensations [79]. Visual prostheses can be divided into two groups: retinal prostheses and brain prostheses. Retinal prostheses are used for treating pathologies that do not affect the visual nerve, while brain prostheses are used if the visual nerve is damaged, and it is necessary to stimulate visual structures of the brain, such as the visual cortex, to evoke visual sensations.

Depending on the severity of retinal damage, several types of retinal prostheses can be used. Epiretinal implants stimulate nerve fibers of retinal ganglion cells by intraocular electrode arrays (up to 60 channels) that receive frames from a video camera. We expect that in the future all components of such prostheses will be implanted inside the eye. Patients with such implants can perceive the shape of objects, the brightness of colors and movement direction.

Subretinal prostheses stimulate ganglion and bipolar cells by electrical signals. They consist of thousands of microphotodiodes that respond to the level of illumination and transmit this information to the electrode array. The studies of these devices are currently at an early experimental stage.

In a transchoroidal prosthesis several dozens of stimulating electrodes are implanted under the choroid. Compared to others, this device can be implanted by a quite simple surgical procedure. Patients perceive stimuli as phosphenes and can detect simple objects.

As a rule, in non-retinal prostheses electrical stimulation of visual cortex is used. In 1974 simple visual perception was restored by implanting 64 electrodes onto the surface of the visual cortex [25]. It is possible that intracortical microelectrode arrays can yield better results.

Bidirectional BCIs (brain-computer-brain interface)

Biderictional, or sensor-connected BCIs decode brain activity and simultaneously transmit artificial sensory signals to the brain, thus creating a feedback loop. Figure 3 shows the schematics of the first brain-computer-brain interface (BCBI) designed in Nicolelis laboratory by O'Doherty, Lebedev and their colleagues [80]. Microelectrode arrays were implanted into motor and somatosensory cortex of monkeys. The first array recorded intentions, the second one transmitted artificial tactile sensations back to the brain using intracortical microstimulation. The BCBI allowed monkeys to explore a virtual object using a cursor or a realistic image (avatar) of monkey's arm. Virtual objects looked alike but had different texture; texture data were transmitted to the brain through microstimulation.

Brain-net

Networks that connect separate nervous systems have recently become a popular subject of research. In general, the task is to create the network that would combine knowledge and effort of several individuals for more effective problem solving. Among such distributed networks are a neuron-net (a community of people and technologies that use neuronal signals for communication), a body-net (a net in which the movements of one individual can be transmitted to another through FES) and a brain-net (an integration of several brains by BCI-technologies [81], fig. 4).

CONCLUSIONS

We are witnessing a rapid growth of BCI technologies. Researchers keep reporting new achievements and are making further progress in the development of methods and devices that will help to restore the lost functionality of the human body. With long-term use of a BCI, an artificial limb can be incorporated into the body schema formed by the brain. Many BCI projects are currently at the stage of lab experiments, but there are a few devices that have been successfully introduced into clinical practice. We envision the future in which a blind, deaf and paralyzed patient can live a life of a healthy person, assisted by neural implants and functional electrical stimulation. Using BCIs for network communication, the mankind can rise to a new level, the most recent projects on creating the “internet of bodies and minds” being the first attempt toward that goal.

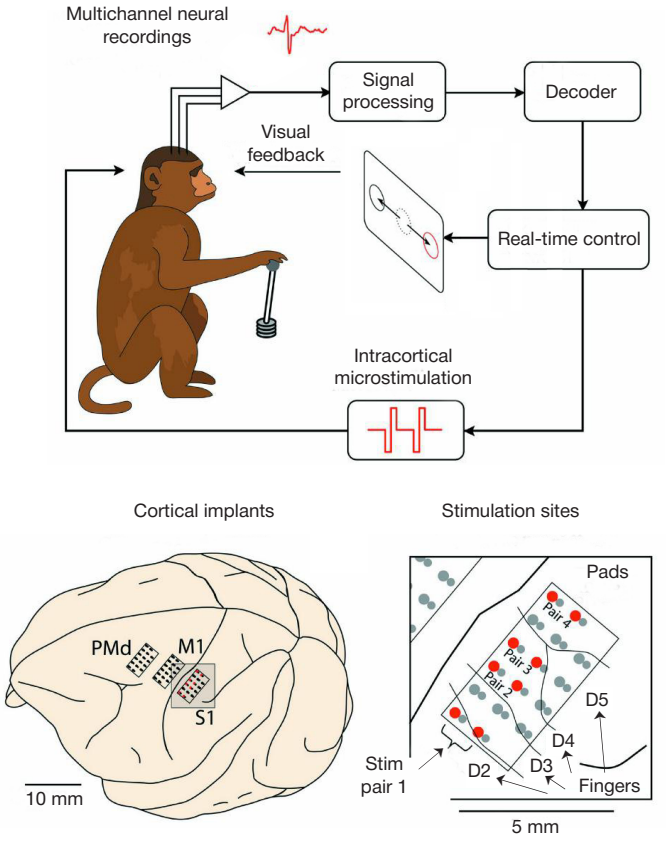

Fig. 3. The schematics of the first brain-computer-brain interface

The motor area of the control loop sets the cursor in motion. The desired position of the cursor is decoded on the basis of motor cortical activity. The sensory part of the loop serves as a feedback tool. It transmits artificial tactile signals into somatosensory cortex through intracortical microstimulation (O'Doherty et al. [80]).

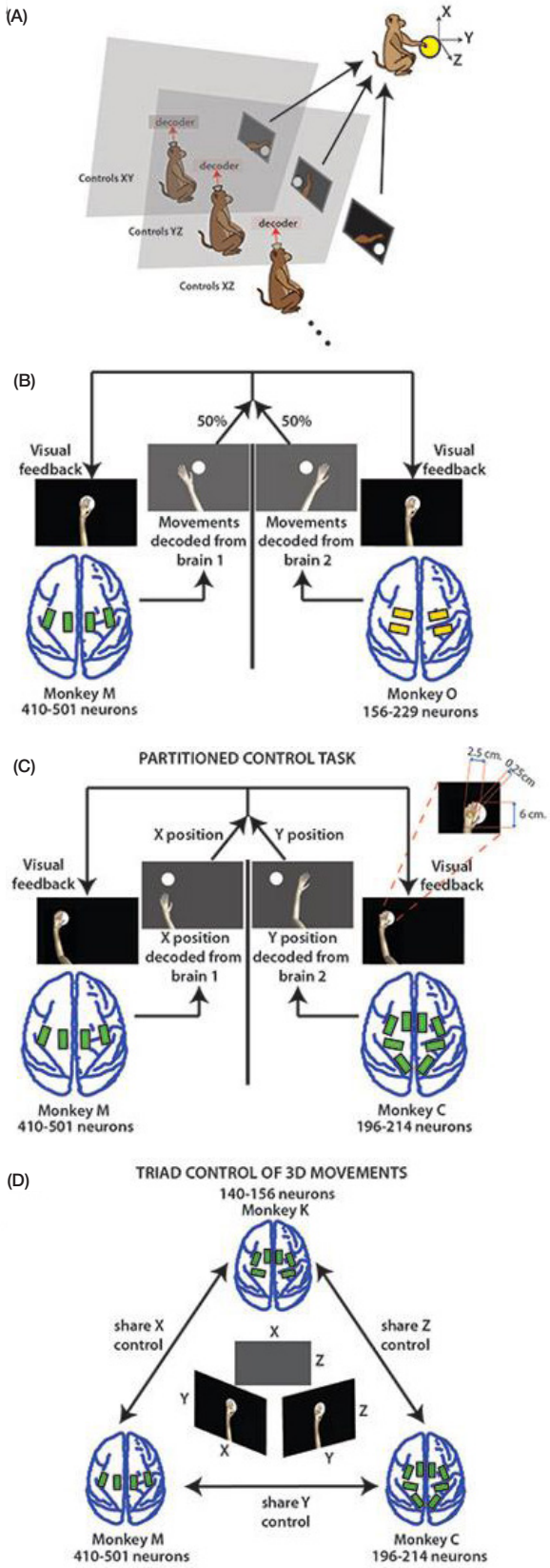

Fig. 4. Integration of brain activity of several subjects using a brain net

Each monkey was seated in a separate room and watched a virtual arm on the screen; the task was to touch the object using the virtual arm **(A)**. Signals from various cortex areas were recorded by a 700-channel invasive electrode array. After decoding, the signals were sent to the virtual arm, with monkeys contributing to coordinates equally **(B)** or with each monkey controlling only one coordinate **(C)** or one plane **(D)**. The tasks were performed more effectively compared to the experiment where only one animal controlled the virtual arm (Ramakrishnan et al., [81]).

References

1. Lebedev MA, Nicolelis MA. Brain-machine interfaces: past, present and future. Trends Neurosci. 2006 Sep; 29 (9): 536–46. Epub 2006 Jul 21.
2. Nicolelis MA, Lebedev MA. Principles of neural ensemble physiology underlying the operation of brain-machine interfaces. Nat Rev Neurosci. 2009 Jul; 10 (7): 530–40.
3. Schwartz AB, Cui XT, Weber DJ, Moran DW. Brain-controlled interfaces: movement restoration with neural prosthetics. Neuron. 2006 Oct 5; 52 (1): 205–20.
4. McFarland DJ, Krusienski DJ, Wolpaw JR. Brain-computer interface signal processing at the Wadsworth Center: mu and sensorimotor beta rhythms. Prog Brain Res. 2006; 159: 411–9.
5. Hatsopoulos NG, Donoghue JP. The science of neural interface systems. Annu Rev Neurosci. 2009; 32: 249–66.
6. Bouton CE, Shaikhouni A, Annetta NV, Bockbrader MA, Friedenberg DA, Nielson DM, et al. Restoring cortical control of functional movement in a human with quadriplegia. Nature. 2016 Apr 13. doi: 10.1038/nature17435.
7. Collinger JL, Wodlinger B, Downey JE, Wang W, Tyler-Kabara EC, Weber DJ, et al. High-performance neuroprosthetic control by an individual with tetraplegia. Lancet. 2013 Feb 16; 381 (9886): 557–64.
8. Hochberg LR, Serruya MD, Friehs GM, Mukand JA, Saleh M, Caplan AH, et al. Neuronal ensemble control of prosthetic devices by a human with tetraplegia. Nature. 2006 Jul 13; 442 (7099): 164–71.
9. Hochberg LR, Bacher D, Jarosiewicz B, Masse NY, Simeral JD, Vogel J, et al. Reach and grasp by people with tetraplegia using a neurally controlled robotic arm. Nature. 2012 May 16; 485 (7398): 372–5.
10. Tangermann M, Krauledat M, Grzeska K, Sagebaum M, Blankertz B, Vidaurre C, Müller KR. Playing pinball with non-invasive BCI. In: Koller D, Schuurmans D, Bengio Y, editors. Advances in Neural Information Processing Systems 21. Neural Information Processing Systems; 2008 Dec 8–11; Vancouver and Whistler, BC, Canada. Cambridge, MA: MIT Press; 2009. p. 1641–8.
11. Lin CT, Chang CJ, Lin BS, Hung SH, Chao CF, Wang IJ. A real-time wireless brain–computer interface system for drowsiness detection. IEEE Trans Biomed Circuits Syst. 2010 Aug; 4 (4): 214–22.
12. Virtual'naya real'nost' i kotiki na khakatone Microsoft i Skolkovo [Internet]. Habrahabr. 2015 Jan. Available from: https://habrahabr.ru/company/microsoft/blog/275837/. Russian.
13. Shannon RV. Advances in auditory prostheses. Curr Opin Neurol. 2012 Feb; 25 (1): 61–6.
14. Wilson BS, Dorman MF. Cochlear implants: a remarkable past and a brilliant future. Hear Res. 2008 Aug; 242 (1–2): 3–21.
15. Lilly JC. Distribution of 'motor' functions in the cerebral cortex in the conscious, intact monkey. Science. 1956; 124: 937.
16. Evarts EV. Motor cortex reflexes associated with learned movement. Science. 1973; 179: 501–3.
17. O'Doherty JE, Lebedev MA, Ifft PJ, Zhuang KZ, Shokur S, Bleuler H, Nicolelis MA. Active tactile exploration using a brain-machine-brain interface. Nature. 2011 Oct 5; 479 (7372): 228–31.
18. Lilly JC. Instantaneous relations between the activities of closely spaced zones on the cerebral cortex; electrical figures during responses and spontaneous activity. Am J Physiol. 1954; 176: 493–504.
19. Dennett DC. Consciousness explained. London, UK: Penguin UK; 1993. 528 p.
20. Frank K. Some approaches to the technical problem of chronic excitation of peripheral nerve. Ann Otol Rhinol Laryngol. 1968 Aug; 77 (4): 761–71.
21. Humphrey DR, Schmidt EM, Thompson WD. Predicting measures of motor performance from multiple cortical spike trains. Science. 1970 Nov 13; 170 (3959): 758–62.
22. Schmidt EM. Single neuron recording from motor cortex as a possible source of signals for control of external devices. Ann Biomed Eng. 1980; 8 (4–6): 339–49.
23. Fetz EE. Operant conditioning of cortical unit activity. Science. 1969 Feb 28; 163 (3870): 955–8.
24. Brindley GS, Lewin WS. The sensations produced by electrical stimulation of the visual cortex. J. Physiol. 1968 May; 196 (2): 479–93.
25. Dobelle WH, Mladejovsky MG, Girvin JP. Artifical vision for the blind: electrical stimulation of visual cortex offers hope for a functional prosthesis. Science. 1974 Feb 1; 183 (4123): 440–4.
26. Chapin JK, Moxon KA, Markowitz RS, Nicolelis MA. Real-time control of a robot arm using simultaneously recorded neurons in the motor cortex. Nat Neurosci. 1999 Jul; 2 (7): 664–70.
27. Wessberg J, Stambaugh CR, Kralik JD, Beck PD, Laubach M, Chapin JK, et al. Real-time prediction of hand trajectory by ensembles of cortical neurons in primates. Nature. 2000 Nov 16; 408 (6810): 361–5.
28. Carmena JM, Lebedev MA, Crist RE, O'Doherty JE, Santucci DM, Dimitrov DF, et al. Learning to control a brain-machine interface for reaching and grasping by primates. PLoS Biol. 2003; 1 (2): e42. doi:10.1371/journal.pbio.0000042.
29. Lebedev MA, Carmena JM, O'Doherty JE, Zacksenhouse M, Henriquez CS, Principe JC, Nicolelis MA. Cortical ensemble adaptation to represent velocity of an artificial actuator controlled by a brain-machine interface. J Neurosci. 2005 May 11; 25 (19): 4681–93.
30. Fitzsimmons NA, Lebedev MA, Peikon ID, Nicolelis MA. Extracting kinematic parameters for monkey bipedal walking from cortical neuronal ensemble activity. Front Integr Neurosci. 2009 Mar 9; 3:3. doi: 10.3389/neuro.07.003.2009.
31. Ifft PJ, Shokur S, Li Z, Lebedev MA, Nicolelis MA. A brain-machine interface enables bimanual arm movements in monkeys. Sci Transl Med. 2013 Nov 6; 5 (210): 210ra154.
32. Kennedy PR, Bakay RA. Restoration of neural output from a paralyzed patient by a direct brain connection. Neuroreport. 1998 Jun 1; 9 (8): 1707–11.
33. Taylor DM, Tillery SI, Schwartz AB. Direct cortical control of 3D neuroprosthetic devices. Science. 2002; 296 (5574): 1829–32.
34. Mountcastle VB. The sensory hand: neural mechanisms of somatic sensation. Cambridge, MA: Harvard University Press: 2005. 640 p.
35. Hubel D.H., Wiesel T.N. (2005). Brain and visual perception: the story of a 25-year collaboration. 744 pp. Oxford University Press.
36. Wise SP. The primate premotor cortex: past, present, and preparatory. Annu Rev Neurosci. 1985; 8: 1–19.
37. Kalaska JF, Scott SH, Cisek P, Sergio LE. Cortical control of reaching movements. Curr Opin Neurobiol. 1997; 7 (6): 849–59.
38. Georgopoulos AP, Kalaska JF, Caminiti R, Massey JT. On the relations between the direction of two-dimensional arm movements and cell discharge in primate motor cortex. J Neurosci. 1982 Nov; 2 (11): 1527–37.
39. Georgopoulos AP, Lurito JT, Petrides M, Schwartz AB, Massey JT. Mental rotation of the neuronal population vector. Science. 1989 Jan 13; 243 (4888): 234–6.
40. Moritz CT, Perlmutter SI, Fetz EE. Direct control of paralysed muscles by cortical neurons. Nature. 2008 Dec 4; 456 (7222): 639–42.
41. Quiroga RQ, Reddy L, Kreiman G, Koch C, Fried I. Invariant visual representation by single neurons in the human brain. Nature. 2005 Jun 23; 435 (7045): 1102–7.
42. Haykin S. Adaptive Filter Theory. 4th ed. Upper Saddle River, New Jersey: Prentice Hall; 2002. 936 p.
43. Sussillo D, Nuyujukian P, Fan JM, Kao JC, Stavisky SD, Ryu S, Shenoy K. A recurrent neural network for closed-loop intracortical brain-machine interface decoders. J Neural Eng. 2012 Apr; 9 (2): 026027. doi: 10.1088/1741-2560/9/2/026027.
44. Birbaumer N, Ghanayim N, Hinterberger T, Iversen I, Kotchoubey B, Kübler A, et al. A spelling device for the paralysed. Nature. 1999 Mar 25; 398 (6725): 297–8.
45. Birbaumer N, Murguialday AR, Cohen L. Brain-computer interface in paralysis. Curr Opin Neurol. 2008 Dec; 21 (6): 634–8.
46. Sherrington CS. The integrative action of the nervous system. New York: Charles Scribner's Sons; 1906. 445 p.
47. Guertin PA. The mammalian central pattern generator for

locomotion. Brain Res Rev. 2009 Dec 11; 62 (1): 45–56.
48. Cordo PJ, Gurfinkel VS. Motor coordination can be fully understood only by studying complex movements. Prog Brain Res. 2004; 143: 29–38.
49. Head H, Holmes G. Sensory disturbances from cerebral lesions. Brain. 1911 Nov 1; 34 (2–3): 102–254.
50. Kawato M. Internal models for motor control and trajectory planning. Curr Opin Neurobiol. 1999 Dec 1; 9 (6): 718–27.
51. Feldman AG, Ostry DJ, Levin MF, Gribble PL, Mitnitski AB. Recent tests of the equilibrium-point hypothesis (lambda model). Motor Control. 1998 Jul; 2 (3): 189–205.
52. Velliste M, Perel S, Spalding MC, Whitford AS, Schwartz AB. Cortical control of a prosthetic arm for self-feeding. Nature. 2008 Jun 19; 453 (7198): 1098–101.
53. Levitskaya OS, Krylov NV, Kapyrin NI. Kostyum funktsional'noy elektrostimulyatsii dlya neiroreabilitatsii s primeneniem virtual'noy real'nosti [Internet]. Skolkovo Robotics sk-news. 2014 Mar [cited 2016 Feb]. Russian.
54. Pfurtscheller G, Müller GR, Pfurtscheller J, Gerner HJ, Rupp R. 'Thought'-control of functional electrical stimulation to restore hand grasp in a patient with tetraplegia. Neurosci. Lett. 2003 Nov 6; 351 (1): 33–6.
55. Ethier C, Oby ER, Bauman MJ, Miller LE. Restoration of grasp following paralysis through brain-controlled stimulation of muscles. Nature. 2012 May 17; 485 (7398): 368–71.
56. Pohlmeyer EA, Oby ER, Perreault EJ, Solla SA, Kilgore KL, Kirsch RF, Miller LE. Toward the restoration of hand use to a paralyzed monkey: brain-controlled functional electrical stimulation of forearm muscles. PLoS One. 2009 Jun 15; 4 (6): e5924.
57. Hick C, Hick A. Intensivkurs Physiologie. 5th ed. München–Jena: Urban&Fischer; 2006. 434 p.
58. Cheron G, Duvinage M, De Saedeleer C, Castermans T, Bengoetxea A, Petieau M,et al. From spinal central pattern generators to cortical network: integrated BCI for walking rehabilitation. Neural Plast. 2012; 2012: 375148.
59. Presacco A, Forrester LW, Contreras-Vidal JL. Decoding intra-limb and inter-limb kinematics during treadmill walking from scalp electroencephalographic (EEG) signals. IEEE Trans Neural Syst Rehabil Eng. 2012 Mar; 20 (2): 212–9.
60. Exoatlet.ru [Internet]. Moscow: ExoAtlet LLC; c2014-2015. Available from: http://www.exoatlet.ru.
61. Courtine G, Gerasimenko Y, van den Brand R, Yew A, Musienko P, Zhong H, et al. Transformation of nonfunctional spinal circuits into functional states after the loss of brain input. Nat Neurosci. 2009 Oct 1; 12 (10): 1333–42.
62. Nicolelis MA. Beyond Boundaries: The New Neuroscience of Connecting Brains with Machines — and How It Will Change Our Lives. New York: Times Books; 2011. 354 p.
63. Iriki A, Tanaka M, Iwamura Y. Coding of modified body schema during tool use by macaque postcentral neurones. Neuroreport. 1996 Oct; 7 (14): 2325–30.
64. Zacksenhouse M, Lebedev MA, Carmena JM, O'Doherty JE, Henriquez C, Nicolelis MA. Cortical modulations increase in early sessions with brain-machine interface. PLoS One. 2011 Jul 18; 2 (7): e619.
65. Galán F, Nuttin M, Lew E, Ferrez PW, Vanacker G, Philips J, Millán JR. A brain-actuated wheelchair: asynchronous and non-invasive brain-computer interfaces for continuous control of robots. Clin Neurophysiol. 2008 Sep 13; 119 (9): 2159–69.
66. Müller-Putz GR, Gernot R, Pfurtscheller G. Control of an electrical prosthesis with an SSVEP-based BCI. IEEE Trans Biomed Eng. 2008 Jan; 55 (1): 361–4.
67. Nicolas-Alonso LF, Gomez-Gil J. Brain computer interfaces, a review. Sensors (Basel). 2012; 12 (2): 1211–79.
68. Sellers EW, Vaughan TM, Wolpaw JR. A brain-computer interface for long-term independent home use. Amyotroph Lateral Scler. 2010 Oct; 11 (5): 449–55.
69. Wolpaw JR, McFarland DJ. Control of a two-dimensional movement signal by a noninvasive brain-computer interface in humans. Proc Natl Acad Sci U S A. 2008 Dec 21;101 (51): 17849–54.
70. Vialatte FB, Maurice M, Dauwels J, Cichocki A. Steady-state visually evoked potentials: focus on essential paradigms and future perspectives. Prog Neurobiol. 2010 Apr; 90 (4): 418–38.
71. Farwell LA, Donchin E. Talking off the top of your head: toward a mental prosthesis utilizing event-related brain potentials. Electroencephalogr Clin Neurophysiol. 1988; 70 (6): 510–23.
72. Mellinger J, Schalk G, Braun C, Preissl H, Rosenstiel W, Birbaumer N, Kübler A. An MEG-based brain–computer interface (BCI). Neuroimage. 2007 Jul 1; 36 (3): 581–93.
73. Sitaram R, Caria A, Birbaumer N. Hemodynamic brain-computer interfaces for communication and rehabilitation. Neural Netw. 2009 Nov; 22 (9): 1320–8.
74. Barton JJ. Disorder of higher visual function. Curr Opin Neurol. 2009 Feb; 24 (1): 1–5.
75. Romo R, Hernández A, Zainos A, Brody CD, Lemus L. Sensing without touching: psychophysical performance based on cortical microstimulation. Neuron. 2000 Apr; 26 (1): 273–78.
76. Fitzsimmons NA, Drake W, Hanson TL, Lebedev MA, Nicolelis MA. Primate reaching cued by multichannel spatiotemporal cortical microstimulation. J Neurosci. 2007 May 23; 27 (21): 5593–602.
77. Zhang F, Aravanis AM, Adamantidis A, de Lecea L, Deisseroth K. Circuit-breakers: optical technologies for probing neural signals and systems. Nat Rev Neurosci. 2007 Aug; 8 (8): 577–81. Erratum in: Nat Rev Nuerosci. 2007 Sep; 8 (9): 732.
78. Jones LA. Tactile communication systems optimizing the display of information. Prog Brain Res. 2011; 192:113–28.
79. Fernandes RA, Diniz B, Ribeiro R, Humayun M. Artificial vision through neuronal stimulation. Neurosci Lett. 2012 Jun 25; 519 (2): 122–8.
80. O'Doherty JE, Lebedev M, Hanson TL, Fitzsimmons N, Nicolelis MA. A brain-machine interface instructed by direct intracortical microstimulation. Front Integr Neurosci. 2009 Sep 1; 3: 20.
81. Ramakrishnan A, Ifft PJ, Pais-Vieira M, Byun YW, Zhuang KZ, Lebedev MA, Nikolelis MA. Computing arm movements with a monkey brained. Sci Rep. 2015 Jul 9; 5: 10767.

Литература

1. Lebedev MA, Nicolelis MA. Brain-machine interfaces: past, present and future. Trends Neurosci. 2006 Sep; 29 (9): 536–46. Epub 2006 Jul 21.
2. Nicolelis MA, Lebedev MA. Principles of neural ensemble physiology underlying the operation of brain-machine interfaces. Nat Rev Neurosci. 2009 Jul; 10 (7): 530–40.
3. Schwartz AB, Cui XT, Weber DJ, Moran DW. Brain-controlled interfaces: movement restoration with neural prosthetics. Neuron. 2006 Oct 5; 52 (1): 205–20.
4. McFarland DJ, Krusienski DJ, Wolpaw JR. Brain-computer interface signal processing at the Wadsworth Center: mu and sensorimotor beta rhythms. Prog Brain Res. 2006; 159: 411–9.
5. Hatsopoulos NG, Donoghue JP. The science of neural interface systems. Annu Rev Neurosci. 2009; 32: 249–66.
6. Bouton CE, Shaikhouni A, Annetta NV, Bockbrader MA, Friedenberg DA, Nielson DM, et al. Restoring cortical control of functional movement in a human with quadriplegia. Nature. 2016 Apr 13. doi: 10.1038/nature17435.
7. Collinger JL, Wodlinger B, Downey JE, Wang W, Tyler-Kabara EC, Weber DJ, et al. High-performance neuroprosthetic control by an individual with tetraplegia. Lancet. 2013 Feb 16; 381 (9886): 557–64.
8. Hochberg LR, Serruya MD, Friehs GM, Mukand JA, Saleh M, Caplan AH, et al. Neuronal ensemble control of prosthetic devices by a human with tetraplegia. Nature. 2006 Jul 13; 442 (7099): 164–71.
9. Hochberg LR, Bacher D, Jarosiewicz B, Masse NY, Simeral JD, Vogel J, et al. Reach and grasp by people with tetraplegia using a

neurally controlled robotic arm. Nature. 2012 May 16; 485 (7398): 372–5.
10. Tangermann M, Krauledat M, Grzeska K, Sagebaum M, Blankertz B, Vidaurre C, Müller KR. Playing pinball with non-invasive BCI. In: Koller D, Schuurmans D, Bengio Y, editors. Advances in Neural Information Processing Systems 21. Neural Information Processing Systems; 2008 Dec 8–11; Vancouver and Whistler, BC, Canada. Cambridge, MA: MIT Press; 2009. p. 1641–8.
11. Lin CT, Chang CJ, Lin BS, Hung SH, Chao CF, Wang IJ. A real-time wireless brain–computer interface system for drowsiness detection. IEEE Trans Biomed Circuits Syst. 2010 Aug; 4 (4): 214–22.
12. Виртуальная реальность и котики на хакатоне Microsoft и Сколково [Интернет]. Хабрахабр. Январь 2015. Доступно по ссылке: https://habrahabr.ru/company/microsoft/blog/275837/.
13. Shannon RV. Advances in auditory prostheses. Curr Opin Neurol. 2012 Feb; 25 (1): 61–6.
14. Wilson BS, Dorman MF. Cochlear implants: a remarkable past and a brilliant future. Hear Res. 2008 Aug; 242 (1–2): 3–21.
15. Lilly JC. Distribution of 'motor' functions in the cerebral cortex in the conscious, intact monkey. Science. 1956; 124: 937.
16. Evarts EV. Motor cortex reflexes associated with learned movement. Science. 1973; 179: 501–3.
17. O'Doherty JE, Lebedev MA, Ifft PJ, Zhuang KZ, Shokur S, Bleuler H, Nicolelis MA. Active tactile exploration using a brain-machine-brain interface. Nature. 2011 Oct 5; 479 (7372): 228–31.
18. Lilly JC. Instantaneous relations between the activities of closely spaced zones on the cerebral cortex; electrical figures during responses and spontaneous activity. Am J Physiol. 1954; 176: 493–504.
19. Dennett DC. Consciousness explained. London, UK: Penguin UK; 1993. 528 p.
20. Frank K. Some approaches to the technical problem of chronic excitation of peripheral nerve. Ann Otol Rhinol Laryngol. 1968 Aug; 77 (4): 761–71.
21. Humphrey DR, Schmidt EM, Thompson WD. Predicting measures of motor performance from multiple cortical spike trains. Science. 1970 Nov 13; 170 (3959): 758–62.
22. Schmidt EM. Single neuron recording from motor cortex as a possible source of signals for control of external devices. Ann Biomed Eng. 1980; 8 (4–6): 339–49.
23. Fetz EE. Operant conditioning of cortical unit activity. Science. 1969 Feb 28; 163 (3870): 955–8.
24. Brindley GS, Lewin WS. The sensations produced by electrical stimulation of the visual cortex. J. Physiol. 1968 May; 196 (2): 479–93.
25. Dobelle WH, Mladejovsky MG, Girvin JP. Artifical vision for the blind: electrical stimulation of visual cortex offers hope for a functional prosthesis. Science. 1974 Feb 1; 183 (4123): 440–4.
26. Chapin JK, Moxon KA, Markowitz RS, Nicolelis MA. Real-time control of a robot arm using simultaneously recorded neurons in the motor cortex. Nat Neurosci. 1999 Jul; 2 (7): 664–70.
27. Wessberg J, Stambaugh CR, Kralik JD, Beck PD, Laubach M, Chapin JK, et al. Real-time prediction of hand trajectory by ensembles of cortical neurons in primates. Nature. 2000 Nov 16; 408 (6810): 361–5.
28. Carmena JM, Lebedev MA, Crist RE, O'Doherty JE, Santucci DM, Dimitrov DF, et al. Learning to control a brain-machine interface for reaching and grasping by primates. PLoS Biol. 2003; 1 (2): e42. doi:10.1371/journal.pbio.0000042.
29. Lebedev MA, Carmena JM, O'Doherty JE, Zacksenhouse M, Henriquez CS, Principe JC, Nicolelis MA. Cortical ensemble adaptation to represent velocity of an artificial actuator controlled by a brain-machine interface. J Neurosci. 2005 May 11; 25 (19): 4681–93.
30. Fitzsimmons NA, Lebedev MA, Peikon ID, Nicolelis MA. Extracting kinematic parameters for monkey bipedal walking from cortical neuronal ensemble activity. Front Integr Neurosci. 2009 Mar 9; 3:3. doi: 10.3389/neuro.07.003.2009.
31. Ifft PJ, Shokur S, Li Z, Lebedev MA, Nicolelis MA. A brain-machine interface enables bimanual arm movements in monkeys. Sci Transl Med. 2013 Nov 6; 5 (210): 210ra154.
32. Kennedy PR, Bakay RA. Restoration of neural output from a paralyzed patient by a direct brain connection. Neuroreport. 1998 Jun 1; 9 (8): 1707–11.
33. Taylor DM, Tillery SI, Schwartz AB. Direct cortical control of 3D neuroprosthetic devices. Science. 2002; 296 (5574): 1829–32.
34. Mountcastle VB. The sensory hand: neural mechanisms of somatic sensation. Cambridge, MA: Harvard University Press: 2005. 640 p.
35. Hubel D.H., Wiesel T.N. (2005). Brain and visual perception: the story of a 25-year collaboration. 744 pp. Oxford University Press.
36. Wise SP. The primate premotor cortex: past, present, and preparatory. Annu Rev Neurosci. 1985; 8: 1–19.
37. Kalaska JF, Scott SH, Cisek P, Sergio LE. Cortical control of reaching movements. Curr Opin Neurobiol. 1997; 7 (6): 849–59.
38. Georgopoulos AP, Kalaska JF, Caminiti R, Massey JT. On the relations between the direction of two-dimensional arm movements and cell discharge in primate motor cortex. J Neurosci. 1982 Nov; 2 (11): 1527–37.
39. Georgopoulos AP, Lurito JT, Petrides M, Schwartz AB, Massey JT. Mental rotation of the neuronal population vector. Science. 1989 Jan 13; 243 (4888): 234–6.
40. Moritz CT, Perlmutter SI, Fetz EE. Direct control of paralysed muscles by cortical neurons. Nature. 2008 Dec 4; 456 (7222): 639–42.
41. Quiroga RQ, Reddy L, Kreiman G, Koch C, Fried I. Invariant visual representation by single neurons in the human brain. Nature. 2005 Jun 23; 435 (7045): 1102–7.
42. Haykin S. Adaptive filter theory. 4th ed. Upper Saddle River, New Jersey: Prentice Hall; 2002. 936 p.
43. Sussillo D, Nuyujukian P, Fan JM, Kao JC, Stavisky SD, Ryu S, Shenoy K. A recurrent neural network for closed-loop intracortical brain-machine interface decoders. J Neural Eng. 2012 Apr; 9 (2): 026027. doi: 10.1088/1741-2560/9/2/026027.
44. Birbaumer N, Ghanayim N, Hinterberger T, Iversen I, Kotchoubey B, Kübler A, et al. A spelling device for the paralysed. Nature. 1999 Mar 25; 398 (6725): 297–8.
45. Birbaumer N, Murguialday AR, Cohen L. Brain-computer interface in paralysis. Curr Opin Neurol. 2008 Dec; 21 (6): 634–8.
46. Sherrington CS. The integrative action of the nervous system. New York: Charles Scribner's Sons; 1906. 445 p.
47. Guertin PA. The mammalian central pattern generator for locomotion. Brain Res Rev. 2009 Dec 11; 62 (1): 45–56.
48. Cordo PJ, Gurfinkel VS. Motor coordination can be fully understood only by studying complex movements. Prog Brain Res. 2004; 143: 29–38.
49. Head H, Holmes G. Sensory disturbances from cerebral lesions. Brain. 1911 Nov 1; 34 (2–3): 102–254.
50. Kawato M. Internal models for motor control and trajectory planning. Curr Opin Neurobiol. 1999 Dec 1; 9 (6): 718–27.
51. Feldman AG, Ostry DJ, Levin MF, Gribble PL, Mitnitski AB. Recent tests of the equilibrium-point hypothesis (lambda model). Motor Control. 1998 Jul; 2 (3): 189–205.
52. Velliste M, Perel S, Spalding MC, Whitford AS, Schwartz AB. Cortical control of a prosthetic arm for self-feeding. Nature. 2008 Jun 19; 453 (7198): 1098–101.
53. Левицкая О. С., Крылов Н. В., Капырин Н. И. Костюм функциональной электростимуляция для нейрореабилитации с применением виртуальной реальности [Интернет]. Сколково Роботикс sk-news. Март 2014 [дата обращения: февраль 2016].
54. Pfurtscheller G, Müller GR, Pfurtscheller J, Gerner HJ, Rupp R. 'Thought'-control of functional electrical stimulation to restore hand grasp in a patient with tetraplegia. Neurosci. Lett. 2003 Nov 6; 351 (1): 33–6.
55. Ethier C, Oby ER, Bauman MJ, Miller LE. Restoration of grasp following paralysis through brain-controlled stimulation of muscles. Nature. 2012 May 17; 485 (7398): 368–71.
56. Pohlmeyer EA, Oby ER, Perreault EJ, Solla SA, Kilgore KL, Kirsch RF, Miller LE. Toward the restoration of hand use to a paralyzed monkey: brain-controlled functional electrical stimulation of forearm muscles. PLoS One. 2009 Jun 15; 4 (6): e5924.
57. Hick C, Hick A. Intensivkurs Physiologie. 5th ed. München–Jena:

Urban&Fischer; 2006. 434 p.
58. Cheron G, Duvinage M, De Saedeleer C, Castermans T, Bengoetxea A, Petieau M,et al. From spinal central pattern generators to cortical network: integrated BCI for walking rehabilitation. Neural Plast. 2012; 2012: 375148.
59. Presacco A, Forrester LW, Contreras-Vidal JL. Decoding intra-limb and inter-limb kinematics during treadmill walking from scalp electroencephalographic (EEG) signals. IEEE Trans Neural Syst Rehabil Eng. 2012 Mar; 20 (2): 212–9.
60. Exoatlet.ru [Internet]. Moscow: ExoAtlet LLC; c2014-2015. Available from: http://www.exoatlet.ru.
61. Courtine G, Gerasimenko Y, van den Brand R, Yew A, Musienko P, Zhong H, et al. Transformation of nonfunctional spinal circuits into functional states after the loss of brain input. Nat Neurosci. 2009 Oct 1; 12 (10): 1333–42.
62. Nicolelis MA. Beyond Boundaries: The New Neuroscience of Connecting Brains with Machines — and How It Will Change Our Lives. New York: Times Books; 2011. 354 p.
63. Iriki A, Tanaka M, Iwamura Y. Coding of modified body schema during tool use by macaque postcentral neurones. Neuroreport. 1996 Oct; 7 (14): 2325–30.
64. Zacksenhouse M, Lebedev MA, Carmena JM, O'Doherty JE, Henriquez C, Nicolelis MA. Cortical modulations increase in early sessions with brain-machine interface. PLoS One. 2011 Jul 18; 2 (7): e619.
65. Galán F, Nuttin M, Lew E, Ferrez PW, Vanacker G, Philips J, Millán JR. A brain-actuated wheelchair: asynchronous and non-invasive brain-computer interfaces for continuous control of robots. Clin Neurophysiol. 2008 Sep 13; 119 (9): 2159–69.
66. Müller-Putz GR, Gernot R, Pfurtscheller G. Control of an electrical prosthesis with an SSVEP-based BCI. IEEE Trans Biomed Eng. 2008 Jan; 55 (1): 361–4.
67. Nicolas-Alonso LF, Gomez-Gil J. Brain computer interfaces, a review. Sensors (Basel). 2012; 12 (2): 1211–79.
68. Sellers EW, Vaughan TM, Wolpaw JR. A brain-computer interface for long-term independent home use. Amyotroph Lateral Scler. 2010 Oct; 11 (5): 449–55.
69. Wolpaw JR, McFarland DJ. Control of a two-dimensional movement signal by a noninvasive brain-computer interface in humans. Proc Natl Acad Sci U S A. 2008 Dec 21;101 (51): 17849–54.
70. Vialatte FB, Maurice M, Dauwels J, Cichocki A. Steady-state visually evoked potentials: focus on essential paradigms and future perspectives. Prog Neurobiol. 2010 Apr; 90 (4): 418–38.
71. Farwell LA, Donchin E. Talking off the top of your head: toward a mental prosthesis utilizing event-related brain potentials. Electroencephalogr Clin Neurophysiol. 1988; 70 (6): 510–23.
72. Mellinger J, Schalk G, Braun C, Preissl H, Rosenstiel W, Birbaumer N, Kübler A. An MEG-based brain–computer interface (BCI). Neuroimage. 2007 Jul 1; 36 (3): 581–93.
73. Sitaram R, Caria A, Birbaumer N. Hemodynamic brain-computer interfaces for communication and rehabilitation. Neural Netw. 2009 Nov; 22 (9): 1320–8.
74. Barton JJ. Disorder of higher visual function. Curr Opin Neurol. 2009 Feb; 24 (1): 1–5.
75. Romo R, Hernández A, Zainos A, Brody CD, Lemus L. Sensing without touching: psychophysical performance based on cortical microstimulation. Neuron. 2000 Apr; 26 (1): 273–78.
76. Fitzsimmons NA, Drake W, Hanson TL, Lebedev MA, Nicolelis MA. Primate reaching cued by multichannel spatiotemporal cortical microstimulation. J Neurosci. 2007 May 23; 27 (21): 5593–602.
77. Zhang F, Aravanis AM, Adamantidis A, de Lecea L, Deisseroth K. Circuit-breakers: optical technologies for probing neural signals and systems. Nat Rev Neurosci. 2007 Aug; 8 (8): 577–81. Erratum in: Nat Rev Nuerosci. 2007 Sep; 8 (9): 732.
78. Jones LA. Tactile communication systems optimizing the display of information. Prog Brain Res. 2011; 192:113–28.
79. Fernandes RA, Diniz B, Ribeiro R, Humayun M. Artificial vision through neuronal stimulation. Neurosci Lett. 2012 Jun 25; 519 (2): 122–8.
80. O'Doherty JE, Lebedev M, Hanson TL, Fitzsimmons N, Nicolelis MA. A brain-machine interface instructed by direct intracortical microstimulation. Front Integr Neurosci. 2009 Sep 1; 3: 20.
81. Ramakrishnan A, Ifft PJ, Pais-Vieira M, Byun YW, Zhuang KZ, Lebedev MA, Nikolelis MA. Computing arm movements with a monkey brained. Sci Rep. 2015 Jul 9; 5: 10767.

PRELIMINARY RESULTS OF A CONTROLLED STUDY OF BCI–EXOSKELETON TECHNOLOGY EFFICACY IN PATIENTS WITH POSTSTROKE ARM PARESIS

Frolov AA[1,2], Mokienko OA[1,3] ✉, Lyukmanov RKh[1,3], Chernikova LA[3], Kotov SV[4], Turbina LG[4], Bobrov PD[1,2], Biryukova EV[1,2], Kondur AA[4], Ivanova GE[1], Staritsyn AN[1], Bushkova YuV[1], Dzhalagoniya IZ[2], Kurganskaya ME[2,3], Pavlova OG[2], Budilin SYu[2], Aziatskaya GA[3], Khizhnikova AE[3], Chervyakov AV[3], Lukyanov AL[5], Nadareyshvily GG[1]

[1] Pirogov Russian National Research Medical University, Moscow, Russia

[2] Institute of Higher Nervous Activity and Neurophysiology, RAS, Moscow, Russia

[3] Research Center of Neurology, Moscow, Russia

[4] Vladimirsky Moscow Regional Research Clinical Institute, Moscow, Russia

[5] Municipal Clinical Hospital no.31, Moscow, Russia

The article presents preliminary results of iMove research study. By the time of this publication, the data of 47 patients have been processed. The patients in the experimental group (n = 36) were trained in kinesthetic motor imagery using brain-computer interface (BCI) and a controllable exoskeleton. In the control group, BCI imitation procedures were carried out. In average, the patients had 9 training sessions with a duration of up to 40 minutes. On completing the training, only the experimental group showed improvement in scores (results are presented as median and quartiles (25 %; 75 %)): grasp score increased from 0.5 (0.0; 13.0) to 3.0 (0.0; 15.5) points (p = 0.003) and pinch score increased from 0.5 (0.0; 7.5) to 1.0 (0.0; 12.0) points (p = 0.005) on ARAT scale. In the experimental group, a significant improvement in motor function was found in 33.3 % patients on ARAT scale, and in 30.5 % patients on Fugl-Meyer scale. In the control group, those scores were lower: 9.1 % and 18.2 % patients, respectively.

Keywords: rehabilitation, stroke, paresis, exoskeleton, brain-computer interface, motor imagery

Funding: the study was supported by the Ministry of Education and Science of the Russian Federation (Grant Agreement no. 14.607.21.0128 dated October 27, 2015), Russian Foundation Basic Research grants no. 16-04-01506a and 16-04-00962a.

✉ **Correspondence should be addressed:** Olesya Mokienko
Volokolamskoye shosse, d. 80, kab.133, Moscow, Russia, 125367; lesya.md@yandex.ru

Received: 30.03.2016 **Accepted:** 07.04.2016

ПРЕДВАРИТЕЛЬНЫЕ РЕЗУЛЬТАТЫ КОНТРОЛИРУЕМОГО ИССЛЕДОВАНИЯ ЭФФЕКТИВНОСТИ ТЕХНОЛОГИИ ИМК–ЭКЗОСКЕЛЕТ ПРИ ПОСТИНСУЛЬТНОМ ПАРЕЗЕ РУКИ

А. А. Фролов[1,2], О. А. Мокиенко[1,3] ✉, Р. Х. Люкманов[1,3], Л. А. Черникова[3], С. В. Котов[4], Л. Г. Турбина[4], П. Д. Бобров[1,2], Е. В. Бирюкова[1,2], А. А. Кондур[4], Г. Е. Иванова[1], А. Н. Старицын[1], Ю. В. Бушкова[1], И. З. Джалагония[2], М. Е. Курганская[2,3], О. Г. Павлова[2], С. Ю. Будилин[2], Г. А. Азиатская[3], А. Е. Хижникова[3], А. В. Червяков[3], А. Л. Лукьянов[5], Г. Г. Надарейшвили[1]

[1] Российский национальный исследовательский медицинский университет имени Н. И. Пирогова, Москва

[2] Институт высшей нервной деятельности и нейрофизиологии РАН, Москва

[3] Научный центр неврологии, Москва

[4] Московский областной научно-исследовательский клинический институт имени М. Ф. Владимирского, Москва

[5] Городская клиническая больница № 31, Москва

В статье представлены предварительные результаты исследования iMove. На момент публикации получены данные по 47 пациентам. Основная группа (n = 36) пациентов проходила обучение кинестетическому воображению движения под контролем интерфейса мозг–компьютер (ИМК) с управляемым экзоскелетом. В контрольной группе проводили процедуры имитации ИМК. В среднем пациенты прошли 9 тренингов длительностью до 40 мин. По завершении тренингов только в основной группе выявлено улучшение по параметрам [Me (25 %; 75 %)]: шаровой захват кисти — с 0,5 (0,0; 13,0) до 3,0 (0,0; 15,5) балла (p = 0,003) и щипковый захват пальцев кисти — с 0,5 (0,0; 7,5) до 1,0 (0,0; 12,0) балла (p = 0,005) по шкале ARAT. В основной группе клинически значимое улучшение двигательной функции по шкале ARAT показали 33,3 % пациентов, а по шкале Fugl-Meyer — 30,5 %. В контрольной группе эти показатели были меньше: 9,1 и 18,2 % пациентов соответственно.

Ключевые слова: реабилитация, инсульт, парез, экзоскелет, интерфейс мозг–компьютер, воображение движения

Финансирование: исследование поддержано Министерством образования и науки Российской Федерации (Соглашение о предоставлении субсидии от 27.10.2015 № 14.607.21.0128), грантами РФФИ № 16-04-01506а и 16-04-00962а.

✉ **Для корреспонденции:** Олеся Александровна Мокиенко
125367, Москва, Волоколамское шоссе, д. 80, каб. 133; lesya.md@yandex.ru

Статья поступила: 30.03.2016 **Статья принята к печати:** 07.04.2016

Assessment of approaches to upper limb function restoration in poststroke patients with hemiparesis is a highpriority task in neurorehabilitation [1, 2]. However, none of the existing methods of motor rehabilitation has been assigned the highest level of evidence and high grades of recommendation strength for arm function restoration. The moderate level of evidence for arm function restoration in poststroke patients is demonstrated by virtual reality technology, robotic tools (due to abundant repetitive task practice) and mental training, including motor imagery [1, 2]. It is important to note that in contrast to motor imagery methods based on active motor paradigms, such as robotic technologies and constraint-induced movement therapy, can be applied to patients with mild or moderate paresis. In case of plegia or severe paresis, robotic therapy often plays a role of passive mechanotherapy.

The impact of motor imagery on motor nervous system activity and neuroplasticity has been demonstrated in multiple neurophysiological studies. It has been shown that during motor imagery, primary motor cortex and brain structures that participate in voluntary movement planning and control are activated [3–6]. In the study that utilized navigated transcranial magnetic stimulation of the brain, the subjects who had been trained in motor imagery exhibited a decreased motor threshold and larger evoked motor responses of the muscles involved in fist clenching [4].

Thus, motor imagery remains the only active paradigm for modulating neroplasticity in motor areas of the brain in patients with plegia and severe paresis [3, 4, 7, 8]. Motor imagery can also be used for the rehabilitation of patients with mild motor dysfunctions as a training tool for more effective motor planning and accurate motor performance [9]. Motor imagery can be controlled by kinesthetic feedback provided by brain-computer-exoskeleton interfaces. Brain-computer interfaces (BCIs) allow for translating brain activity signals into commands for the external device [10, 11]. With motor imagery, such signals are represented by sensorimotor rhythm modulation [12]. If a limb exoskeleton is used as an external device, the BCI operator receives kinesthetic feedback (the operator needs to imagine the movement that the exoskeleton is able to perform).

A number of controlled trials have been carried out to study the efficacy of non-invasive BCIs with external assistive devices that implement kinesthetic feedback. Those studies enrolled up to 32 patients with poststroke arm paresis. Haptic Knob [13] and MIT-Manus [14] robots and orthoses [15], which are not exoskeletons by design, were used as external devices.

Clinical trials of the efficacy of a BCI-based system where kinesthetic feedback is implemented by a hand exoskeleton have been conducted in Russia [16–18]. Biryukova et al. [19] studied one clinical case. However, none of those works compared the obtained results with the controls. Besides, clinical effectiveness of training in using a BCI technology to control the external assistive device has not been studied in patients at different rehabilitation stages and with different paresis severity; the effect of repetitive training using a BCI-external assistive device technology has not been investigated.

In this work we present preliminary results of a multicenter blind randomized controlled study of the efficacy of the hand exoskeleton controlled by non-invasive brain-computer interface for the rehabilitation of patients with poststroke paresis. The study will be open for participant recruitment until the number of participants reaches 120.

METHODS

The study was approved by the Ethics Committee of the Research Center of Neurology (protocol no. 12/14 dated December 10, 2014). All patients gave written informed consent. The protocol of iMove study is listed in the international registry of clinical trials of the U.S. National Institutes of Health (ClinicalTrials.gov; study indentifier is NCT02325947).

This blind randomized controlled study has been carried out at three clinical centers since December, 2014. Among site selection criteria were the presence of a neurorehabilitation unit or a motor rehabilitation service and a pool of patients with a history of stroke at various time points in the past or hemiparesis of various degrees.

The study included male and female patients aged 18–80 years with a prior stroke (1 month to 2 years before screening); with a poststroke hand paresis (from mild to plegia on Medical Research Council Weakness Scale sums score, MRC-SS [20]); with a supratentorial focal ischemic or hemorrhagic stroke confirmed by MRI or CT scan; all patients gave written informed consent. Study participants were either admitted to the clinical centers or received outpatient therapy.

The following exclusion criteria were applied: left-handedness according to Edinburgh Handedness Inventory [21]; severe cognitive impairment (Montreal Cognitive Assessment Score >10) [22]; sensory aphasia; severe motor aphasia; severe vision impairment that would not allow the patient to follow visual instructions on the computer screen; arm muscle contracture (Modified Ashworth Scale score of 4) [23].

Withdrawal criteria were as follows: patient's refusal to participate in the study; development of acute disease or decompensation of chronic disease that could possibly affect the study outcome, including recurrent cerebrovascular events, acute myocardial infarction, decompensated diabetes, etc.; therapy with systemic muscle relaxants that started after the participant had been enrolled (or medication dosage change); injections of botulinum toxins in paretic arm muscles after the patient had been enrolled.

Patients who gave informed consent to participate in the study and met inclusion/exclusion criteria were screened; their data were submitted to the automated system of information support for clinical trials (ImagerySoft, Russia); each participant was given an identification number. Then participants were randomly allocated to the experimental or control group (3 : 1).

Patients from the experimental group were trained to use the BCI-exoskeleton technology; patients from the control group were trained to use the BCI-imitating system. Each group attended up to 12 training sessions (each 40 min long) every day except weekends (the acceptable idle interval was up to 3 days). Patients from both groups also underwent standard rehabilitation procedures, such as therapeutic exercises with the instructor and massage.

In this study we used a BCI based on EEG pattern analysis and recognition of synchronization/desynchronization of sensorimotor rhythms during arm movement imagery. EEG signals were band-pass filtered between 5–30 Hz. We used the EEG pattern classification based on Bayesian method [24, 25]. To assess classification accuracy, we used Cohen's kappa coefficient ($\kappa = 1$ represented perfect recognition, $\kappa = 0$ represented due-to-chance recognition [26]) and the percentage of right responses suggested by the classifier (>33 % value represented more than chance recognition, because patients performed three mental tasks). The components of the BCI-exoskeleton system are presented in fig. 1.

During the session, the patient was wearing an electrode cap for EEG recording. Electrode gel was applied underneath

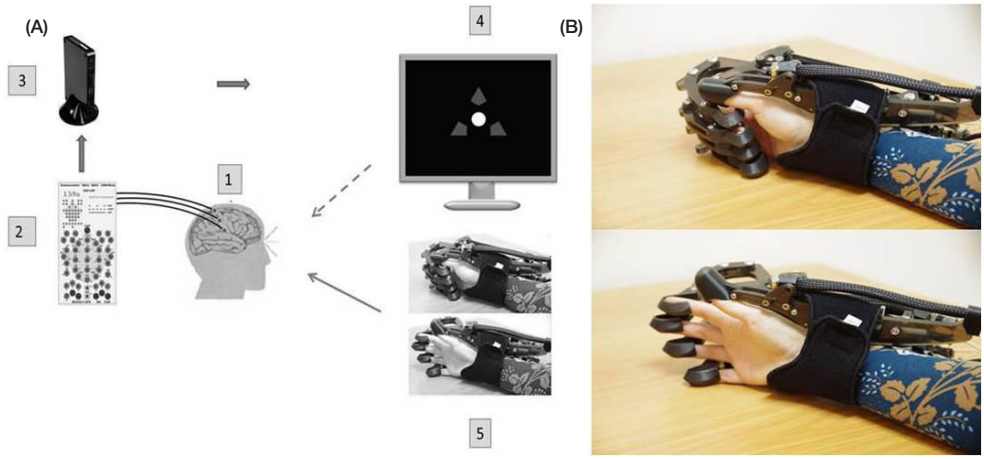

Fig. 1. BCI-exoskeleton system. **(A)** Schematic of the BCI used in the study: 1 — 32 Ag/AgCl EEG electrodes; 2 — NVX52 encephalograph (Medical Computer Systems, Russia); 3 — a computer (OS: Windows 7); data are transmitted in real time, EEG parameters are extracted; control command is recognized; 4 — a screen; 5 — the hand exoskeleton; dotted and solid arrows represent visual and kinesthetic feedback, respectively. **(B)** The hand exoskeleton (Neurobotics, Russia) with pneumatic actuator for finger extension

each electrode. The exoskeleton was fixed to the paretic arm. The exoskeleton used in this study is a polymer carcass for the hand and fingers with robotic pneumatic drive, intended for finger extension that does not exceed the physiological norm. During the training session, the patient was sitting in front of the computer screen; his arms were on the armrest or on the desk in a comfortable position.

In the middle of the dark screen there was a circle for gaze fixation with 3 arrows around it; the arrows changed colors to indicate a new instruction. The patient followed one of three instructions: to relax and, to imagine a slow extension of the left hand fingers or the right hand fingers kinesthetically. The instructions to imagine the extension of the right or left hand fingers (right or left arrow changed its color respectively) were presented on the screen in random order for 10 min. Following the instruction to relax, the patient had to sit still and watch the center of the screen.

Results of mental task recognition were presented to the patient via visual and kinesthetic feedback. If the classifier successfully recognized the task the patient had been instructed with, the circle in the middle of the screen turned green and the exoskeleton extended fingers. When other tasks were recognized, the circle did not change its color and the exoskeleton did not perform any action.

One training procedure consisted of up to three sessions described above; each session lasted for 10 s. The patient rested for 5 s between the sessions.

With the controls, the same components of the BCI system were used and the same conditions were applied. The patients in the control group also followed the instruction to relax and watch the arrow color. The color changed at random, each change lasted for 10 s, and the exoskeleton opened the fingers of the paretic hand when the corresponding arrow appeared on the screen.

Thus, the patient in the control group did not imagine the movement and did not try to control the exoskeleton, but received passive mechanotherapy for the paretic hand. EEG signals were recorded for monitoring.

The researcher who performed clinical assessment of the patients did not know what group the patient was included into. This information was only available to the researchers who conducted rehabilitation sessions using BCI-exoskeleton system or its dummy.

Before and after the training course, the patients underwent a procedure for arm movement and arm force assessment based on Fugl–Meyer Assessment scale (FM) and Action Research Arm Test (ARAT) [27, 28]. Besides, dynamics across different scale sections were analyzed. The degree of spasticity was assessed using MAS scale.

We also estimated the percentage of patients with improvements by 5 points or more on ARAT scale and by 7 points or more in the motor function of upper extremities on FM scale (A–H sections).

Statistical analysis was done using Mann–Whitney test (for independent samples). Wilcoxon test (for dependent samples), Spearman correlation coefficient, RM-ANOVA analysis of variance, and a maximum likelihood χ^2 test on the PC with installed Statsoft Statistica 6.0 software.

The data are presented as median and quartiles (25 %; 75 %). Differences were considered statistically significant with $p < 0.05$.

RESULTS

232 patients were screened for eligibility. Out of 58 patients who met the inclusion criteria 11 patients refused to participate after the first or second training procedure. Thus, the study included 47 patients (33 male and 14 female) with a mean age of 56 years (48 and 64 years respectively), median time elapsed after stroke was 8 months (4 and 13 months respectively). There were 35 patients with ischemic stroke and 12 patients with hemorrhagic stroke. All enrolled patients were right-handed and Caucasian. The experimental group consisted of 36 patients; they attended BCI-exoskeleton training sessions. The control group included 11 patients who had training sessions with a dummy. The groups were comparable in terms of age, time elapsed after stroke, and the degree of neurological deficit. Patients' demographics and the initial data are presented in table 1. No statistical differences were found between the groups with respect to age, time elapsed after stroke, lesion localization and lateralization and the degree of neurological deficit. No statistical differences were found between the patients from three clinical centers with respect to time elapsed after stroke, type, localization and severity of neurological deficit.

Mean number of training sessions was 9.5 (8.0; 10.0) in the experimental group and 10.0 (6.0; 10.0) in the control group, with $p > 0.05$

In both groups, improvement of arm motor activity assessed by ARAT and FM scales (arm function sections: A–D,

Table 1. Patients demographics and initial data (both groups)

Parameter	Experimental group (n = 36)	Control group (n = 11)
Age, years	56.0 (47.0; 64.0)	58.0 (48.0; 73.0)
Sex, male, n	27 (75.0%)	6 (54.5%)
Time elapsed after stroke, months	9.0 (5.0; 13.5)	2.0 (1.0; 12.0)
Lesion lateralization, n left right	 19 (52.8%) 17 (47.2%)	 8 (72.7%) 3 (27.3%)
Lesion localization, n cortical subcortical cortical - subcortical	 2 (5.5%) 19 (52.8%) 15 (41.7%)	 2 (18.2 %) 8 (72.7%) 1 (9.1%)
Rehabilitation period, n early (1–6 months) late (7–12 months) residual (over 12 months)	 14 (38.8%) 11 (30.6%) 11 (30.6%)	 6 (54.5%) 2 (18.2%) 3 (27.3%)
ARAT score, points	4.5 (0.0; 33.0)	1.0 (0.0; 22.0)
FM score, upper extremity (A–D, H, I), points	75.5 (61.0; 92.0)	65.0 (61.0; 104.0)
FM score, arm motor function (A–D), points	27.5 (11.0; 40.5)	12.0 (11.0; 49.0)
MAS score, points	2.0 (1.0; 3.0)	2.0 (1.0; 2.0)
Number of training sessions	9.5 (8.0; 10.0)	10.0 (6.0; 10.0)

H, I) was observed. The following improvements on ARAT scale were observed in the experimental group only: grasp scores increased from 0.5 (0.0; 13.0) to 3.0 (0.0; 15.5) points, with $p = 0.003$; pinch scores increased from 0.5 (0.0; 7.5) to 1.0 (0.0; 12.0) points, with $p = 0.005$; gross arm movement scores increased from 2.0 (0.0; 4.5) to 3.0 (1.0; 6.5) points, with $p < 0.001$ (tab. 2). No statistically significant differences were found between the groups in motor function improvement using RM-ANOVA analysis.

In the experimental group, a clinically significant improvement in the arm motor function on ARAT scale (by 5 points or more) and on FM scale (by 7 points or more, sections A-D) was found in 33.3 % patient and 30.5 % patients, respectively. A clinically significant improvement of arm motor function on both scales was found in 16.7 % patients of the experimental group. The observed improvement was associated with the restoration of wrist motor function. In the control group, the percentage of patients with clinically significant improvement of arm motor function was lower: 9.1 and 18.2 % on ARAT and FM scales, respectively (tab. 2).

In both group, restoration of arm function did not depend on the time elapsed after stroke and patient's age (on both ARAT and FM scales and subscales). In each group, a moderate or medium correlation between the restoration degree of arm function (wrist in particular) assessed by ARAT scale and the initial severity of neurological deficit ($r = 0.4$, $p < 0.05$) was found; however, in the experimental group, statistically significant improvement of wrist function was observed in the subgroup of patients with initially severe paresis, as well as in the subgroup of patients with mild or moderate paresis (tab. 3).

Three patients of the experimental group from the second study site took a second BCI-exoskeleton training course during another planned hospitalization. The time interval between the courses was 6 to 9 months. Every course consisted of 8–10 training sessions. As shown in fig. 2, by the time of the second hospitalization, arm motor function assessed by ARAT scale had not deteriorated in any patient. The score of patient 1 on FM scale (C–D) was lower at the time of the second hospitalization, but still considerably higher than the initial score. During the second rehabilitation therapy course with BCI-exoskeleton training sessions included, all three patients displayed improvement of arm motor function parameters.

None of the patients displayed deterioration of arm functions on ARAT or FM scale during the study.

During the training sessions, 3 patients had mild headache, namely, 2 patients from the experimental group (one of them observed headache during two training sessions out of ten, the other had headache over the course of all ten sessions) and 1 patient from the control group (during 3 sessions out of 10).

The majority of patients reported attention fatigue 20 to 30 min after the training session. Fatigue was more conspicuous if a patient had been insomniac the night before the training (2 patients in the experimental group), was prone to depression (2 patients in the experimental group), had other tiring therapeutic procedures before the session (1 patient in the experimental group), or was initially weak. The majority of patients thought that fatigue was the evidence of training effectiveness and felt good about it.

If there were complaints about headache or fatigue, the training session was discontinued for that day. For one patient, the time between the sessions within one training course was extended to 2–3 min (in agreement with his doctor and following the patient's wish). Due to fatigue and bad general condition, the time between the sessions was increased up to 2–3 days for one patient from the experimental group.

One patient from the experimental group had an episode of high blood pressure (200/100 mmHg) after the third training session during the second therapy course, but was able to respond to medication.

On the whole, none of the patients withdrew from the study on account of adverse effects.

DISCUSSION

Preliminary results of iMove multicenter blind controlled study conducted in Russia have shown that a 2–3 week rehabilitation therapy using a BCI-exoskeleton technology increases the number of patients with clinically significant improvement in arm motor function. This improvement is associated with the recovery of hand function, the motor imagery of which was practiced by the patients. It was also shown that only in the

Table 2. Changes in basic ARAT and Fugl–Meyer scores in each group before and after the study

Parameter	Experimental group (n = 36)		Control group (n = 11)		Possible range
	Before	After	Before	After	
ARAT Scale					
Total score	4.5 (0.0; 33.0)	7.0 (1.0; 43.5)	1.0 (0.0; 22.0)	6.0 (0.0; 24.0)	0–57
	< 0.001		**0.018**		
Grasp	0.5 (0.0; 13.0)	3.0 (0.0; 15.5)	0.0 (0.0; 5.0)	1.0 (0.0; 6.0)	0–18
	0.003		0.423		
Grip	0.5 (0.0; 8.0)	1.5 (0.0; 10.0)	0.0 (0.0; 6.0)	1.0 (0.0; 7.0)	0–12
	< 0.001		**0.043**		
Pinch	0.5 (0.0; 7.5)	1.0 (0.0; 12.0)	0.0 (0.0; 4.0)	0.0 (0.0; 5.0)	0–18
	0.005		0.423		
Total hand score	3.0 (0.0; 29.5)	5.0 (0.0; 37.0)	0.0 (0.0; 16.0)	3.0 (0.0; 18.0)	0–48
	< 0.001		**0.028**		
Gross movement	2.0 (0.0; 4.5)	3.0 (1.0; 6.5)	1.0 (0.0; 6.0)	3.0 (0.0; 6.0)	0–9
	< 0.001		0.109		
Improvements by 5 points and more on ARAT scale, % (n)	33.3 (12)		9.1 (1)		0–100
Fugl-Meyer Scale					
Upper extremity (A–D, H,I)	75.5 (61.0; 92.0)	84.5 (63.0; 103.0)	65.0 (61.0; 104.0)	72 (65.0; 108.0)	0–126
	< 0.001		**0.004**		
Upper extremity motor function (A–D)	27.5 (11.0; 40.5)	33.5 (15.5; 48.0)	12.0 (11.0; 49.0)	17.0 (13.0; 54.0)	0–66
	< 0.001		**0.005**		
Proximal arm active movements (A)	21.0 (10.5; 26.5)	24.5 (13.5; 32.0)	11.0 (10.0; 27.0)	15.0 (11.0; 28.0)	0–36
	< 0.001		**0.008**		
Hand active movements (B–C)	6.0 (1.0; 14.5)	8.0 (2.0; 18.0)	2.0 (1.0; 19.0)	3.0 (2.0; 19.0)	0–24
	< 0.001		**0.049**		
Number of cases with arm motor function (A–D) improved by 7 points or more, % (n)	30.5 (11)		18.2 (2)		0–100

Note: center-aligned are p values obtained from comparing the corresponding scores in each group before and after the study. Statistically significant differences are shown in bold.

Table 3. Improvement of hand motor function in the experimental group patients depending on the initial severity of paresis

Initial paresis severity on FM scale (B–C)	n	FM scale, points		p
		Before the study	After the study	
Plegia or severe paresis, 0–12 points	24	2.0 (1.0; 6.0)	3.0 (1.0; 8.0)	0.004
(of which) 0–7 points	20	1.0 (1.0; 2.5)	2.0 (1.0; 6.0)	0.003
Mild or moderate paresis, 13–24 points	12	17.5 (14.5; 21.5)	22.0 (18.0; 23.5)	0.005

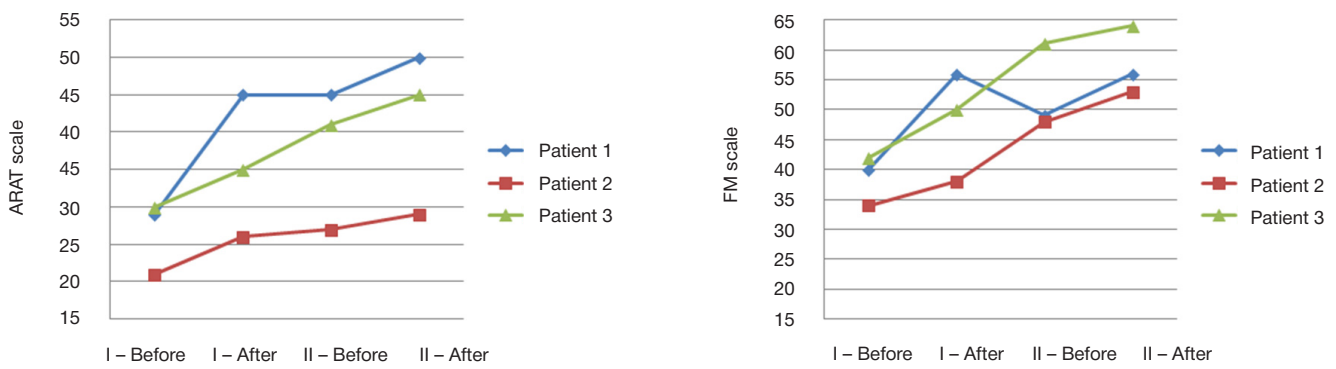

Fig. 2. Arm motor function dynamics in patients who completed two training courses. I and II represent the number of hospital admissions (or the training course), "Before" and "After" represent scores before and after each training course. Time elapsed after stroke with respect to the first and second hospital admissions: 21 and 30 months for Patient 1, 9 and 14 months for Patient 2, 6 and 12 months for Patient 3, respectively

BCI-exoskeleton group, grasp and pinch movements were improved. It is important to note that to grasp a big object (for example, a special object for ARAT-based assessment), the intact ability for hand opening movement is necessary. During BCI-exoskeleton training sessions, the patients imagined hand opening and feedback was provided kinesthetically by the exoskeleton that implemented the movement. No statistically significant difference in the degree of motor function restoration was found between the control and the experimental groups, which can be explained by the insufficient training duration and the length of observation period [14].

The results of our study are consistent with the data provided by other controlled studies in a given area of research. In Ramos–Murguialday study, 16 patients with poststroke hemiparesis were trained to use a BCI-orthesis system and 16 other patients were included in the control group. In the control group, the orthesis was not connected to the BCI and opened at random. Both groups had training sessions for 4 weeks, except weekends (in average, the patients had about 18 training sessions). As a result, the BCI group showed improvement in motor function on FM scale and scored 3.41 points more than the control group ($p = 0.018$) [15].

With 26 patients enrolled in the study, Ang investigated the efficacy of treatment in the group that received BCI-Manus training sessions compared to the group that received only MIT-Manus robotic therapy. In the second group, training intensity was considerably higher than in the first group (1040 movements against 136 during one session). After the 4-week course, the efficacy of treatment was comparable in both groups; however, 12 weeks after the observation had started, further motor function improvements were observed in 63.6 % patients from the BCI-Manus group and in 35.7 % controls [14].

In another study that enrolled 21 patients and was conducted by the same research team [13], three approaches were compared: a BCI with Haptic Knob robotic device for hand opening (the BCI-HK group), a Haptic Knob without BCI control, and a standard rehabilitation therapy. Compared to the standard therapy, a considerable hand function improvement was found only in the BCI-HK group during the 3rd, 12th and 24th weeks of the observation (by 2.14, 1.82 and 2.28 points on FM scale (C–D), respectively, with $p < 0.05$).

It is important to note that in contrast to our study, in the experiments mentioned above, patients were tested for the ability to control a BCI by motor imagery. Another important difference is higher training intensity: 18 h in total [13, 14], compared to 5 h in our study. However, in our case it is impossible to increase training intensity due to the specifics of the centers where the study is conducted and limited hospital admission periods.

Our study is characterized by the use of several scales for the assessment of arm motor function restoration. FM scale is more universal and detailed [13, 27], while ARAT scale is more functional and allows for the assessment of various hand movements needed for daily tasks [28].

Unlike other studies in this area of research, our study utilizes the exoskeleton as an assistive device. Although there are no data indicating the higher efficacy of the use of this particular device during BCI training sessions, the movement it implements is kinematically closer to the hand and finger physiological movement. It becomes possible due to the use of flexible pneumatic muscles, exo-joints and finger fixators designed with regard to human hand anatomy, which improves ergonomic parameters, helps to avoid rapid fatigue onset during the session, and also excludes traumas if all safety measures are taken. On the other hand, it should be emphasized that it is still impossible to implement a complex functional movement. The exoskeleton contributes to human finger extension; flexion of the fingers is passive, as they are brought back to the initial position by the spring. Such exoskeleton can be only used to stimulate surface and proprioceptive afferentation coming from fingers and hands and as a passive mechanotherapeutic complex with one degree of freedom for the distal arm. The second disadvantage of the exoskeleton is noise from the pneumatic pump that can distract the BCI operator from motor imagery.

Our study demonstrated that arm restoration assessed by ARAT and FM tests did not depend on the time elapsed after stroke and patient's age in both the experimental and the control groups; thus, this method can be used at various rehabilitation stages and can contribute to better health restoration, which is consistent with the results obtained by other authors [13, 14, 29].

In spite of moderate or medium correlation between the degree of hand function recovery on ARAT scale and the initial severity of neurological deficit, improvement of hand function was observed in the subgroups of patients with initially severe paresis and in the subgroup of patients with initially mild or moderate paresis. Earlier, improvement of hand motor function in patients with severe hand paresis was demonstrated associated with BCI-exoskeleton training [19]. Thus, the severity of motor deficiency cannot be seen as the criteria of exclusion from a BCI-exoskeleton training course. Moreover, for patients with plegia or severe paresis, such training courses are the only available method among those based on active motor paradigm.

The distinctive feature of this study is participation of patients from three clinical centers with statistically negligible differences in sex, time elapsed after stroke, type, localization and lateralization of stroke. Patient screening performed by different experts from different clinical centers and the blind design of the study reduced the influence of subjective factors [27] on the assessment of clinical test results.

Patients who had 2 training courses spaced 6 to 9 months apart observed further improvement of motor activity during the second training course. It is important to study the specifics of motor function restoration throughout several training courses separated by rest periods. Within the framework of this study, the observation will be continued for patients who are scheduled for further hospital admissions.

The most common adverse effect was fatigue; however, none of the patients withdrew from the study because of a serious adverse effect, and on the whole the technology is safe. Because conspicuous fatigue was preceded by insomnia, considerable exercise load during therapeutic procedures before the training session, predisposition to depression and generalized weakness, the probability of this adverse effect can be reduced by selecting the optimal sequence of rehabilitation procedures and by questioning the patient about his condition and sleep problems before each training session.

CONCLUSIONS

Although there is no screening for the ability of a patient to control the brain–computer interface and training sessions based on this technology are not so intensive, preliminary results of this study demonstrate its efficacy with respect to the percentage of patients with clinically significant improvement on ARAT and FM scales.

References

1. Langhorne P, Coupar F, Pollock A. Motor recovery after stroke: a systematic review. Lancet Neurol. 2009 Aug; 8 (8): 741–54.
2. Pollock A, Farmer SE, Brady MC, Langhorne P, Mead GE, Mehrholz J, et al. Interventions for improving upper limb function after stroke. Cochrane Database Syst Rev. 2014 Nov 12; 11: CD010820. doi: 10.1002/14651858.CD010820.pub2.
3. Shih JJ, Krusienski DJ, Wolpaw JR. Brain–computer interfaces in medicine. Mayo Clin Proc. 2012 Mar; 87 (3): 268–79.
4. Mokienko OA, Chervyakov AV, Kulikova SN, Bobrov PD, Chernikova LA, Frolov AA, et al. Increased motor cortex excitability during motor imagery in brain–computer interface trained subjects. Front Comput Neurosci. 2013 Nov 22; 7: 168.
5. Frolov AA, Gusek D, Bobrov PD, Mokienko OA, Chernikova LA, Konovalov RN. Localization of brain electrical activity sources and hemodynamic activity foci during motor imagery. Hum Physiol. 2014 May–Jun; 40 (3): 273–83.
6. Mokienko OA, Chernikova LA, Frolov AA, Bobrov PD. Motor imagery and its practical application. Neurosci Behav Physiol. 2014 Jun; 44 (5): 483–9.
7. Soekadar SR, Birbaumer N, Slutzky MW, Cohen LG. Brain–machine interfaces in neurorehabilitation of stroke. Neurobiol Dis. 2015 Nov; 83: 172–9.
8. Grosse-Wentrup M, Mattia D, Oweiss K. Using brain–computer interfaces to induce neural plasticity and restore function. J Neural Eng. 2011 Apr; 8 (2): 025004. doi: 10.1088/1741-2560/8/2/025004.
9. Steenbergen B, Crajé C, Nilsen DM, Gordon AM. Motor imagery training in hemiplegic cerebral palsy: a potentially useful therapeutic tool for rehabilitation. Dev Med Child Neurol. 2009 Sep; 51 (9): 690–6.
10. Nicolas-Alonso LF, Gomez-Gil J. Brain computer interfaces, a review. Sensors (Basel). 2012; 12 (2): 1211–79.
11. Vidal JJ. Toward direct brain–computer communication. Annu Rev Biophys Bioeng. 1973; 2: 157–80.
12. Pfurtscheller G, Aranibar A. Evaluation of event-related desynchronization (ERD) preceding and following voluntary self-paced movement. Electroencephalogr Clin Neurophysiol. 1979 Feb; 46 (2): 138–46.
13. Ang KK, Guan C, Phua KS, Wang C, Zhou L, Tang KY, et al. Brain–computer interface–based robotic end effector system for wrist and hand rehabilitation: results of a three-armed randomized controlled trial for chronic stroke. Front Neuroeng. 2014 Jul 29; 7: 30.
14. Ang KK, Chua KS, Phua KS, Wang C, Chin ZY, Kuah CW, et al. A Randomized Controlled Trial of EEG-Based Motor Imagery Brain–Computer Interface Robotic Rehabilitation for Stroke. Clin EEG Neurosci. 2015 Oct; 46 (4): 310–20.
15. Ramos-Murguialday A, Broetz D, Rea M, Läer L, Yilmaz O, Brasil FL, et al. Brain–machine interface in chronic stroke rehabilitation: a controlled study. Ann Neurol. 2013 Jul; 74 (1): 100–8.
16. Kotov SV, Turbina LG, Bobrov PD, Frolov AA, Pavlova OG, Kurganskaya ME, et al. Reabilitatsiya bol'nykh, perenesshikh insul't, s pomoshch'yu bioinzhenernogo kompleksa «interfeis mozg–komp'yuter + ekzoskelet». Zh Nevrol Psikhiatr Im S S Korsakova. 2014; 114 (12-2): 66–72. Russian.
17. Kotov SV, Turbina LG, Bobrov PD, Frolov AA, Pavlova OG, Kurganskaya ME, et al. Primenenie kompleksa «interfeis "mozg–komp'yuter" i ekzoskelet» i tekhniki voobrazheniya dvizheniya dlya reabilitatsii posle insul'ta. Almanac of Clinical Medicine. 2015; (39): 15–21. Russian.
18. Mokienko OA, Lyukmanov RKh, Chernikova LA, Suponeva NA, Piradov MA, Frolov AA. Brain–computer interface: The first experience of clinical use in Russia. Hum Physiol. 2016 Jan; 42 (1): 24–31.
19. Biryukova EV, Pavlova OG, Kurganskaya ME, Bobrov PD, Turbina LG, Frolov AA, et al. Recovery of the motor function of the arm with the aid of a hand exoskeleton controlled by a brain–computer interface in a patient with an extensive brain lesion. Hum Physiol. 2016; 42 (1): 13–23.
20. Compston A. Aids to the investigation of peripheral nerve injuries. Medical Research Council: Nerve Injuries Research Committee. His Majesty's Stationery Office: 1942; pp. 48 (iii) and 74 figures and 7 diagrams; with aids to the examination of the peripheral nervous system. By Michael O'Brien for the Guarantors of Brain. Saunders Elsevier: 2010; pp. [8] 64 and 94 Figures. Brain. 2010 Oct; 133 (10): 2838–44.
21. Oldfield RC. The assessment and analysis of handedness: the Edinburgh inventory. Neuropsychologia. 1971 Mar; 9 (1): 97–113.
22. Bocti C, Legault V, Leblanc N, Berger L, Nasreddine Z, Beaulieu-Boire I, et al. Vascular cognitive impairment: most useful subtests of the Montreal Cognitive Assessment in minor stroke and transient ischemic attack. Dement Geriatr Cogn Disord. 2013; 36 (3–4): 154–62.
23. Bohannon RW, Smith MB. Interrater reliability of a modified Ashworth scale of muscle spasticity. Phys Ther. 1987 Feb; 67 (2): 206–7.
24. Frolov A, Húsek D, Bobrov P. Comparison of four classification methods for brain–computer interface. Neural Network World. 2011; 21 (2): 101–5.
25. Bobrov PD, Korshakov AV, Roshchin V, Frolov AA. Baiesovskii podkhod k realizatsii interfeisa mozg–komp'yuter, osnovannogo na predstavlenii dvizhenii. Zh Vyssh Nerv Deiat Im I P Pavlova. 2012; 62 (1): 89–99. Russian.
26. Kohavi R, Provost F. Glossary of terms. Special Issue of Applications of Machine Learning and the Knowledge Discovery Process. Mach Learn. 1998; 30 (2–3): 271–4.
27. Sanford J, Moreland J, Swanson LR, Stratford PW, Gowland C. Reliability of the Fugl-Meyer assessment for testing motor performance in patients following stroke. Phys Ther. 1993 Jul; 73 (7): 447–54.
28. Doussoulin SA, Rivas SR, Campos SV. [Validation of «Action Research Arm Test» (ARAT) in Chilean patients with a paretic upper limb after a stroke]. Rev Med Chil. 2012 Jan; 140 (1): 59–65. Spanish.
29. Buch ER, Modir Shanechi A, Fourkas AD, Weber C, Birbaumer N, Cohen LG. Parietofrontal integrity determines neural modulation associated with grasping imagery after stroke. Brain. 2012 Feb; 135 (Pt 2): 596–614.

Литература

1. Langhorne P, Coupar F, Pollock A. Motor recovery after stroke: a systematic review. Lancet Neurol. 2009 Aug; 8 (8): 741–54.
2. Pollock A, Farmer SE, Brady MC, Langhorne P, Mead GE, Mehrholz J, et al. Interventions for improving upper limb function after stroke. Cochrane Database Syst Rev. 2014 Nov 12; 11: CD010820. doi: 10.1002/14651858.CD010820.pub2.
3. Shih JJ, Krusienski DJ, Wolpaw JR. Brain–computer interfaces in medicine. Mayo Clin Proc. 2012 Mar; 87 (3): 268–79.
4. Mokienko OA, Chervyakov AV, Kulikova SN, Bobrov PD, Chernikova LA, Frolov AA, et al. Increased motor cortex excitability during motor imagery in brain–computer interface trained subjects. Front Comput Neurosci. 2013 Nov 22; 7: 168.
5. Frolov AA, Gusek D, Bobrov PD, Mokienko OA, Chernikova LA, Konovalov RN. Localization of brain electrical activity sources and hemodynamic activity foci during motor imagery. Hum Physiol. 2014 May–Jun; 40 (3): 273–83.
6. Mokienko OA, Chernikova LA, Frolov AA, Bobrov PD. Motor imagery and its practical application. Neurosci Behav Physiol. 2014 Jun; 44 (5): 483–9.
7. Soekadar SR, Birbaumer N, Slutzky MW, Cohen LG. Brain–

machine interfaces in neurorehabilitation of stroke. Neurobiol Dis. 2015 Nov; 83: 172–9.
8. Grosse-Wentrup M, Mattia D, Oweiss K. Using brain–computer interfaces to induce neural plasticity and restore function. J Neural Eng. 2011 Apr; 8 (2): 025004. doi: 10.1088/1741-2560/8/2/025004.
9. Steenbergen B, Crajé C, Nilsen DM, Gordon AM. Motor imagery training in hemiplegic cerebral palsy: a potentially useful therapeutic tool for rehabilitation. Dev Med Child Neurol. 2009 Sep; 51 (9): 690–6.
10. Nicolas-Alonso LF, Gomez-Gil J. Brain computer interfaces, a review. Sensors (Basel). 2012; 12 (2): 1211–79.
11. Vidal JJ. Toward direct brain–computer communication. Annu Rev Biophys Bioeng. 1973; 2: 157–80.
12. Pfurtscheller G, Aranibar A. Evaluation of event-related desynchronization (ERD) preceding and following voluntary self-paced movement. Electroencephalogr Clin Neurophysiol. 1979 Feb; 46 (2): 138–46.
13. Ang KK, Guan C, Phua KS, Wang C, Zhou L, Tang KY, et al. Brain–computer interface–based robotic end effector system for wrist and hand rehabilitation: results of a three-armed randomized controlled trial for chronic stroke. Front Neuroeng. 2014 Jul 29; 7: 30.
14. Ang KK, Chua KS, Phua KS, Wang C, Chin ZY, Kuah CW, et al. A Randomized Controlled Trial of EEG-Based Motor Imagery Brain–Computer Interface Robotic Rehabilitation for Stroke. Clin EEG Neurosci. 2015 Oct; 46 (4): 310–20.
15. Ramos-Murguialday A, Broetz D, Rea M, Läer L, Yilmaz O, Brasil FL, et al. Brain–machine interface in chronic stroke rehabilitation: a controlled study. Ann Neurol. 2013 Jul; 74 (1): 100–8.
16. Котов С. В., Турбина Л. Г., Бобров П. Д., Фролов А. А., Павлова О. Г., Курганская М. Е. и др. Реабилитация больных, перенесших инсульт, с помощью биоинженерного комплекса «интерфейс мозг–компьютер + экзоскелет». Журн неврол. и психиатр. 2014; 114 (12-2): 66–72.
17. Котов С. В., Турбина Л. Г., Бобров П. Д., Фролов А. А., Павлова О. Г., Курганская М. Е. и др. Применение комплекса «интерфейс «мозг–компьютер» и экзоскелет» и техники воображения движения для реабилитации после инсульта. Альм. клин. мед. 2015; (39): 15–21.
18. Mokienko OA, Lyukmanov RKh, Chernikova LA, Suponeva NA, Piradov MA, Frolov AA. Brain–computer interface: The first experience of clinical use in Russia. Hum Physiol. 2016 Jan; 42 (1): 24–31.
19. Biryukova EV, Pavlova OG, Kurganskaya ME, Bobrov PD, Turbina LG, Frolov AA, et al. Recovery of the motor function of the arm with the aid of a hand exoskeleton controlled by a brain–computer interface in a patient with an extensive brain lesion. Hum Physiol. 2016; 42 (1): 13–23.
20. Compston A. Aids to the investigation of peripheral nerve injuries. Medical Research Council: Nerve Injuries Research Committee. His Majesty's Stationery Office: 1942; pp. 48 (iii) and 74 figures and 7 diagrams; with aids to the examination of the peripheral nervous system. By Michael O'Brien for the Guarantors of Brain. Saunders Elsevier: 2010; pp. [8] 64 and 94 Figures. Brain. 2010 Oct; 133 (10): 2838–44.
21. Oldfield RC. The assessment and analysis of handedness: the Edinburgh inventory. Neuropsychologia. 1971 Mar; 9 (1): 97–113.
22. Bocti C, Legault V, Leblanc N, Berger L, Nasreddine Z, Beaulieu-Boire I, et al. Vascular cognitive impairment: most useful subtests of the Montreal Cognitive Assessment in minor stroke and transient ischemic attack. Dement Geriatr Cogn Disord. 2013; 36 (3–4): 154–62.
23. Bohannon RW, Smith MB. Interrater reliability of a modified Ashworth scale of muscle spasticity. Phys Ther. 1987 Feb; 67 (2): 206–7.
24. Frolov A, Húsek D, Bobrov P. Comparison of four classification methods for brain–computer interface. Neural Network World. 2011; 21 (2): 101–5.
25. Бобров П. Д., Коршаков А. В., Рощин В. Ю., Фролов А. А. Байесовский подход к реализации интерфейса мозг–компьютер, основанного на представлении движений. Журн. высш. нервн. деят. 2012; 62 (1): 89–99.
26. Kohavi R, Provost F. Glossary of terms. Special Issue of Applications of Machine Learning and the Knowledge Discovery Process. Mach Learn. 1998; 30 (2–3): 271–4.
27. Sanford J, Moreland J, Swanson LR, Stratford PW, Gowland C. Reliability of the Fugl-Meyer assessment for testing motor performance in patients following stroke. Phys Ther. 1993 Jul; 73 (7): 447–54.
28. Doussoulin SA, Rivas SR, Campos SV. [Validation of «Action Research Arm Test» (ARAT) in Chilean patients with a paretic upper limb after a stroke]. Rev Med Chil. 2012 Jan; 140 (1): 59–65. Spanish.
29. Buch ER, Modir Shanechi A, Fourkas AD, Weber C, Birbaumer N, Cohen LG. Parietofrontal integrity determines neural modulation associated with grasping imagery after stroke. Brain. 2012 Feb; 135 (Pt 2): 596–614.

STUDYING THE ABILITY TO CONTROL HUMAN PHANTOM FINGERS IN P300 BRAIN-COMPUTER INTERFACE

Kaplan AYa[1,2]✉, Zhigulskaya DD[1], Kirjanov DA[1]

[1] Laboratory for Neurophysiology and Nero-Computer Interfaces, Faculty of Biology, Lomonosov Moscow State University, Moscow, Russia

[2] Laboratory for Brain-Machine Interfaces and Applied Neuroengineering, Lobachevsky National Research State University of Nizhny Novgorod, Nizhny Novgorod, Russia

In this work we have tested the assumption that an individual can control a target finger of a phantom by voluntarily focusing his attention on the luminous marker located on that finger in the complex of a P300 wave–based brain-computer interface (P300 BCI) and an anthropomorphic phantom. Because each correct movement of phantom fingers indicates a sufficient mental effort aimed at this action, creating a new ideomotor training simulator of smaller movements of the hand becomes possible. Our study included 21 volunteer subjects of both sexes aged 18–25. It was shown that with P300 BCI complex the subjects learned to control phantom fingers on the first day of the experiment, the percentage of successful attempts being no less than 69 %. Failures were mainly related to the insufficient attention focus on luminous markers on the target phantom fingers. We hypothesize that P300 BCI — Hand Phantom complex can be a basis for developing a fine motor skills simulator.

Keywords: brain-computer interface, BCI, electroencephalogram, neurorehabilitation, stroke, evoked potentials, P300

Funding: this work was partially supported by the Skolkovo Foundation, grant no. 1110034, and the Russian Science Foundation, grant no. 15-19-20053.

✉ **Correspondence should be addressed:** Alexandr Kaplan
ul. Leninskie gory, d. 1, str. 12, Moscow, Russia, 117234; akaplan@mail.ru

Received: 11.04.2016 **Accepted:** 15.04.2016

ИЗУЧЕНИЕ ВОЗМОЖНОСТИ УПРАВЛЕНИЯ ОТДЕЛЬНЫМИ ПАЛЬЦАМИ ФАНТОМА КИСТИ РУКИ ЧЕЛОВЕКА В КОНТУРЕ ИНТЕРФЕЙСА МОЗГ–КОМПЬЮТЕР НА ВОЛНЕ P300

А. Я. Каплан[1,2]✉, Д. Д. Жигульская[1], Д. А. Кирьянов[1]

[1] Лаборатория нейрофизиологии и нейрокомпьютерных интерфейсов, биологический факультет, Московский государственный университет имени М. В. Ломоносова, Москва

[2] Лаборатория разработки мозго-машинных интерфейсов и прикладной нейроинженерии, Национальный исследовательский Нижегородский государственный университет им. Н. И. Лобачевского, Нижний Новгород

В исследовании проверяли предположение, что в контуре предложенного комплекса интерфейса мозг–компьютер на основе волны P300 (ИМК-P300) и антропоморфного фантома кисти руки человек сможет управлять сгибанием целевого пальца фантома, произвольно фокусируя свое внимание на расположенном на этом пальце световом маркере. Поскольку каждое правильное срабатывание пальцев фантома будет свидетельствовать о достаточной выраженности направленных на это действие мысленных усилий, открывается перспектива создания на этой основе идеомоторного тренажера мелких движений кисти. В качестве испытуемых-добровольцев были задействованы 21 человек обоих полов в возрасте 18–25 лет. Было показано, что испытуемые действительно уже в первый экспериментальный день приобретали навык управления пальцами фантома руки в контуре ИМК-P300 с надежностью не менее 69 % успешных попыток. При этом основные ошибки управления были связаны с недостаточной концентрацией внимания на сигналах светового маркера целевых пальцев фантома. Сделано предположение, что разработанный комплекс «ИМК-P300 — Фантом кисти» может послужить основой для создания тренажера мелкой моторики кисти.

Ключевые слова: интерфейс мозг–компьютер, ИМК, электроэнцефалограмма, нейрореабилитация, инсульт, вызванные потенциалы, P300

Финансирование: работа выполнена при частичной поддержке Фонда «Сколково», грант № 1110034, и РНФ, грант № 15-19-20053.

✉ **Для корреспонденции:** Александр Яковлевич Каплан
117234, г. Москва, ул. Ленинские горы, д. 1, стр. 12; akaplan@mail.ru

Статья поступила: 11.04.2016 **Статья принята к печати:** 15.04.2016

Including the elements of mental practice into rehabilitation programs for patients with impaired motor skills after stroke or neurological trauma is becoming a new trend in modern neurorehabilitation [1-4]. This approach is based on Nikolai Bernstein's concept according to which creating a mental plan for executing the motor act rather than performing the act itself would be a true response to the tasks set by the environment. [5]. Such activity boosts neural plasticity processes that drive restoration of neuronal pools for motor control [6, 7]. Motor imagery that triggers restructuring of the motor act plan in

neuronal networks can be as effective for the restoration of impaired motor coordination as the actual execution of the movement [1, 3, 4]. Indeed, the studies based on transcranial magnetic stimulation used to test cortical excitability demonstrated the activation of cortical structures associated with motor representation during motor imagery [8, 9].

However, despite the seeming simplicity of motor imagery, whether it is effective in triggering cortical restructuring depends on mental effort intensity, stability and direction [10, 11]. Yet, an individual needs a feedback on motor imagery quality, otherwise his or her mental effort will weaken if repeated multiple times, motor images will fade, and he or she will gradually lose interest in the training procedure. The feedback loop can be provided by brain-computer interface (BCI) technologies that make use of mu-rhythm depression recorded by EEG to detect mental representations of movements and thansform those events into commands for controlling virtual reality objects or real objects [2,9,10,12]. Thus, the operator's mental effort shaped as movement representation can be translated into the actions of physical objects or virtual objects on the screen via BCI. Given a person is motivated, his or her motor imagery skills can develop sufficient intensity and sustainability over time. Using such skills during training sessions is an effective trigger for adaptive plasticity processes in the corresponding brain structures [1, 9, 12].

The weakness of this approach is the extremely low level of differentiation of mental movement representations in relation to their subsequent BCI-based identification. Only 2 to 3 motor images can be reliably (with 0.6-0.7 probability) identified by motor imagery based BCIs. Usually, those are left or right arm/leg movements [10, 12]. It is insufficient for establishing several feedback channels for mental rehearsal of fine motor skills, such as movements of individual fingers, which are the hardest to restore.

At the same time, there is a BCI technology that makes use of reliable EEG-based detection of human focus of attention on external screen characters and provides for a library of no less than 36 commands [13]. Detection of the attention focus is based on EEG responses to short flashes of external objects, such as symbols on the screen; response to a target stimulus is identified on the basis of specific response parameters, a P300 wave in particular [1, 14, 15]. Still, due to the necessity of using a stimulus medium formed by symbols, application of BCI-P300 in rehabilitation could be reduced to communicators, such as for text entry in patients with severe motor and speech impairment, and for activation of remote control buttons [16].

In this work we test the hypothesis that BCI-P300 can be used non-conventionally, namely, as a basis for a training simulator for improving fine motor skills (of fingers) with a multichannel feedback. In such a simulator, the anthropomorphic hand phantom with movable fingers can be used as an actuator. We speculate that using a BCI-P300 system proposed in this work, an individual will be able to control phantom finger flexion by focusing his or her attention on the fingers.

The onset of finger movement will indicate sufficient intensity of mental effort aimed at focusing attention on the process.

METHODS

The study enrolled 12 right-handed volunteers (6 male and 15 female, 18–25 years of age) with normal or corrected-to-normal vision. The study was approved by Bioethics Committee of Lomonosov Moscow State University. All participants gave written informed consent. The subjects were seated in a comfortable armchair, arms on armrests. Above the right arm of the subject covered with non-transparent fabric, the anthropomorphic hand was placed, its movable fingers were connected to servo-motors by flexible cords. Light markers (light-emitting diodes) were attached to the distal phalanx of each phantom finger, light intensity being 5 cd/m2. Turning them on and off was a visual stimulus for event-related potentials (ERPs) recorded by EEG.

For unipolar EEG recording, 8 electrodes (Cz, Pz, PO3, PO4, PO7, PO8, O1, O2), the referential indifferent ear electrode and the Ground Electrode in Fpz position were used. To record biopotentials, NVX52 electroencephalograph (MKS, Russia) was set up to a sampling frequency of 500 Hz, a passband of 0.1-30 Hz (second order Butterworth filter), a band-reject filter of 50 Hz

To identify ERPs associated with target stimuli, i.e., flashes of the light markers on the phantom finger that the subject's attention was focused on, a classifier based on Fisher's linear discriminant analysis (LDA) was used; its output was transformed into a finger-flexion command for the phantom if the preset threshold was exceeded. The classifier analyzed short intervals of 10 ms long that the 0-800 ms EEG signal was split into (0-800 ms is time from stimulus presentation). Commands for stimuli and servomotors activation were executed by phantom hand components, namely, two programmed microcomputers Freeduino Nano v5ATmega328 (Russia). Both microcomputers were connected to the computer via USB ports. The phantom was connected to NVX52 amplifier for EEG recording, which facilitated synchronized ERP recording, their processing by the classifier and command generation.

During the experimental session, a randomized sequence of ten flashes on each phantom finger was presented to the subject to implement one command, i.e., to flex one phantom finger that the subject's attention was drawn to by flashes. Each command was preceded by instructing the subject on what phantom finger had to be chosen. Light-emitting diodes were on for 50 ms; the interval between the stimuli was 150 ms. Every subject had 20 experimental sessions spaced by small breaks; their results were used to assess how effectively the subject operated the hand phantom.

The classifier was trained right before the experimental session on non-random sampling sets of target and non-target ERPs. The procedure lasted for 4 min.

To estimate which operating mode was the most effective for attention focus control, two types of signals were tested, with subject's attention focused on flash offset and flash onset. In both cases the length of the signal was set to 50 ms.

To assess how effectively the phantom fingers were operated, control accuracy was measured by the number of right, wrong or zero phantom finger flexions resulting from the subject focusing the attention on a certain phantom finger. Statistical analysis of data obtained from all subjects was carried out using Stasoft Statistica 7.0 software. To estimate the difference in the effectiveness of both operating modes Wilcoxon sign ranked test was used.

RESULTS

Fig.1 shows statistical data on subjects' performance accuracy during the procedure of selecting a target phantom finger for its further flexion by shifting the focus of attention to it. The data are presented as a percentage of the total number of trials. The accuracy rates of control of phantom fingers were averaged across the groups for various operating modes (using

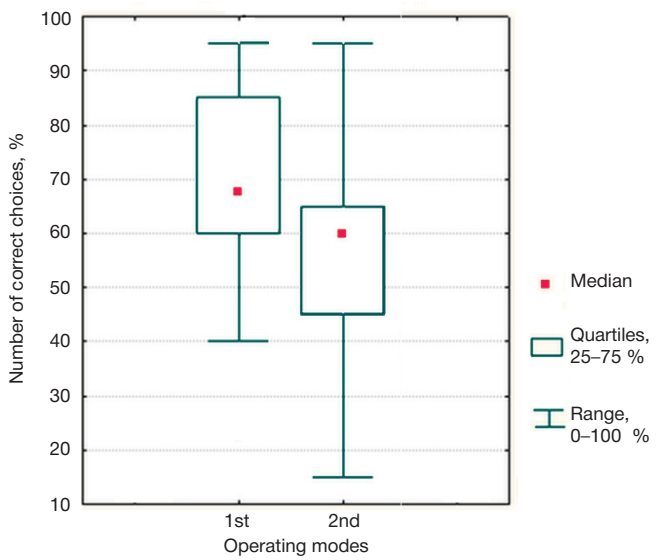

Fig. 1. Accuracy of phantom finger control in two BCI operating modes

In the first and second operating modes, the stimuli used were flashing events onset and offset, respectively.

flash onset and offset as stimuli). The results did not show any statistical difference and were 69 % and 57 % , respectively, with maximal control accuracy being 95 % for some subjects in both modes. The range of accuracy scores for each subject in the second mode was substantially wider than in the first mode. It leads us to conclude that using BCI-P300 technology with light markers placed on phantom fingers controlled via BCI can be seen as a basis for developing a neurosimulator for fine motor skills, with a customized set-up of light signaling for each operating mode.

As shown in fig. 1, the subjects could not issue a command to flex the target finger by shifting their attention to the light marker placed on the phantom hand even in the optimal operating mode. In case of errors, either a non-target finger is flexed or no movement occurs; therefore, analysis of errors of both types was carried out; its results are presented in fig. 2. Scores are presented as absolute values of the number of errors of both types that occurred during 20 attempts to initiate target finger flexion. It should be reminded that each trial could result in one right and five wrong responses (four non-target finger responses and one zero movement response).

As shown in fig. 2, subjects rarely failed to select the target finger for flexion. In average, there were no more than 1.5 errors in 20 trials. But in a greater number of cases (5–6 depending on the operating mode), subjects failed to initiate flexion of any finger leaving the phantom hand motionless. Wilcoxon test showed significant differences ($p < 0.05$) between the number of type 1 and type 2 errors for each operating mode.

Initiating a non-target finger movement is possibly related to the weak sustained attention; attention is drawn to the non-target finger, and the latter is wrongly detected as a flexion target. At the same time, the absence of commands for phantom fingers on completing another attempt to activate the target finger indicates insufficient attention focus on flashing events. As a result, no distinct ERPs are generated in response to target stimuli, and classifier output does not reach the threshold value for command issue.

DISCUSSION

The obtained data confirmed that it is possible to design a BCI-P300 – Phantom Hand system, in which an individual can control flexion of phantom fingers by voluntarily focusing his or her attention on them. Because flexion of a finger that an individual selects in his mind indicates the sufficient intensity of his mental effort to focus his attention on triggering the movement, development of the effective training simulator for fine motor skills that makes use of this technology is highly possible.

However, up to now no attempts to use a BCI-P300 technology for feedback in motor function training have been reported. It is probably due to the fact that the operator does not need to perform motor imagery or his attention is shifted to external objects

However, since pivotal works of Botvinnik and Cohen [17] were published, their findings confirmed multiple times thereafter [18,19], it has been known that under certain conditions the external object, such as a rubber hand, can be easily and reliably identified with the internal representation of one's own hand. Moreover, there is no need to imagine the movement of one's own hand to activate the neurons in the motor cortex, it is enough to watch the hand of the other person or its artificial replica move [20, 21]. Coupled with the data obtained in this work confirming the possibility of using the BCI-P300 technology for controlling individual fingers of the hand phantom, the facts mentioned above hold promise for creating a fine motor skills training neurosimulator based on the BCI-P300 — Phantom Hand system.

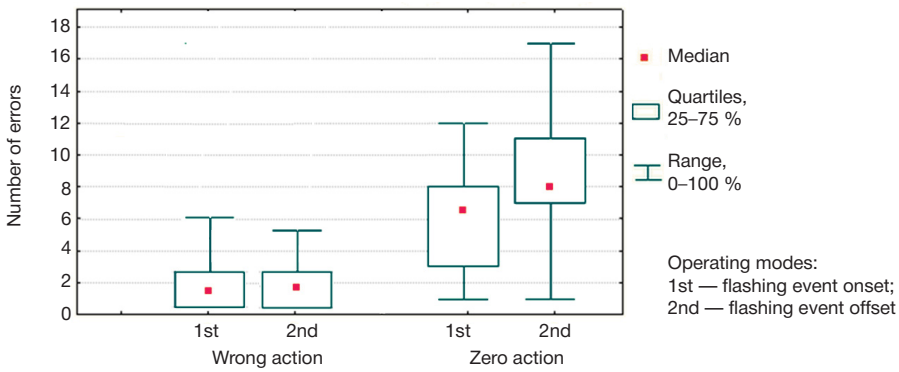

Fig. 2. Number of type 1 and type 2 errors in both operating modes with subjects attempting to issue a command to flex the target finger by focusing their attention on the light marker

Statistically significant difference (Wilcoxon test, $p<0.05$) was observed when comparing averaged type 1 and type 2 errors for each operating mode.

CONCLUSIONS

The BCI-P300 technology can be used to generate commands for mental control of fingers of the human hand phantom with reliability of no less than 69 %, which is sufficient to develop a fine motor skills neurosimulator.

The majority of the BCI-P300 operator's errors in controlling the fingers of the human hand phantom are associated with insufficient focus on the signals of the light markers placed on phantom fingers, which necessitates the improvement of the stimulus medium.

References

1. Kaplan AYa. Nerofiziologicheskie osnovaniya i prakticheskie realizatsii tehnologii mozg-mashinnykh interfeisov v nevrologicheskoi reabilitatsii. Hum Physiol. 2016; 42 (1): 118–27. Russian.
2. Mokienko OA, Chernikova LA, Frolov AA, Bobrov PD. [Motor imagery and its practical application]. Zh Vyssh Nerv Deiat Im I P Pavlova. 2013 Mar–Apr; 63 (2): 195–204. Russian.
3. Park J, Lee N, Cho M, Kim D, Yang Y. Effects of mental practice on stroke patients' upper extremity function and daily activity performance. J Phys Ther Sci. 2015 Apr; 27 (4): 1075–7.
4. Kho AY, Liu KP, Chung RC. Meta-analysis on the effect of mental imagery on motor recovery of the hemiplegic upper extremity function. Aust Occup Ther J. 2014 Apr; 61 (2): 38–48.
5. Bernshtein NA. Fiziologiya dvizhenii i aktivnost'. Gazenko OG, editor. Moscow: Nauka; 1990. 494 p. Russian.
6. Skvortsova VI, Krylov VV. Gemorragicheskii insul't: Prakticheskoe rukovodstvo. Moscow: GEOTAR-Media; 2005. 160 p. Russian.
7. Hara Y. Brain plasticity and rehabilitation in stroke patients. J Nippon Med Sch. 2015; 82 (1): 4–13.
8. Mokienko OA, Chervyakov AV, Kulikova SN, Bobrov PD, Chernikova LA, Frolov AA, et al. Increased motor cortex excitability during motor imagery in brain-computer interface trained subjects. Front Comput Neurosci. 2013 Nov 22; 7: 168.
9. Yuan H, He B. Brain-computer interfaces using sensorimotor rhythms: current state and future perspectives. IEEE Trans Biomed Eng. 2014 May; 61 (5): 1425–35.
10. Vasil'ev AN, Liburkina SP, Kaplan AYa. Lateralizatsiya patternov EEG u cheloveka pri predstavlenii dvizhenii rukami v interfeise mozg–komp'yuter. Zh Vyssh Nerv Deiat Im I P Pavlova. 2016; 66 (3): 1–11. Russian.
11. Machado S, Lattari E, de Sá AS, Rocha NB, Yuan TF, Paes F, et al. Is mental practice an effective adjunct therapeutic strategy for upper limb motor restoration after stroke? A systematic review and meta-analysis. CNS Neurol Disord Drug Targets. 2015; 14 (5): 567–75.
12. Frolov AA, Biryukova EV, Bobrov PD, Mokienko OA, Platonov AK, Pryanichnikov VE, et al. Printsipy neiroreabilitatsii, osnovannye na ispol'zovanii interfeisa "mozg-komp'yuter" i biologicheski adekvatnogo upravleniya ekzoskeletonom. Hum Physiol. 2013; 39 (2): 99–105. Russian.
13. Powers JC, Bieliaieva K, Wu S, Nam CS. The Human Factors and Ergonomics of P300-Based Brain-Computer Interfaces. Brain Sci. 2015 Aug 10; 5 (3): 318–56.
14. Bamdad M, Zarshenas H, Auais MA. Application of BCI systems in neurorehabilitation: a scoping review. Disabil Rehabil Assist Technol. 2015; 10 (5): 355–64.
15. Kaplan AY, Shishkin SL, Ganin IP, Basyul IA, Zhigalov AY. Adapting the P300-based brain-computer interface for gaming: a review. IEEE Trans Comput Intell AI Games (Special Issue on Brain/Neuronal-Computer Games Interfaces and Interaction). 2013; 5 (2): 141–9.
16. Cipresso P, Carelli L, Solca F, Meazzi D, Meriggi P, Poletti B, et al. The use of P300-based BCIs in amyotrophic lateral sclerosis: from augmentative and alternative communication to cognitive assessment. Brain Behav. 2012 Jul; 2 (4): 479–98.
17. Botvinick M, Cohen J. Rubber hands 'feel' touch that eyes see. Nature. 1998 Feb 19; 391 (6669): 756.
18. Kammers MP, de Vignemont F, Verhagen L, Dijkerman HC. The rubber hand illusion in action. Neuropsychologia. 2009 Jan; 47 (1): 204–11.
19. Kalckert A, Ehrsson HH. The moving rubber hand illusion revisited: comparing movements and visuotactile stimulation to induce illusory ownership. Conscious Cogn. 2014 May; 26: 117–32.
20. Rizzolatti G, Fogassi L, Gallese V. Neurophysiological mechanisms underlying the understanding and imitation of action. Nat Rev Neurosci. 2001 Sep; 2 (9): 661–70.
21. Gatti R, Tettamanti A, Gough PM, Riboldi E, Marinoni L, Buccino G. Action observation versus motor imagery in learning a complex motor task: a short review of literature and a kinematics study. Neurosci Lett. 2013 Apr 12; 540: 37–42.

Литература

1. Каплан А. Я. Нерофизиологические основания и практические реализации технологии мозг-машинных интерфейсов в неврологической реабилитации. Физиол. чел. 2016; 42 (1): 118–27.
2. Мокиенко О. А., Черникова Л. А., Фролов А. А., Бобров П. Д. Воображение движения и его практическое применение. Журн. высш. нервн. деят. 2013. 63 (2): 195–204.
3. Park J, Lee N, Cho M, Kim D, Yang Y. Effects of mental practice on stroke patients' upper extremity function and daily activity performance. J Phys Ther Sci. 2015 Apr; 27 (4): 1075–7.
4. Kho AY, Liu KP, Chung RC. Meta-analysis on the effect of mental imagery on motor recovery of the hemiplegic upper extremity function. Aust Occup Ther J. 2014 Apr; 61 (2): 38–48.
5. Бернштейн Н. А. Физиология движений и активность. Газенко О. Г., редактор. М.: Наука; 1990. 494 с.
6. Скворцова В. И., Крылов В. В. Геморрагический инсульт: Практическое руководство. М: ГЭОТАР-Медиа; 2005. 160 с.
7. Hara Y. Brain plasticity and rehabilitation in stroke patients J Nippon Med Sch. 2015; 82 (1): 4–13.
8. Mokienko OA, Chervyakov AV, Kulikova SN, Bobrov PD, Chernikova LA, Frolov AA, et al. Increased motor cortex excitability during motor imagery in brain-computer interface trained subjects. Front Comput Neurosci. 2013 Nov 22; 7: 168.
9. Yuan H, He B. Brain-computer interfaces using sensorimotor rhythms: current state and future perspectives. IEEE Trans Biomed Eng. 2014 May; 61 (5): 1425–35.
10. Васильев А. Н., Либуркина С. П., Каплан А. Я. Латерализация паттернов ЭЭГ у человека при представлении движений руками в интерфейсе мозг–компьютер. Журн. высш. нервн. деят. 2016; 66 (3): 1–11.
11. Machado S, Lattari E, de Sá AS, Rocha NB, Yuan TF, Paes F, et al. Is mental practice an effective adjunct therapeutic strategy for upper limb motor restoration after stroke? A systematic review and meta-analysis. CNS Neurol Disord Drug Targets. 2015; 14 (5): 567–75.
12. Фролов А. А., Бирюкова Е. В., Бобров П. Д., Мокиенко О. А., Платонов А. К., Пряничников В. Е. и др. Принципы нейрореабилитации, основанные на использовании интерфейса «мозг–компьютер» и биологически адекватного управления экзоскелетоном. Физиол. чел. 2013; 39 (2): 99–105.
13. Powers JC, Bieliaieva K, Wu S, Nam CS. The Human Factors and Ergonomics of P300-Based Brain-Computer Interfaces. Brain Sci. 2015 Aug 10; 5 (3): 318–56.
14. Bamdad M, Zarshenas H, Auais MA. Application of BCI systems

in neurorehabilitation: a scoping review. Disabil Rehabil Assist Technol. 2015; 10 (5): 355–64.
15. Kaplan AY, Shishkin SL, Ganin IP, Basyul IA, Zhigalov AY. Adapting the P300-based brain-computer interface for gaming: a review. IEEE Trans Comput Intell AI Games (Special Issue on Brain/Neuronal-Computer Games Interfaces and Interaction). 2013; 5 (2): 141–9.
16. Cipresso P, Carelli L, Solca F, Meazzi D, Meriggi P, Poletti B, et al. The use of P300-based BCIs in amyotrophic lateral sclerosis: from augmentative and alternative communication to cognitive assessment. Brain Behav. 2012 Jul; 2 (4): 479–98.
17. Botvinick M, Cohen J. Rubber hands 'feel' touch that eyes see. Nature. 1998 Feb 19; 391 (6669): 756.
18. Kammers MP, de Vignemont F, Verhagen L, Dijkerman HC. The rubber hand illusion in action. Neuropsychologia. 2009 Jan; 47 (1): 204–11.
19. Kalckert A, Ehrsson HH. The moving rubber hand illusion revisited: comparing movements and visuotactile stimulation to induce illusory ownership. Conscious Cogn. 2014 May; 26: 117–32.
20. Rizzolatti G, Fogassi L, Gallese V. Neurophysiological mechanisms underlying the understanding and imitation of action. Nat Rev Neurosci. 2001 Sep; 2 (9): 661–70.
21. Gatti R, Tettamanti A, Gough PM, Riboldi E, Marinoni L, Buccino G. Action observation versus motor imagery in learning a complex motor task: a short review of literature and a kinematics study. Neurosci Lett. 2013 Apr 12; 540: 37–42.

DEVELOPMENT OF A NEURODEVICE WITH A BIOLOGICAL FEEDBACK FOR COMPENSATING FOR LOST MOTOR FUNCTIONS

Bogdanov EA[1]✉, Petrov VA[1], Botman SA[1], Sapunov VV[1], Stupin VA[2], Silina EV[3], Sinelnikova TG[3], Patrushev MV[1], Shusharina NN[1]

[1] Institute of Chemistry and Biology,
Immanuel Kant Baltic Federal University, Kaliningrad, Russia

[2] Department of Hospital Surgery no.1, Faculty of General Medicine,
Pirogov Russian National Research Medical University, Moscow, Russia

[3] Department of Human Pathology, Faculty of Postgraduate Professional Training of Physicians,
The First Sechenov Moscow State Medical University, Moscow

Concurrent use of electrophysiological signals of various types, such as obtained from electroencephalogram (EEG), electromyogram (EMG), electrooculogram (EOG), and others, increases the effectiveness of systems for external device control, namely, neural prostheses, exoskeletons, robotic wheelchairs and teleoperated robots. This article presents the results of the first tests of a multifunctional neurodevice capable of detecting EEG, EMG and EOG signals simultaneously (with EOG signals, photoplethysmogram, SpO2 and temperature modules of the neurodevice were used). Measurement results were then compared to the data obtained from KARDi3 device (Medical Computer Systems, Russia) and Fluke 17b multimeter with a plug-in thermistor (Fluke Corporation, USA). The informative value and accuracy of both datasets were comparable. We also studied the effectiveness of EEG and EMG signal hybridization on the basis of the neurodevice of interest; it allowed for an increase of classification accuracy in all subjects by an average of 12.5 % up to the mean of 86.8 % (from 75 to 97 %).

Keywords: neurodevice, exoskeleton, brain-computer interface, electroencephalogram, electromyogram, electrooculogram, biological feedback

Funding: the work was supported by the Ministry of Education and Science of the Russian Federation (Grant Agreement no. RFMEFI57815X0140 dated October 27, 2015).

Acknowledgements: the authors thank Alexandr Romanov of the Rehabilitation Center of the Administrative Department of the President of the Russian Federation, Moscow; Raphael Oganov of State Research Center for Preventive Medicine, Moscow; Daniil Borchevkin, Alexey Belousov, Vladimir Savinov, Sergey Sokolov, and Alexey Medvedev for their scientific contribution and productive collaboration.

✉ **Correspondence should be addressed:** Evgeny Bogdanov
ul. A. Nevskogo, d. 14, Kaliningrad, Russia, 236041; eubogdanov@gmail.com

Received: 31.03.2016 **Accepted:** 07.04.2016

РАЗРАБОТКА НЕЙРОУСТРОЙСТВА С БИОЛОГИЧЕСКОЙ ОБРАТНОЙ СВЯЗЬЮ ДЛЯ ВОСПОЛНЕНИЯ УТРАЧЕННЫХ ДВИГАТЕЛЬНЫХ ФУНКЦИЙ

Е. А. Богданов[1]✉, В. А. Петров[1], С. А. Ботман[1], В. В. Сапунов[1], В. А. Ступин[2], Е. В. Силина[3], Т. Г. Синельникова[3], М. В. Патрушев[1], Н. Н. Шушарина[1]

[1] Химико-биологический институт,
Балтийский федеральный университет имени Иммануила Канта, Калининград

[2] Кафедра госпитальной хирургии № 1, лечебный факультет,
Российский национальный исследовательский медицинский университет имени Н. И. Пирогова, Москва

[3] Кафедра патологии человека, Институт профессионального образования,
Первый Московский государственный медицинский университет имени И. М. Сеченова, Москва

Одновременное использование электрофизиологических сигналов нескольких типов (данных электроэнцефалограммы (ЭЭГ), электромиограммы (ЭМГ), электроокулограммы (ЭОГ) и др.) обеспечивает более высокую эффективность систем управления внешними устройствами — нейропротезами, экзоскелетами, роботизированными инвалидными креслами и телеуправляемыми роботами. В статье представлены результаты первых испытаний многофункционального нейроустройства, способного распознавать одновременно ЭЭГ-, ЭМГ- и ЭОГ-сигналы (последние — с подключением модулей фотоплетизмограммы, SpO2 и температуры). Результаты измерений сигналов с помощью разработки сравнивали с данными прибора KARDi3 («Медицинские компьютерные системы», Россия) и мультиметра Fluke 17b с подключаемым термистором (Fluke Corporation, США). По информативности и точности данные были сопоставимы. Также исследовали эффективность гибридизации ЭЭГ- и ЭМГ-сигналов с помощью нейроустройства: она позволила увеличить точность классификации у всех испытуемых в среднем на 12,5 % — до среднего значения 86,8 % (от 75 до 97 %).

Ключевые слова: нейроустройство, экзоскелет, интерфейс мозг–компьютер, электроэнцефалограмма, электромиограмма, электроокулограмма, биологическая обратная связь

Финансирование: работа выполнена при поддержке Министерства образования и науки Российской Федерации (Соглашение о предоставлении субсидии от 27.10.2015 № RFMEFI57815X0140).

Благодарности: авторы благодарят Александра Романова из Центра реабилитации Управления делами Президента РФ (Москва), Рафаэля Оганова из Государственного научно-исследовательского центра профилактической медицины (Москва), Даниила Борчевкина, Алексей Белоусова, Владимира Савинова, Сергея Соколова и Алексея Медведева за плодотворное научное сотрудничество и вклад в работу.

✉ **Для корреспонденции:** Евгений Анатольевич Богданов
236041, г. Калининград, ул. А. Невского, д. 14; eubogdanov@gmail.com

Статья получена: 31.03.2016 **Статья принята к печати:** 07.04.2016

Applied biorobotics improves the quality of life in patients with neurological disorders and traumas. Neuroprostheses, exoskeletons, robotic wheelchairs and telecontrol robots contribute to rehabilitation of patients, substitute for lost functions and enhance physical abilities of healthy people.

Choosing the right control scheme is very important for the development of such devices. It must ensure the accuracy, stability and safety of the device performance, given that the device will be used continuously. The majority of existing solutions are based on recording human body biopotentials using electromyography (EMG), electroencephalography (EEG), electrooculography (EOG) and electrocardiography (ECG) [1–6].

Robotic wheelchairs, prostheses and exoskeletons are good examples of the effectiveness of EMG-based schemes [7–9]. However, EMG alone is not enough if an individual who had a stroke or a spinal cord injury cannot generate a muscle signal of the required intensity. In such cases we turn to brain-computer interfaces (BCIs) that transform signals from damaged brain areas into commands for external devices. One of the recent works [10] has demonstrated a high effectiveness of a BCI for neuroprosthesis control tested by a tetraplegic patient with intact sensory and cognitive functions.

Among various methods of brain signals recording, EEG is the most convenient due to its availability, safety, cost-effectiveness and portability. The brain cortex consists of multiple areas of functional specialization in which waves of different frequency are observed [11]. The EEG spectrum is unique for every individual and changes constantly depending on a person's physiological condition and the activity performed, as long-term measurements have proved [12] By decoding EEG signals, we can discriminate between limb movements quite accurately. For example, the algorithm proposed for the reconstruction of the trajectory of finger joint angles during reach to grasp movements ensured 76 % accuracy of EEG signal [13]. Another work showed that it was possible to correctly identify one out of five actual or imaginary movements of the wrist and fingers with 65–71 % accuracy [14].

For better classification accuracy,a large number of EEG channels is thought to be necessary. However, Yang et al. [15] were able to remove irrelevant noise and improve the EEG signal classification technique that can be applied to a neural network or used for robotic device control. EEG was recorded with only 6 channels out of 32; still, the classification accuracy reached 86 % in some motor tasks. However, EEG-based BCIs have certain drawbacks resulting from incorrect electrode placement, shifting of electrodes, noises, artifacts, imperfect algorithms of filtration and signal processing.

Some researchers suggested that EMG and EEG methods should be fused [16–18]. For example, in case of paresis or limb loss, EEG signals can be used to compensate for weak EMG signals, ensuring that a prosthesis or exoskeleton is moved by mental effort. If EMG signals are of normal intensity, EEG signals can help reduce the impact of tremor, fatigue or artifacts.

Leeb et al. [19] proposed a hybrid EEG-EMG-based control system; it was tested on 6 healthy individuals. The subjects moved their left or right arm for 5 seconds (there were 60 trials in total). Brain activity was recorded by 16 sensors placed in accordance with the international 10–20 system. Muscular activity was recorded over left and right forearm flexors and extensors. The obtained EMG signals were rectified and averaged (0.3 s) to get the envelopes. The data from two classifiers were fused together to get one control signal. The hybrid system showed high classification accuracy in all subjects. Despite the fact that EMG signals were quite informative (classification accuracy was 83 % in average), the hybrid approach was more effective (classification accuracy was 91 %), especially in case of increasing muscle fatigue.

Xie et al. also developed a hybrid EEG-EMG-based BCI (visualization of movement intention) [20]. Their study enrolled 10 post stroke patients with non-severe hemiparesis, 10 patients with peripheral nerve injury and 10 healthy individuals. All patients were between 20 and 58 years of age. For calibration, subjects were asked to lie on the bed and perform knee flexion and extension tasks. The sensor measured the angle and the force of movements; the obtained data were later used as target levels. Then EEG/EMG sensors were attached, and the experiment was carried out. The aim of the experiment was to establish the correlation between EEG/EMG signals and leg movements and to measure the accuracy of potential control commands for the external device. First, EEG data were processed followed by EMG data processing; in the third experiment the hybrid approach was applied. The results showed that the hybrid approach led to increased classification accuracy in all groups of subjects, compared to single modality approach. In healthy individuals, classification accuracy was 98 %, in post stroke patients — 84 %, for patients with peripheral nerve injury — 85 %.

Kiguchi et al. [21] carried out a study of a hybrid EEG-EMG system for controlling arm movements using SUEFUL-7 robotic device, and assessed its effectiveness [22]. The robot was equipped with a video camera and could detect arm position by rotational angle and force sensors. A 16-channel EMG interface for recording signals coming from arms and shoulders was used as a control system. The experiment enrolled four 23-year-old healthy individuals. Some of them wore an exoskeleton and a device for EEG recording and response monitoring. In the first experiment, the subjects performed arm flexion/extension tasks, and the robot did the opposite impeding the movement. In the second experiment, one full and two empty cups were put on the table. When the subject grasped the empty cup, the robot used the assistance algorithm that estimated the position of empty cups using the video camera, and randomly selected one of them; after that, the robot assisted the subject in pouring the liquid. The accuracy of choice was assessed using EEG and EMG signals. If the subject did not resist, the robot inferred that the target had been chosen correctly. In that experiment, the flexibility of the robot and its ability to correctly interpret the intentions of the subject were tested. The results showed the increased accuracy of interpretation of human actions by the robot.

BCI performance can be improved by oculography data recorded parallel to EEG. A group of scientists designed a hybrid EEG-EOG-based BCI to enhance the reliability of hand exoskeleton for continuous grasping movements [23]. EEG signals were recorded at 5 EEG sites in accordance with the international 10–20 system. The experiment consisted of two parts. In the first part, the subjects controlled the exoskeleton through EEG signals only; they made grasping movements when the visual indicator appeared (green for the movement onset, red for rest). The robotic hand opened automatically if the commands issued by the operator's brain were not intense enough to get over a preset threshold. In the second part of the experiment, EOG signals were used as a switch. When the subject looked to the left or to the right, the exoskeleton hand opened regardless of EEG signals. The hybrid model increased system safety. When only EEG signals were used, the motion of the robotic hand exceeded 25 % of a full hand closing in half of subjects at rest. The hybrid system showed the increase in

the threshold value in 10.4 % of subjects, with maximal grasp being less than 28 % of a full hand closing (in a single modality system it was 60 %) .

Cardiovascular system performance is usually assessed by monitoring arterial blood pressure and heart rate (HR); it correlates to brain activity, including that, during motor tasks [24–26]. Studies of the effect of changing mental activity on heart activity assessed by EEG show that hybrid EEG-ECG systems are a promising practical tool [27–29]. In the experiment involving 6 healthy right-handed men (mean age was 28 years), who imagined movements of their left leg or left arm, researchers assessed classification accuracy of EEG signals and ECG signals separately; then a fused EEG-ECG recording was processed [29]. For every subject, 180 sessions were held (60 sessions for each assessment method). They consisted of three parts; the subject rested for the first 6 seconds (while, data from previous sessions were processed); then the subject was presented with an indicator that randomly indicated the action that the subject had to perform (arm or leg movement visualization or rest); that part of the experiment lasted for 6 s; finally, there was a pause of unfixed length (up to several seconds). Three EEG channels were recorded (C3, C4, Cz, according to the international 10–20 system) along with ECG, R–R intervals were calculated as a difference between QRS complexes, which show heart rate, filtered at 5–10 Hz frequencies. The obtained data allowed for a few interesting conclusions. First, active visualization of limb movements induced heart rate change. Second, ECG classification accuracy was very high in almost all subjects: in many subjects the use of ECG modality was more effective than EEG. Third, the hybrid approach increased classification accuracy in almost all subjects, especially in those, whose results in a single modality mode were low.

Thus, a hybrid approach to the implementation of systems for external device control is very promising. Considering how fast these technologies are developing, we believe that such high-accuracy neurodevices will appear in the market in the nearest future. The laboratory of Neurobiology and Medical Physics of the Institute of Chemistry and Biology of Immanuel Kant Baltic Federal University is working on a multifunctional neurodevice capable of detecting different electrophysiological signals simultaneously (EEG, EMG, EOG supported by the use of photoplethysmogram, SpO2 and temperature modules), ensuring a biological feedback and transmitting the processed data to exoskeletons and robotic devices in real time. This article presents the results of the first tests of the prototype model of such a neurodevice and assesses the possibility of fused EEG and EMG signal recording based on it.

METHODS

We have implemented a prototype model of electrophysiological and biometrical recorder capable of converting biosignals into commands for an electromechanical device; we have also tested our model in a two-stage experiment. At the first stage, the neurodevice was used to study the motor activity of the subjects by recording electrophysiological signals. For the unbiased assessment of the device performance, the resulting data were compared to the data obtained with analytical devices that had proved to be reliable and are now successfully applied in medical practice. At that stage, 2 healthy men participated in the experiment, (22 and 23 years of age, height of 175 and 177 cm, respectively, weight of 70 and 75 kg). At the second stage, a possibility of fused EEG and EMG recording using the neurodevice was assessed. The experiment enrolled 10 healthy right-handed men aged 22–29 years (mean age was 25 years).

Brain electrical activity was measured by encephalogram via scalp leads; bioelectrical potentials in skeletal muscles were measured by electromyography; bioelectrical potentials related to eye ball movements were measured by oculography; body temperature was measured by thermometry; pulse rate was measured using photoplethysmography. The obtained data were recorded digitally and graphically.

For EEG recording, silver cup electrodes (Ag/AgCl) were used; EEG caps were used to place the electrodes on subjects' heads. For EMG and EOG recording, silver plate electrodes were used. In the experiments aimed at the assessment of physiological signal parameters, the most common artifacts were detected, such as artifacts resulting from bad electrode attachment or electrical noise caused by subject's movements, artifacts caused by upper body muscle tension and forehead wrinkling, muscle potentials, skin potentials, eye blinking, pulse waves.

To study motor activity, the subjects were asked to do physical exercises, including bending and turning the head to the right and left, tilting it down and back, with the prototype model of the neurodevice attached to it. Before the experiment, we had written a program for real-time visual representation of Euler angles rotation.

Results of EEG, EMG and EOG signal recording and pulse rate data were compared to those obtained with KARDi3 device (Medical Computer Systems, Russia), intended for recording and analyzing ECG, EOG, EEG and some other parameters. Measurements were first done with KARDi3, then with the neurodevice of interest. The subject remained in the same position throughout the experiment. The electrodes attached to the body were not moved when switching from KARDi3 to the neurodevice prototype model. To reduce the amount of artifacts, electrode cables were bundled and twisted.

During EEG recording, we focused on alpha-rhythm, which is normally the most stable electrophysiological signal. To record the alpha rhythm, a bipolar lead system was used. Electrodes were attached to the back of the subject's neck, reference electrodes were attached to ear lobes. To achieve the maximal relaxation of neck and head muscles and to reduce myographic artifacts, the subject was seated in the reclined position. In total, 100 trials were conducted. For both the neurodevice prototype model and KARDi3, the same recording mode was used, with a 30 Hz low-pass filter, a 0.5 Hz high-pass filter, a 50 Hz band-reject filter, speed of 30 mm/s (X-axis), sensitivity of 50 mcV/mm (Y-axis).

EOG signals were recorded during the eye movement task. The total number of trials was 100. The subjects were asked to do the following exercises: look at the yellow dot in the center of the board – then up (red circle) – center (yellow dot) – down (blue circle) – center (yellow dot) – left (red cross) – center (yellow dot) – right (blue cross) – center (yellow dot). The subject was seated in front of the board with graphic symbols. To register the signal, a bipolar montage scheme was used. Electrodes were attached to the temples, close to the right eye and on the forehead. For both the neurodevice prototype model and KARDi3, the same recording mode was used, with a 40 Hz low-pass filter, a 1 Hz high-pass filter, a 50 Hz band-reject filter, speed of 15 mm/s (X-axis), sensitivity of 50 mcV/mm (Y-axis).

To record EMG signals during thigh muscles contraction, the subject was asked to move the right leg forward for a step-like movement. There were 100 trials in total. The left leg did not move, the subject did not lean on the right leg on which electrodes were placed. The subject was standing, using his left leg and right arm as points of support; his right leg

with electrodes on it was relaxed. Electrodes were placed 5 cm apart from each other. To record the signal, a referential montage scheme was used. Electrodes were placed over the femoral muscle using adhesive rings. For both the neurodevice prototype model and KARDi3, the same recording mode was used, with a 100 Hz low-pass filter, a 1 Hz high-pass filter, a 50 Hz band-reject filter, speed of 120 mm/s (X-axis), sensitivity of 10 mcV/mm (Y-axis).

To record EEG, EMG and EOG signals using our neurodevice prototype, neurodevice, we have developed original software. To record EEG, EMG and EOG by KARDi3, Neurocortex software by Neurobotics, Russia was used.

To measure the pulse rate the subject was seated. For ECG recording (100 trials in total), KARDi3 electrodes were attached to the wrists by adhesive rings. A referential montage scheme was used. Then, the subject put his finger on the photoplethysmogram module of the neurodevice, the output being the pulse-related signal. Pulse measurement was supported by pulse oximetry (SpO2). The following recording mode was chosen for both the neurodevice and KARDi3: a 0.1 Hz low-pass filter, a 50 Hz high-pass filter, a 50 Hz band-reject filter, speed of 60 mm/s (X-axis), sensitivity of 20 mcV/mm (Y-axis). To process data obtained with KARDi3, Neocortex software was used; to process data obtained with the neurodevice, Heart Rate Monitor Demo software was used (Silicon Labs, USA).

To compare temperature measurement accuracy, Fluke 17b multimeter with a plug-in thermistor was used. The temperature sensor was attached to the subject's forehead by the adhesive ring. The total number of trials was 136. Temperature data were transmitted to the PC via Blootooth protocol every second.

At the second stage of the experiment, a possibility of EEG and EMG fused recording by the neurodevice of interest was studied to ensure its good performance in a complex with robotic devices, such as an exoskeleton.

The subjects were instructed to imagine their left leg movements and then to flex and extend the thigh (10 sessions for every participant). Classification accuracy was first assessed for EMG signals only and then for a hybrid EMG-EEG system.

Physiological parameters were continuously monitored during motor tasks and idle periods (5 s long). Fisher linear discriminant analysis was used for classification.

STUDY RESULTS

We studied motor activity involved in performing such tasks as turning and bending the head to the right or left, tilting it down and back. The results demonstrate high accuracy and precision of the data obtained with the motor sensor of the studied neurodevice. The diagram in fig. 1 shows Euler angles rotation (X-axis represents time, Y-axis represents angle): 1) pitch is rotation around the transverse axis (green line); 2) roll is rotation around the longitudinal axis (blue line); 3) yaw is rotation around the vertical axis (red line).

EEG data obtained with the studied neurodevice showed the same artifacts as EEG data obtained with KARDi3, and their amounts were comparable. It indicates that the studied neurodevice could compete with similar tools for EEG recording. Muscular activity artifacts were associated with small neck and head movements resulting from subject's fatigue. Quite a few encephalograms showed traces of cardiogram artifacts, which is possibly related to the individual specifics of the subject's cardiovascular system and the placement of electrodes over subcutaneous blood arteries.

EOG data obtained with the neurodevice were comparable to the data obtained with KARDi3 in their informative value; in case of our neurodevice, the amount of artifacts was lower. The most common artifact was eye blinking, which appeared on EOG as a sharp amplitude increase; artifacts of mimic muscles that accompanied the subject's growing fatigue were also present.

During EMG signal quality assessment, it was found that the data obtained with our neurodevuce were as informative as the data obtained with KARDi3. No artifacts were detected.

The results of temperature measurements obtained with the neurodevice were comparable to the data from Fluke 17b reference device. In average, temperature variance was 0.3%.

Pulse signal was obtained from the electrocardiogram recorded with KARDi3 and the neurodevice photoplethysmogram module. ECG R–R interval data from KARDi3 showed the same pulse values as data from the photoplethysmogram module. The mean HR in the first subject was 78 and 77 beats per minute (measured with KARDi3 and the neurodevice, respectively). The mean HR in the second subject was 72 and 71 beats per minute (measured with KARDi3 and the neurodevice, respectively). No artifacts that could affect the result were observed (fig. 2).

It is worth mentioning that the module for the assessment of cardiovascular system performance estimates blood oxygen saturation, thus providing some valuable data that can be used for exoskeleton control.

Our study of EEG and MG signal hybridization yielded results that support the idea electrophysiological signal fusion approach. The experiment showed that mean classification accuracy of EMG signals was 74.3 %. EMG-EEG hybridization led to the increased classification accuracy by an average of 12.5 % with a mean of 86.8 % (75–97 %) in all subjects. The results are presented in the table below.

DISCUSSION

It is obvious that development of a high-accuracy multifunctional neurodevice that allows for continuous recording of physiological signals and transmits data to the external device (exoskeleton) can yield very inspiring results. We have carried out a truly multidisciplinary study, at the first stage of which a prototype model of such a neurodevice was created and tested. It was demonstrated that the signals obtained with our device were identical to those obtained with reliable analytical tools.

During some motor activity measurement procedures, gyroscope drift was observed associated with a changing magnetic field generated by the accumulator battery. It was

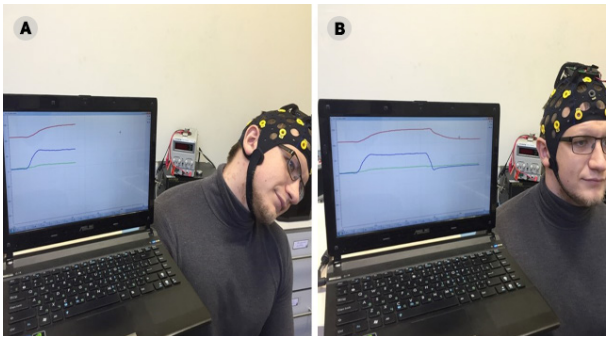

Fig. 1. Euler angles rotation during head exercises. **(A)** Head is bent to the left. **(B)** Head is back to the initial position (the yaw and roll angles change, the pitch angle remains unchanged, gyroscope returns to the initial position)

the result of the relatively weak attachment of the accumulator to the model; rigid fixation of the accumulator helped to solve the issue. With weak attachment of the model to the subject's body, a simultaneous change of two angles was observed occasionally when the subject was performing a task. It can be explained by the "multilayered" scheme used in the experiment: gyroscope components were placed on the motor module, and the motor module was placed on the subject's head. Steady movements of the subject's head also made their contribution. We will consider it in the fabrication of the experimental sample and will use software and hardware automatic calibration of the device position with respect to the subject's position The main motor activity parameters measured by the experimental sample that we plan to fabricate will be linear acceleration of the accelerometer, angular acceleration of the gyroscope and a magnetic field vector of a magnetometer. EMG and EOG muscular artifacts will be removed using additional band-reject filters or special software. Cardiogram artifacts can be removed by changing electrode attachment mode from stationary to dynamic, with a possibility to shift electrodes by no less than 10 mm. Thus, the electrode can be moved if it has been placed over an artery. Besides, improving accessories for electrode attachment will also reduce the amount of artifacts.

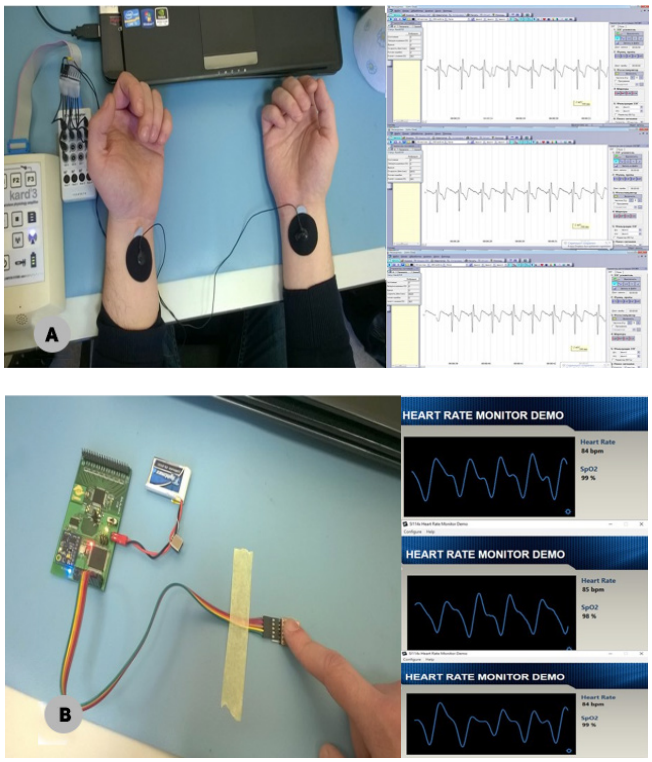

Fig. 2. Studying heart activity. **(A)** Electrode placement and ECG data obtained with KARDi3. **(B)** Electrode placement for photoplethysmogram and SpO2 analysis using the prototype model of the neurodevice

The results of EEG-EMG fusion experiment showed the considerable advantage of hybrid BCIs over single-modality BCIs and confirmed the feasibility of simultaneous recording of various physiological signals [19–21, 23, 29]. Due to the increased classification accuracy and flexibility, a hybrid system is more reliable and exhibits higher performance. The obtained results lead us to conclude that fused EEG-EMG recording improves the interpretation of intended and actual physical activity. EEG signals unrelated to muscular activity are an additional identification tool that can be used in robotics. We speculate that improvements to the system and simultaneous use of various physiological signals will result in almost 100 % classification accuracy.

By now, very few works describing such experiments have been published. All of them are non-representative with respect to the number of participants. To increase signal classification accuracy and safety of robotic devices, further research is necessary. Still, certain difficulties remain. First, electrode shifting is a problem, because the correct placement of electrodes is what defines intensity, quality and reproducibility of signals. With respect to that, non-contact technologies can be a solution. Second, complex movements involving several muscles (hand, forearm, shoulder girdle and trunk muscles) are generated by a large number of motor cortex areas, and the size of each area is unique for every person, which impedes reconstruction of complex movements. To solve this problem, new technologies capable of isolating target movements from unrelated ones are necessary. Some solutions have been proposed so far, including invasive interfaces based on electrocorticography [30, 31].

CONCLUSIONS

The tests of the neurodevice prototype capable of simultaneous detection of different electrophysiological signals confirmed the feasibility of hybrid approach to the development of systems for external device control. Fusion of several modalities or switching from one to another to select the one that best interprets human intention increases signal classification accuracy and can possibly improve robotic device performance. Further research is necessary with a larger number of participants involved, including those with different pathologies.

EMG and EEG signal classification accuracy in single modality and hybrid approaches, %

Subject	EMG	EMG + EEG	Dynamics
1	84.0	93.0	+ 9.0
2	72.0	84.0	+ 12.0
3	77.0	88.0	+ 11.0
4	92.0	97.0	+ 5.0
5	70.0	93.0	+ 23.0
6	63.0	79.0	+ 16.0
7	69.0	81.0	+ 12.0
8	75.0	90.0	+ 15.0
9	61.0	75.0	+ 14.0
10	80.0	88.0	+ 8.0
Mean	74.3	86.8	+ 15.0

References

1. Singh RM, Chatterji S, Kumar A. Trends and challenges in EMG based control scheme of exoskeleton robots — a review. Int J Sci Eng Res. 2012; 3 (9): 933–40.
2. Artemiadis P. EMG-based robot control interfaces: past, present and future. Adv Robot Autom. 2012, 1 (2): e107.
3. Li G. Electromyography pattern-recognition-based control of powered multifunctional upper-limb prostheses. In: Mizrahi J, editor. Advances in applied electromyography. InTech; 2011. 224 p.
4. Kim Y, Doh NL, Youm Y, Chung WK. Robust discrimination method of the electrooculogram signals for human-computer interaction controlling mobile robot. Intell Autom Soft Comp. 2007; 13 (3): 319–36.
5. Oonishi Y, Oh S, Hori Y. New control method for power-assisted wheelchair based on upper extremity movement using surface myoelectric signal. 2008 10th IEEE International Workshop on Advanced Motion Control. 2008; 498–503.
6. Gu Y, Dremstrup K, Farina D. Single-trial discrimination of type and speed of wrist movements from EEG recordings. Clin Neurophysiol. 2009 Aug; 120 (8): 1596–600.
7. Shenoy P, Miller KJ, Crawford B, Rao RP. Online electromyographic control of a robotic prosthesis. IEEE Trans Biom Eng. 2008 Mar; 55 (3): 1128–35.
8. Kiguchi K, Hayashi Y. An EMG-based control for an upper-limb power-assist exoskeleton robot. IEEE Trans Syst Man Cybern B Cybern. 2012 Aug; 42 (4): 1064–71.
9. Rosen J, Brand M, Fuchs MB, Arcan M. A myosignal-based powered exoskeleton system. IEEE Trans Syst Man Cybern A Syst Hum. 2001; 31 (3): 210–22.
10. Collinger JL, Wodlinger B, Downey JE, Wang W, Tyler-Kabara EC, Weber DJ, et al. High-performance neuroprosthetic control by an individual with tetraplegia. Lancet. 2013 Feb 16; 381 (9866): 557–64.
11. Nunez PL, Srinivasan R. Electric fields of the brain: the neurophysics of EEG. Oxford, UK: Oxford university press; 2006. 611 p.
12. Arai M, Nishinaka Y, Miki N. Long-term electroencephalogram measurement using polymer-based dry microneedle electrode. In: 2015 Transducers – 2015 18th International Conference on Solid-State Sensors, Actuators and Microsystems (TRANSDUCERS); 2015 June 21–25; Anchorage, AK. IEEE; 2015. p. 81–4.
13. Agashe H, Contreras-Vidal JL. Reconstructing hand kinematics during reach to grasp movements from electroencephalographic signals. Conf Proc IEEE Eng Med Biol Soc. 2011; 2011: 5444–7. doi: 10.1109/IEMBS.2011.6091389.
14. Mohamed AK, Marwala T, John LR. Single-trial EEG discrimination between wrist and finger movement imagery and execution in a sensorimotor BCI. Conf Proc IEEE Eng Med Biol Soc. 2011; 2011: 6289–93.
15. Yang J, Singh H, Hines EL, Schlaghecken F, Iliescu DD, Leesonc MS, Stocks NG. Channel selection and classification of electroencephalogram signals: an artificial neural network and genetic algorithm-based approach. Artif Intell Med. 2012; 55 (2):117–26.
16. Feldman Y, Ishai PB, Raicu V. Electrode polarization. Dielectric relaxation in biological systems: physical principles, methods, and applications. 2015 Jul 23: 140.
17. Allison BZ, Leeb R, Brunner C, Müller-Putz GR, Bauernfeind G, Kelly JW, Neuper C. Toward smarter BCIs: extending BCIs through hybridization and intelligent control. J Neural Eng. 2012 Feb; 9 (1): 013001.
18. Pfurtscheller G, Allison BZ, Brunner C, Bauernfeind G, Solis-Escalante T, Scherer R, et al. The hybrid BCI. Front Neurosci. 2010 Apr 21; 4: 30.
19. Leeb R, Sagha H, Chavarriaga R, Mill J. Multimodal fusion of muscle and brain signals for a hybrid-BCI. Conf Proc IEEE Eng Med Biol Soc. 2010; 2010: 4343–6.
20. Xie P, Chen X, Ma P, Li X, Su P. Identification Method of Human Movement Intention based on the Fusion Feature of EEG and EMG. In: Proceedings of the World Congress on Engineering 2013, vol. 2; 2013 Jul 3–5; London, UK. IAENG; 2013.
21. Kiguchi K, Hayashi Y. A study of EMG and EEG during perception-assist with an upper-limb power-assist robot. In: 2012 IEEE International Conference on Robotics and Automation (ICRA); 2012 May 14–18; Saint Paul, MN. IEEE; 2012. p. 2711–6.
22. Gopura RARC, Kiguchi K, Li Y. SUEFUL-7: A 7DOF upper-limb exoskeleton robot with muscle-model-oriented EMG-based control. In: 2009 IEEE/RSJ International Conference on Intelligent Robots and Systems; 2009 Oct 11–19; St. Louis, USA. IEEE; 2009. p. 1126–31.
23. Witkowski M, Cortese M, Cempini M, Mellinger J, Vitiello N, Soekadar SR. Enhancing brain-machine interface (BMI) control of a hand exoskeleton using electrooculography (EOG). J Neuroeng Rehabil. 2014 Dec 16; 11: 165.
24. Rumyantseva SA, Stupin VA, Oganov RG, Silina EV, Petrov VA, Kasymov VA, et al. The ways of long-term blood pressure control systems development. Cardiovascular Therapy and Prevention. 2015; (14) 1: 78–82.
25. Stupin VA, Silina EV, Oganov RG, Bogdanov YA, Shusharina NN. Development of an invasive device for long-term remote monitoring of cardiovascular system parameters, including blood pressure, in patients with comorbid conditions. Biosciences Biotechnology Research Asia, Aug 2015. Vol. 12(2), p. 1255-1263.
26. Silina EV., Stupin VA., Kolesnikova EA., Rumyantseva SA., Oganov RG. New devices for invasive blood pressure detection and the prototype for a long-term invasive distance control of cardiovascular system. Biology and medicine. 2014; 6 (3): BM-045-14, 5 p.
27. Pfurtscheller G, Leeb R, Slater M. Cardiac responses induced during thought-based control of a virtual environment. Int J Psychophysiol. 2006 Oct; 62 (1): 134–40.
28. Pfurtscheller G, Ortner R, Bauernfeind G, Linortner P, Neuper C. Does conscious intention to perform a motor act depend on slow cardiovascular rhythms? Neurosci Lett. 2010 Jan 1; 468 (1): 46–50.
29. Shahid S, Prasad G, Sinha RK. On fusion of heart and brain signals for hybrid BCI. In 2011 5th International IEEE/EMBS Conference Neural Engineering (NER); 2011 Apr 27 – May 11; Cancun, Mexico. IEEE; 2011. p. 48–52.
30. Judy JW. Neural interfaces for upper-limb prosthesis control: opportunities to improve long-term reliability. IEEE Pulse. 2012 Mar; 3 (2): 57–60.
31. Yanagisawa T, Hirata M, Saitoh Y, Goto T, Kishima H, Fukuma R, et al. Real-time control of a prosthetic hand using human electrocorticography signals: technical note. J Neurosurg. 2011 Jun; 114 (6): 1715–22.

Литература

1. Singh RM, Chatterji S, Kumar A. Trends and challenges in EMG based control scheme of exoskeleton robots — a review. Int J Sci Eng Res. 2012; 3 (9): 933–40.
2. Artemiadis P. EMG-based robot control interfaces: past, present and future. Adv Robot Autom. 2012, 1 (2): e107.
3. Li G. Electromyography pattern-recognition-based control of powered multifunctional upper-limb prostheses. In: Mizrahi J, editor. Advances in applied electromyography. InTech; 2011. 224 p.
4. Kim Y, Doh NL, Youm Y, Chung WK. Robust discrimination method of the electrooculogram signals for human-computer interaction controlling mobile robot. Intell Autom Soft Comp. 2007; 13 (3): 319–36.
5. Oonishi Y, Oh S, Hori Y. New control method for power-assisted wheelchair based on upper extremity movement using surface myoelectric signal. 2008 10th IEEE International Workshop on Advanced Motion Control. 2008; 498–503.
6. Gu Y, Dremstrup K, Farina D. Single-trial discrimination of type and speed of wrist movements from EEG recordings. Clin

Neurophysiol. 2009 Aug; 120 (8): 1596–600.
7. Shenoy P, Miller KJ, Crawford B, Rao RP. Online electromyographic control of a robotic prosthesis. IEEE Trans Biom Eng. 2008 Mar; 55 (3): 1128–35.
8. Kiguchi K, Hayashi Y. An EMG-based control for an upper-limb power-assist exoskeleton robot. IEEE Trans Syst Man Cybern B Cybern. 2012 Aug; 42 (4): 1064–71.
9. Rosen J, Brand M, Fuchs MB, Arcan M. A myosignal-based powered exoskeleton system. IEEE Trans Syst Man Cybern A Syst Hum. 2001; 31 (3): 210–22.
10. Collinger JL, Wodlinger B, Downey JE, Wang W, Tyler-Kabara EC, Weber DJ, et al. High-performance neuroprosthetic control by an individual with tetraplegia. Lancet. 2013 Feb 16; 381 (9866): 557–64.
11. Nunez PL, Srinivasan R. Electric fields of the brain: the neurophysics of EEG. Oxford, UK: Oxford university press; 2006. 611 p.
12. Arai M, Nishinaka Y, Miki N. Long-term electroencephalogram measurement using polymer-based dry microneedle electrode. In: 2015 Transducers – 2015 18th International Conference on Solid-State Sensors, Actuators and Microsystems (TRANSDUCERS); 2015 June 21–25; Anchorage, AK. IEEE; 2015. p. 81–4.
13. Agashe H, Contreras-Vidal JL. Reconstructing hand kinematics during reach to grasp movements from electroencephalographic signals. Conf Proc IEEE Eng Med Biol Soc. 2011; 2011: 5444–7. doi: 10.1109/IEMBS.2011.6091389.
14. Mohamed AK, Marwala T, John LR. Single-trial EEG discrimination between wrist and finger movement imagery and execution in a sensorimotor BCI. Conf Proc IEEE Eng Med Biol Soc. 2011; 2011: 6289–93.
15. Yang J, Singh H, Hines EL, Schlaghecken F, Iliescu DD, Leesonc MS, Stocks NG. Channel selection and classification of electroencephalogram signals: an artificial neural network and genetic algorithm-based approach. Artif Intell Med. 2012; 55 (2):117–26.
16. Feldman Y, Ishai PB, Raicu V. Electrode polarization. Dielectric relaxation in biological systems: physical principles, methods, and applications. 2015 Jul 23: 140.
17. Allison BZ, Leeb R, Brunner C, Müller-Putz GR, Bauernfeind G, Kelly JW, Neuper C. Toward smarter BCIs: extending BCIs through hybridization and intelligent control. J Neural Eng. 2012 Feb; 9 (1): 013001.
18. Pfurtscheller G, Allison BZ, Brunner C, Bauernfeind G, Solis-Escalante T, Scherer R, et al. The hybrid BCI. Front Neurosci. 2010 Apr 21; 4: 30.
19. Leeb R, Sagha H, Chavarriaga R, Mill J. Multimodal fusion of muscle and brain signals for a hybrid-BCI. Conf Proc IEEE Eng Med Biol Soc. 2010; 2010: 4343–6.
20. Xie P, Chen X, Ma P, Li X, Su P. Identification Method of Human Movement Intention based on the Fusion Feature of EEG and EMG. In: Proceedings of the World Congress on Engineering 2013, vol. 2; 2013 Jul 3–5; London, UK. IAENG; 2013.
21. Kiguchi K, Hayashi Y. A study of EMG and EEG during perception-assist with an upper-limb power-assist robot. In: 2012 IEEE International Conference on Robotics and Automation (ICRA); 2012 May 14–18; Saint Paul, MN. IEEE; 2012. p. 2711–6.
22. Gopura RARC, Kiguchi K, Li Y. SUEFUL-7: A 7DOF upper-limb exoskeleton robot with muscle-model-oriented EMG-based control. In: 2009 IEEE/RSJ International Conference on Intelligent Robots and Systems; 2009 Oct 11–19; St. Louis, USA. IEEE; 2009. p. 1126–31.
23. Witkowski M, Cortese M, Cempini M, Mellinger J, Vitiello N, Soekadar SR. Enhancing brain-machine interface (BMI) control of a hand exoskeleton using electrooculography (EOG). J Neuroeng Rehabil. 2014 Dec 16; 11: 165.
24. Румянцева С. А., Ступин В. А., Оганов Р. Г., Силина Е. В., Петров В. А., Касымов В. А. и др. Пути развития систем длительного контроля артериального давления. Кардиоваскулярная терапия и профилактика. 2015; (14) 1: 78–82.
25. Stupin VA, Silina EV, Oganov RG, Bogdanov YA, Shusharina NN. Development of an invasive device for long-term remote monitoring of cardiovascular system parameters, including blood pressure, in patients with comorbid conditions. Biosciences Biotechnology Research Asia, Aug 2015. Vol. 12(2), p. 1255-1263.
26. Silina EV., Stupin VA., Kolesnikova EA., Rumyantseva SA., Oganov RG. New devices for invasive blood pressure detection and the prototype for a long-term invasive distance control of cardiovascular system. Biology and medicine. 2014; 6 (3): BM-045-14, 5 p.
27. Pfurtscheller G, Leeb R, Slater M. Cardiac responses induced during thought-based control of a virtual environment. Int J Psychophysiol. 2006 Oct; 62 (1): 134–40.
28. Pfurtscheller G, Ortner R, Bauernfeind G, Linortner P, Neuper C. Does conscious intention to perform a motor act depend on slow cardiovascular rhythms? Neurosci Lett. 2010 Jan 1; 468 (1): 46–50.
29. Shahid S, Prasad G, Sinha RK. On fusion of heart and brain signals for hybrid BCI. In 2011 5th International IEEE/EMBS Conference Neural Engineering (NER); 2011 Apr 27 – May 11; Cancun, Mexico. IEEE; 2011. p. 48–52.
30. Judy JW. Neural interfaces for upper-limb prosthesis control: opportunities to improve long-term reliability. IEEE Pulse. 2012 Mar; 3 (2): 57–60.
31. Yanagisawa T, Hirata M, Saitoh Y, Goto T, Kishima H, Fukuma R, et al. Real-time control of a prosthetic hand using human electrocorticography signals: technical note. J Neurosurg. 2011 Jun; 114 (6): 1715–22.

IMPROVING EYE-BRAIN-COMPUTER INTERFACE PERFORMANCE BY USING ELECTROENCEPHALOGRAM FREQUENCY COMPONENTS

Shishkin SL[1]✉, Kozyrskiy BL[1,3], Trofimov AG[1,3], Nuzhdin YO[1], Fedorova AA[1], Svirin EP[1], Velichkovsky BM[2]

[1] Department of Neurocognitive Technologies, Kurchatov Complex of NBICS Technologies, National Research Centre Kurchatov Institute, Moscow, Russia

[2] Kurchatov Complex of NBICS Technologies, National Research Centre Kurchatov Institute, Moscow, Russia

[3] Faculty of Cybernetics and Information Security, National Research Nuclear University MEPhI, Moscow, Russia

Eye-brain-computer interfaces (EBCIs) could combine the advantages of eye tracking systems used for operating technical devices and brain-computer interfaces. Such systems are intended for both patients with various motor impairments and healthy individuals. The effectiveness of EBCIs is largely dependent on their ability to detect the user's intent to give a command on the encephalogram (EEG) recorded during gaze fixation, that is, just within hundreds of milliseconds. These strict requirements necessitate a full use of data contained in EEG for more accurate classification of gaze fixations as spontaneous and "control". This work describes our attempt to use for classification not only amplitude statistical features, but also wavelet features specific to oscillatory EEG components within the interval of 50-500 ms from gaze fixation onset. Integral index of classification accuracy AUC significantly depended on the feature set, reaching the highest value (0.75, average over the group of 8 participants) for the combined amplitude and wavelet set. We believe that further improvement of this method will facilitate the practical application of EBCIs.

Keywords: brain-computer interface, eye-brain-computer interface, electroencephalogram, EEG, gaze-based control, control gaze fixation, eye tracking, video-oculography, classification, wavelets

Funding: this work was partially supported by the Russian Science Foundation, grant no. 14-28-00234 (acquisition and preprocessing of experimental data), and the Russian Foundation for Basic Research, grant no. 15-29-01344 (evaluation of wavelet features significance for classification).

✉ **Correspondence should be addressed:** Sergey Shishkin
pl. Akademika Kurchatova, d. 1, Moscow, Russia, 123182; sergshishgkin@mail.ru

Received: 08.04.2016 **Accepted:** 15.04.2016

УЛУЧШЕНИЕ РАБОТЫ ИНТЕРФЕЙСА ГЛАЗ–МОЗГ–КОМПЬЮТЕР ПРИ ИСПОЛЬЗОВАНИИ ЧАСТОТНЫХ КОМПОНЕНТОВ ЭЛЕКТРОЭНЦЕФАЛОГРАММЫ

С. Л. Шишкин[1]✉, Б. Л. Козырский[1,3], А. Г. Трофимов[1,3], Ю. О. Нуждин[1], А. А. Федорова[1], Е. П. Свирин[1], Б. М. Величковский[2]

[1] Отдел нейрокогнитивных технологий, Курчатовский комплекс НБИКС-технологий, Национальный исследовательский центр «Курчатовский институт», Москва

[2] Курчатовский комплекс НБИКС-технологий, Национальный исследовательский центр «Курчатовский институт», Москва

[3] Факультет кибернетики и информационной безопасности, Национальный исследовательский ядерный университет «МИФИ», Москва

Интерфейсы глаз–мозг–компьютер (ИГМК) могли бы совместить в себе достоинства айтрекинговых систем управления техническими устройствами и интерфейсов мозг–компьютер. Такие системы предназначены как для пациентов с различными моторными нарушениями, так и здоровых людей. Эффективность ИГМК во многом определяется возможностью распознать намерение пользователя отдать команду по электроэнцефалограмме (ЭЭГ), регистрируемой во время фиксации взгляда, т. е. в течение всего сотен миллисекунд. Эти жесткие требования диктуют необходимость добиваться как можно более полного использования заключенной в ЭЭГ информации для повышения точности классификации фиксаций взгляда на «управляющие» и спонтанные. В настоящей работе предприняли попытку использовать для классификации не только амплитудные статистические признаки, но также вейвлетные признаки, характеризующие осцилляторные компоненты ЭЭГ в интервале 50…500 мс относительно начала фиксации взгляда. Значения интегрального показателя точности классификации AUC при этом значимо выросли и составили 0,75 в среднем по группе из 8 человек. Предполагается, что дальнейшее совершенствование методики позволит превратить ИГМК в практически полезную технологию.

Ключевые слова: интерфейс мозг–компьютер, интерфейс глаз–мозг–компьютер, электроэнцефалограмма, ЭЭГ, управление с помощью взгляда, управляющая фиксация взгляда, айтрекинг, видеоокулография, классификация, вейвлеты

Финансирование: работа выполнена при частичной поддержке Российского научного фонда, грант № 14-28-00234 (получение экспериментальных данных и их предварительная обработка), и Российского фонда фундаментальных исследований, грант № 15-29-01344 (оценка вклада вейвлетных признаков в классификацию).

✉ **Для корреспонденции:** Сергей Львович Шишкин
123182, г. Москва, пл. Академика Курчатова, д. 1; sergshishgkin@mail.ru

Статья поступила: 08.04.2016 **Статья принята к печати:** 15.04.2016

Brain-computer interfaces (BCIs) are systems for operating computers and other devices connected to them that make use of the detection of brain activity patterns associated with control commands. They have been designed primarily to assist paralyzed patients [1–3]. At the same time, the accuracy and operating speed of a vast majority of BCIs are still low. It is unclear if BCIs can be used outside the range of tasks where it is sufficient to issue very simple commands but important that these commands be given "straight from the brain" (for example, in poststroke rehabilitation [4]). Using BCI, a satisfactory spelling rate (50 characters per minute in healthy individuals) was achieved only in the recent study [5], in which rhythmic visual stimulation was used; it is still unclear if the use of such stimulation in BCI is safe.

Interestingly, all non-invasive BCIs with high accuracy and high speed rates utilize EEG response to visual stimuli the user directs his or her gaze at. It means that they can be used only if a patient does not suffer from any serious vision impairment or eye movement disorders and still has the ability to voluntarily direct his gaze towards specific screen areas associated with control commands (to fixate the gaze on virtual "buttons"). When this is the case, however, it is possible to control computers and other devices connected to them by detecting gaze direction using eye tracking (video-oculography).

Current methods of gaze-based control demonstrate relatively good accuracy, speed and usability when used for text entry [6]. However, attempts to apply them to a wider range of tasks are hampered by the so-called "Midas touch" problem [7]. Just like King Midas from the ancient Greek myth turned all things into gold by touching them, technical devices are non-selective in translating gaze fixations or eye movements into commands: their user issues commands even without an intent to issue them. This is because eye movements are a crucial component of visual function and are normally spontaneous, slipping conscious control easily even if attention is focused on them. Current solutions to this problem either make the control process very slow and tiring or can be used for a limited range of tasks.

As early as 1996, it was proposed to solve the Midas touch problem and create a high-performance universal interface by combining "eye-mouse" control with BCI [8]. Over a number of years the combination of those two technologies [9] was quite mechanical in nature and did not result in creating systems with fast response and good ergonomic properties. An innovative solution was suggested by Torsten Zander's group who turned to the idea of natural combination of eye tracking and BCI [8] within the framework of a new trend, namely, the development of the so-called "passive BCIs". This name was given to BCIs that responded to patterns of brain activity unrelated to deliberate efforts to issue a command using BCI [10]. Zander and his colleagues showed that eye fixations used for control ("control" fixations) can be differentiated from spontaneous (visual) fixations using the encephalogram (EEG) recorded during fixations, even if control markers appearing on EEG were not evoked intentionally (the subjects were not given additional tasks and were not presented with stimuli in the "control" position) [11]. However, in their study control could be implemented only by a long (1,000 ms) gaze fixation on a single screen target.

Our group has developed a method for an eye-brain-computer interface (EBCI) that allows for EEG–based classification of shorter fixations with a duration of 500 ms. In our experiment, subjects played Lines, a computer game, with their gaze only. Each move was made by fixating the gaze on one of 50 elements on the board. The classifier was trained to differentiate between the EEG signals recorded during those fixations and EEG signals recorded during fixations on the same elements but with control switched off, i.e., during supposedly spontaneous fixations [12; Shishkin et al., in prep.]. Due to the reduction of fixation length, subjects perceived control as natural and comfortable. The number and location of control-sensitive visual elements in our method was limited by eye tracker capacities only. However, fixation-related amplitude features of the EEG components (we used those features in our early works) did not provide sufficient control detection accuracy for practical application of the technology.

In this study we analyze the possibility to improve the accuracy of the EBCI classifier that automatically differentiates between control gaze fixations and spontaneous ones by using features of oscillatory EEG components in addition to EEG amplitude features. Since short EEG intervals should be used, during which both amplitude and frequency components can display time dependency, and because of the high dimensionality of time-frequency data and other significant differences between them and amplitude data, it was necessary to develop a special scheme for extracting quantitative parameters of EEG components recorded during gaze fixations.

METHODS

The experiment

We used EEG recordings obtained in our early experimental study. Its results will be presented in another article [Shishkin et al., in prep.]; the article will also provide a detailed description of the methods used in the experiment.

Our study was conducted in compliance with the guidelines of the Declaration of Helsinki. The study enrolled 8 relatively healthy individuals (7 male and 1 female) aged 21-48 (mean age was 29). The subjects gave their informed consent. Gaze was recorded using EyeLink 1000 Plus eyetracker (SR Research, Canada). Fixations were detected on-line using variance criterion. Sinchronously, EEG from 19 electrodes (Fz, F3, F4, Cz, C3, C4, Pz, P1, P2, P3, P4, POz, PO3, PO4, PO7, PO8, Oz, O1, O2) and electrooculogram (EOG) were recorded using the actiCHamp system (BrainProducts, Germany). EOG was used to monitor EEG artifacts. Gaze direction, EEG and EOG were recorded at 500 Hz frequency.

Gaze-based control algorithms and the task the subjects performed were exactly the same as described in our preliminary study [12]. Here, only the most important details are listed. The subjects played Lines, a computer game that was modified so that all moves during the game could be performed by a sequence of 3 fixations, each exceeding a 500 ms duration threshold. Each sequence started with the fixation on a particular screen area, where a special "control on" indicator appeared after the threshold had been reached. EEG recorded during those fixations constituted the first class of data (control fixations). Another data class (non-control fixations) was constituted by EEG recorded during fixations that also exceeded the threshold but did not result in a move, according to game rules. Fixation-based game control, EEG/EOG synchronization and recording of gaze fixation data were performed using the original software.

An average of 155 (from 120 to 184) control and 159 (from 114 to 208) non-control fixations was recorded for each subject.

Feature extraction

To extract EEG wavelet features, we chose the interval 50–500 ms after fixation onset, because the preceding interval contained artifacts related to gaze shifts, and the subsequent interval could not be used for detecting the intention to issue a command in the on-line mode. In the analyzed interval there were almost no artifacts, so we did not apply any procedures for their correction or removal. In our early work we showed [12; Shishkin et al., in prep.] that in our EBCI paradigm, a considerable difference in EEG amplitudes between control and non-control fixations was typical for the second half of fixation interval only. Therefore, we used the interval 200–500 ms after fixation onset to obtain amplitude features in the current study.

Amplitude features were obtained by averaging amplitude values in each EEG channel separately in overlapping 50 ms windows. To reduce the influence of slow oscillations and direct current component, the baseline was corrected by subtracting the mean value for the interval 200–300 ms after fixation onset from those averaged values. The obtained "raw" amplitude features constituted a feature vector that characterized a trial corresponding to one fixation.

Wavelet features were obtained using Morlet wavelet transform. The scale range corresponded to the frequency range of 5–30 Hz. The higher frequency corresponded to the scale, the more wavelet coefficients were used to describe the trial. To reduce noise produced by irrelevant features, only 30 % of the wavelet time-frequency features were used, namely those that differed most considerably between spontaneous and control fixations (those that had the highest coefficient of determination, R^2).

Selected features were processed using Principal Component Analysis (PCA). It was applied separately to amplitude features and wavelet features. 80 components with highest variance for each feature type were selected. They constituted new sets of features. Before and after PCA, z-score normalization was applied either to all values of each feature (in all trials) or to all features within a single trial (for amplitude features and wavelet features separately). Normalization within a single trial was considered a way of adaptation to local feature level that could gradually vary over time.

EEG-based classification of control and non-control fixations

For classification, linear discriminant analysis with shrinkage regularization was used. It ensured effective training with small training sets (like the one that was available in this study) even if feature dimensionality was relatively high; it also proved to be highly effective in the BCIs based on event-related potentials [13, 14].

Classification quality was assessed using 5-fold cross-validation. Classifier training, feature selection, calculation of mean values and standard deviations for feature normalization (in case it was applied trialwise), as well as dimensionality reduction, were carried out on the data used as the training set. The derived feature selection rule, mean and standard deviations for corresponding value sets, weight matrix for selected components, and weight of the trained classifier were applied to the rest of data regarded as a test sample. Due to such arrangement of cross-validation, it was possible to reconstruct a real situation of how a classifier can be used online in a BCI.

As a classification quality metric, we used AUC (Area Under Curve; here, "Curve" refers to the Receiver Operating Characteristic (ROC) curve), an integral performance index widely applied in similar studies. It shows to what extent classification results differ from random for various classifier threshold values that can be selected to separate classes with various ratios of various types of errors, depending on the specific purpose the classifier is used for. If classification results do not differ from random guess, AUC value goes to 0.5; if the classifier does not make any errors, AUC equals to 1. To compare AUC values in case of various feature sets, multivariate analysis of variance (MANOVA) and Bonferroni post hoc test were applied using Statistica 7.0 software (StatSoft, USA).

RESULTS

With all methods of feature extraction, individual values of classification accuracy (AUC) were above 0.5, group mean was no less than 0.66; however, AUC mean values were considerably different (fig. 1).

3-way MANOVA (see table below; all three factors were with repeated measures) applied to individual AUC values showed that classification accuracy was dependent on the feature set factor ($\lambda = 0.06$, $F(2.6) = 49$, $p = 0.0002$), while the effects of other factors and interaction between factors in all their combinations were not statistically significant. Benferroni post hoc test showed that the difference between amplitude and amplitude-wavelet feature sets was statistically significant ($p = 0.006$); no statistically significant difference between amplitude and wavelet ($p = 0.34$) and between wavelet and amplitude-wavelet ($p = 0.16$) feature sets was found. The set that consisted of amplitude features only had the lowest classification accuracy. The best results were shown by the combined set (amplitude and wavelet features grouped together). With the combined EEG feature set, AUC group mean increased by 0.05–0.08 (depending on the method used for normalization) compared to the amplitude set. AUC group mean was 0.75 ± 0.04 (M ± SD) with features normalized both before and after PCA, and 0.75 ± 0.06 with features normalized before PCA and within trials after PCA.

Fig. 2 shows individual results for the feature extraction

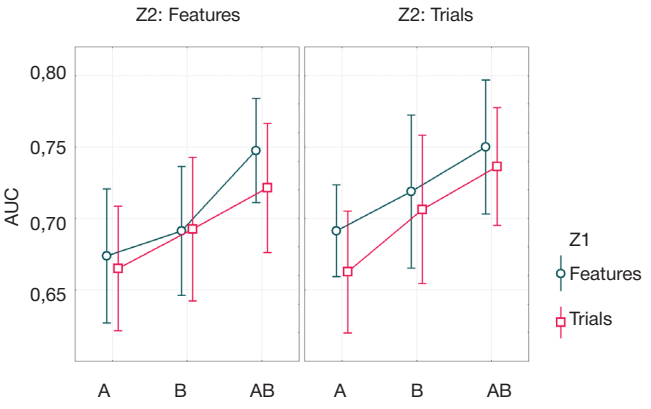

Fig. 1. Dependence of classification accuracy (AUC) for gaze fixations (control and non-control) on the method used for feature extraction from EEG recorded during gaze fixation

Legend: A — amplitude features only, B — wavelet features only, AB — combined (amplitude-wavelet) set of features; Z1 — normalization type before PCA; Z2 — normalization type after PCA; features: normalization of separate features; trials — normalization of features within a single trial. Vertical lines represent 95 % confidence intervals.

Effect of feature extraction methods on classification accuracy (AUC)

Factors	Wilks' λ	F	df (Effect, Error)	p
Z1 (normalization before PCA)	0.71	2.85	1, 7	0.1354
Z2 (normalization after PCA)	0.67	3.43	1, 7	0.1064
Feature set (A, B, AB)	**0.06**	**49.01**	**2, 6**	**0.0002**
Z1 × Z2	0.86	1.18	1, 7	0.3139
Z1 × features	0.48	3.26	2, 6	0.1101
Z2 × features	0.68	1.41	2, 6	0.3138
Z1 × Z2 × features	0.79	0.81	2, 6	0.4881

Note. Using multivariate analysis of variance (MANOVA), AUC dependence on normalization before PCA (Z1), normalization after PCA (Z2), feature set type (amplitude, wavelet, amplitude-wavelet) and their interaction (represented by ×) were analyzed. Statistically significant effect is shown in bold ($p < 0.05$).

method that resulted in the highest group averaged AUC. Individual curves on the graph provide values of various types of errors that could be observed with various classification threshold values. Specifically, of particular importance is EBCI classifier sensitivity, i.e., the rate of correctly identified control fixations, under the condition of low false positive rate. As shown in fig. 2, when fixating false positive rate at 0.1 (which can be achieved by selecting the corresponding classifier threshold using a separate set); only one subject demonstrated sensitivity lower than 0.2, while another subject had sensitivity above 0.5 and the rest scores were in the interval between those two values.

DISCUSSION

Improvement of classifier performance is the key factor in the development of an EBCI that could detect relatively short control gaze fixations using EEG intervals recorded during such fixations, as only single signal intervals with the duration of a few hundred milliseconds are available for analysis in such a BCI paradigm.

Quality of classification with low level of false alarms should be discussed separately. In EBCI, it is easy to provide a safety net in case control fixation is not identified. If the interface does not respond when the threshold of 500 ms has been reached, the users can continue fixate their gaze, and the system will respond after the additional (for example, 1,000 ms) threshold has been reached, even without the response from the EEG classifier. We can make a supposition that with the EBCI that has this kind of safety net, the brain of the user interested in speeding up interface activation can learn to produce the EEG pattern that accompanies control fixations and ensures a considerably more frequent response of the classifier. However, for that a minimum entry-level control is necessary. As fig. 2 demonstrates, the scheme for signal preprocessing and feature extraction developed by the authors of this work would help some subjects evoke a faster interface response in half of control fixations with relatively low false alarm rate (0.1)

While we already can speculate on the nature of amplitude features that can be used for classification in our EBCI, assuming that they might be related to the presence of negative potential associated with feedback expectation in case of interface response [Shishkin et al., in prep.], the nature of wavelet features still requires further elucidation. It should be noted that patterns of EEG frequency components typical for various brain states are highly individual and their specifics can be only partially observed on the group level. However, they can be successfully classified if the classifier is trained on individual data, in particular in the BCI paradigm [15–18]. Still, high dimensionality of such data requires an especially elaborated approach to different stages of analysis, with a larger number of subjects involved in such studies whenever possible. We have just made our first steps in this direction, but similar results obtained with various methods of data normalization may indicate a relatively high robustness of the proposed scheme for data preprocessing and informative features extraction, and its good prospects for the EBCI development.

CONCLUSIONS

In this work we made the first attempt to use the spatiotemporal EEG representation, i.e. representation of EEG frequency components as a function of time from the fixation onset. The use of these features allowed us to achieve classification accuracy at least as good as classification accuracy based on amplitude features we used in previous works. Moreover, a combination of both feature sets led to classification accuracy improvement. We believe that further improvement of computation methods will allow us to closely approach a practical application of eye-brain-computer interfaces that combine the main advantages of standard BCIs and control systems based on eye tracking.

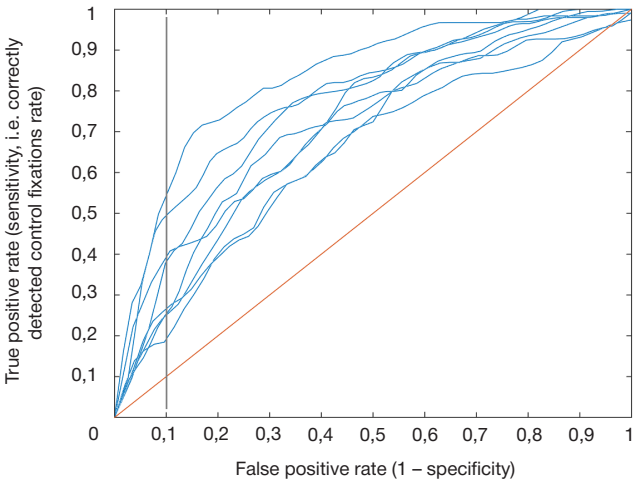

Fig. 2. ROC curves (Receiver Operating Characteristic curves) for all subjects when using the amplitude-wavelet feature set, feature normalization before PCA, trial normalization after PCA (feature extraction method that allowed for the highest group averaged AUC value). Red line shows random classification, grey vertical line provides an example of strict requirements to the specificity of classifier (false positive rate = 0.1)

References

1. Wolpaw JR, Birbaumer N, McFarland DJ, Pfurtscheller G, Vaughan TM. Brain–computer interfaces for communication and control. Clin Neurophysiol. 2002; 113 (6): 767–791.
2. BNCI Horizon 2020. The Future of Brain/Neural Computer Interaction: Horizon 2020. Appendix C: End Users. 7th Framework Programme of the European Union. Available from: http://bnci-horizon-2020.eu/roadmap.
3. Kaplan AYa, Kochetova AG, Shishkin SL, Basyul IA, Ganin IP, Vasilyev AN, Liburkina SP. Experimental and theoretical foundations and practical implementation of brain-computer interface technology. Bulletin of Siberian Medicine. 2013; 12 (2): 21-9. Russian.
4. Kaplan AYa. Neurophysiological foundations and practical realizations of the brain–machine interfaces in the technology in neurological rehabilitation. Human Physiology. 2016; 42 (1): 103–10. Russian.
5. Chen X, Wang Y, Nakanishi M, Gao X, Jung TP, Gao S. High-speed spelling with a noninvasive brain–computer interface. Proc Natl Acad Sci U S A. 2015; 112 (44): E6058–67.
6. Majaranta P. Text entry by eye gaze [dissertation]. Tampere, Finland: University of Tampere; 2009. Available from: http://tampub.uta.fi/handle/10024/66483.
7. Jacob RJK. The use of eye movements in human-computer interaction techniques: what you look at is what you get. ACM Transactions on Information Systems. 1991; 9 (2): 152–69.
8. Velichkovsky BM, Hansen JP. New technological windows into mind: there is more in eyes and brains for human-computer interaction. In: Proceedings of the SIGCHI conference on Human factors in computing systems; 1996 Apr 13–18; Vancouver, BC, Canada. New York: ACM; 1996. p. 496–503.
9. Pfurtscheller G, Allison BZ, Bauernfeind G, Brunner C, Escalante TS, Scherer R, et al. The hybrid BCI. Front Neurosci. 2010; 4: 42. Available from: http://journal.frontiersin.org/article/10.3389/fnpro.2010.00003/full.
10. Zander TO, Kothe C. Towards passive brain–computer interfaces: applying brain–computer interface technology to human–machine systems in general. J Neural Eng. 2011; 8 (2): 025005.
11. Protzak J, Ihme K, Zander TO. A passive brain-computer interface for supporting gaze-based human-machine interaction. In: Stephanidis C, Antona M, editors. Universal Access in Human-Computer Interaction. Design Methods, Tools, and Interaction Techniques for eInclusion. Springer; 2013. p. 662–71.
12. Shishkin SL, Svirin EP, Nuzhdin YO, Fedorova AA, Trofimov AG, Slobodskoy-Plusnin JY, et al. Learn waiting! Contingent negative variation may help you to control with your eye-gaze. In: Pechenkova EV, Falikman MV, editors. Cognitive Science in Moscow: New Studies. Ed. by E. V. Pechenkova, M. V. Falikman. M.: BukiVedi; 2015. p. 486–91. Russian.
13. Blankertz B, Lemm S, Treder M, Haufe S, Muller KR. Single-trial analysis and classification of ERP components — a tutorial. NeuroImage. 2011; 56 (2): 814–25.
14. Schultze-Kraft M, Birman D, Rusconi M, Allefeld C, Gorgen K, Dahne S, et al. The point of no return in vetoing self-initiated movements. Proc Natl Acad Sci U S A. 2016; 113 (4): 1080–5.
15. Ivanitsky GA. Recognition of the task type in the process of its mental solving by a few-second EEG record using the learned classifier. Zh Vyssh Nerv Deiat I P Pavlova. 1997; 47: 743–7. Russian.
16. Dat TH, Shue L, Guan C. Electrocorticographic signal classification based on time-frequency decomposition and nonparametric statistical modeling. In: 28th Annual International Conference of the IEEE Engineering in Medicine and Biology Society. 2006. P. 2292-5.
17. Roik AO, Ivanitskii GA. A neurophysiological model of the cognitive space. Neuroscience and Behavioral Physiology. 2013; 43 (2): 193–9.
18. Frolov A, Husek D, Bobrov P. Comparison of four classification methods for brain-computer interface. Neural Network World. 2011; 21 (2): 101–15.
19. Frolov A, Husek D, Bobrov P, Mokienko O, Tintera J. Sources of electrical brain activity most relevant to performance of brain-computer interface based on motor imagery. In: Fazel-Rezai R, editor. Brain-Computer Interface Systems: Recent Progress and Future Prospects. InTech; 2013. p. 175–93.

Литература

1. Wolpaw JR, Birbaumer N, McFarland DJ, Pfurtscheller G, Vaughan TM. Brain–computer interfaces for communication and control. Clin Neurophysiol. 2002; 113 (6): 767–791.
2. BNCI Horizon 2020. The Future of Brain/Neural Computer Interaction: Horizon 2020. Appendix C: End Users. 7th Framework Programme of the European Union. Доступно по ссылке: http://bnci-horizon-2020.eu/roadmap
3. Каплан А. Я., Кочетова А. Г., Шишкин С. Л., Басюл И. А., Ганин И. П., Васильев А. Н., Либуркина С. П. Экспериментально-теоретические основания и практические реализации технологии «интерфейс мозг–компьютер». Бюллетень сибирской медицины. 2013; 12 (2): 21–9.
4. Каплан А. Я. Нерофизиологические основания и практические реализации технологии мозг-машинных интерфейсов в неврологической реабилитации. Физиология человека. 2016; 42 (1): 118–27.
5. Chen X, Wang Y, Nakanishi M, Gao X, Jung TP, Gao S. High-speed spelling with a noninvasive brain–computer interface. Proc Natl Acad Sci U S A. 2015; 112 (44): E6058–67.
6. Majaranta P. Text entry by eye gaze [диссертация]. Tampere, Finland: University of Tampere; 2009. Доступно по ссылке: http://tampub.uta.fi/handle/10024/66483.
7. Jacob RJK. The use of eye movements in human-computer interaction techniques: what you look at is what you get. ACM Transactions on Information Systems. 1991; 9 (2): 152–69.
8. Velichkovsky BM, Hansen JP. New technological windows into mind: there is more in eyes and brains for human-computer interaction. In: Proceedings of the SIGCHI conference on Human factors in computing systems; 1996 Apr 13–18; Vancouver, BC, Canada. New York: ACM; 1996. p. 496–503.
9. Pfurtscheller G, Allison BZ, Bauernfeind G, Brunner C, Escalante TS, Scherer R, et al. The hybrid BCI. Front Neurosci. 2010; 4: 42. Доступно по ссылке: http://journal.frontiersin.org/article/10.3389/fnpro.2010.00003/full.
10. Zander TO, Kothe C. Towards passive brain–computer interfaces: applying brain–computer interface technology to human–machine systems in general. J Neural Eng. 2011; 8 (2): 025005.
11. Protzak J, Ihme K, Zander TO. A passive brain-computer interface for supporting gaze-based human-machine interaction. In: Stephanidis C, Antona M, editors. Universal Access in Human-Computer Interaction. Design Methods, Tools, and Interaction Techniques for eInclusion. Springer; 2013. p. 662–71.
12. Шишкин С. Л., Свирин Е. П., Нуждин Ю. О., Федорова А. А., Трофимов А. Г., Слободской-Плюснин Я. Ю. и др. Учитесь ждать! Условно-негативная волна поможет отдавать команды взглядом? В сборнике: Печенкова Е. В., Фаликман М. В., редакторы. Когнитивная наука в Москве: новые исследования. М.: БукиВеди; 2015. с. 486–91.
13. Blankertz B, Lemm S, Treder M, Haufe S, Muller KR. Single-trial analysis and classification of ERP components — a tutorial. NeuroImage. 2011; 56 (2): 814–25.
14. Schultze-Kraft M, Birman D, Rusconi M, Allefeld C, Gorgen K, Dahne S, et al. The point of no return in vetoing self-initiated movements. Proc Natl Acad Sci U S A. 2016; 113 (4): 1080–5.
15. Иваницкий Г. А. Распознавание типа решаемой в уме задачи по нескольким секундам ЭЭГ с помощью обучаемого классификатора. Журнал высшей нервной деятельности им. И. П. Павлова. 1997; 47: 743–7.

16. Dat TH, Shue L, Guan C. Electrocorticographic signal classification based on time-frequency decomposition and nonparametric statistical modeling. Conf Proc IEEE Eng Med Biol Soc. 2006; 1: 2292–5. PMID: 17945704.
17. Роик А. О., Иваницкий Г. А. Нейрофизиологическая модель когнитивного пространства. Журнал высшей нервной деятельности им. И. П. Павлова. 2011; 60 (6): 688–96.
18. Frolov A, Husek D, Bobrov P. Comparison of four classification methods for brain-computer interface. Neural Network World. 2011; 21 (2): 101–15.
19. Frolov A, Husek D, Bobrov P, Mokienko O, Tintera J. Sources of electrical brain activity most relevant to performance of brain-computer interface based on motor imagery. In: Fazel-Rezai R, editor. Brain-Computer Interface Systems: Recent Progress and Future Prospects. InTech; 2013. p. 175–93.

STABILITY OF SPONTANEOUS ELECTRICAL ACTIVITY OF NEURAL NETWORKS *IN VITRO*

Sokolov IS[1,2]✉, M Tatarintsev MK[1,3], Khasanov RY[1,4], Azieva AM[1], Makarenko EYu[2], Burtsev MS[1,3,5]

[1] Department of Neurosciences, Kurchatov Complex of NBICS Technologies, National Research Centre Kurchatov Institute, Moscow, Russia

[2] Department of Physiology, Biomedical Faculty, Pirogov Russian National Research Medical University, Moscow, Russia

[3] Department of NBIC Technologies, Faculty of Nano-, Bio-, Information and Cognitive Technologies, Moscow Institute of Physics and Technology (State University), Dolgoprudny, Russia

[4] Department of Human and Animal Physiology, Faculty of Biology, Lomonosov Moscow State University, Moscow, Russia

[5] National Research Nuclear University MEPhI, Moscow, Russia

Using brain-computer interfaces, one can both read data from and transmit them to the brain. However, these data are only a set of sensor system signals and not the knowledge or experience. Neural networks are a basis for cognitive activity and can simulate processes similar to learning *in vitro*. In this work we tested the hypothesis of a neural network's ability to learn by detecting deviations from its stereotypical activity and modifying them in a way that allows it to get rid of external electrical stimulation. Spontaneous activity of several neuronal cultures *in vitro* was analyzed by clustering method. The results showed that activity of untrained cultures remained stable for a long time, and external electrical stimulation led to switching between various spontaneous activity patterns.

Keywords: neuronal cultures, neural networks, learning, spontaneous activity, cluster analysis, bursting activity analysis

Funding: this work was supported by the Russian Science Foundation, grant no. 15-11-30014.

✉ **Correspondence should be addressed:** Ilya Sokolov
ul. Chertanovskaya, d. 49, k. 2, kv. 121, Moscow, Russia, 117534; ilsersokolov@gmail.com

Received: 01.04.2016 **Accepted:** 07.04.2016

УСТОЙЧИВОСТЬ СПОНТАННОЙ ЭЛЕКТРИЧЕСКОЙ АКТИВНОСТИ НЕЙРОННЫХ СЕТЕЙ *IN VITRO*

И. С. Соколов[1,2]✉, М. К. Татаринцев[1,3], Р. Ю. Хасанов[1,4], А. М. Азиева[1], Е. Ю. Макаренко[2], М. С. Бурцев[1,3,5]

[1] Отдел нейронаук, Курчатовский центр НБИКС-технологий, Национальный исследовательски центр «Курчатовский институт», Москва

[2] Кафедра физиологии, медико-биологический факультет, Российский национальный исследовательский медицинский университет имени Н. И. Пирогова, Москва

[3] Кафедра НБИК-технологий, факультет нано-, био-, информационных и когнитивных технологий, Московский физико-технический институт (государственный университет), Долгопрудный

[4] Кафедра физиологии человека и животных, биологический факультет, Московский государственный университет имени М. В. Ломоносова, Москва

[5] Национальный исследовательский ядерный университет «МИФИ», Москва

С помощью нейро-компьютерных интерфейсов можно как считывать информацию с мозга, так и передавать ее в мозг. Однако эта информация — сигналы сенсорных систем, а не знание и опыт. Нейронные сети, представляющие собой основу когнитивной деятельности, способны *in vitro* воспроизводить процессы, аналогичные обучению. В работе проверена гипотеза о том, что нейронная сеть реализует обучение путем обнаружения отклонения от своей стереотипной активности и модификации ее таким образом, чтобы избавиться от внешней электрической стимуляции. Спонтанная активность нескольких нейрональных культур *in vitro* была проанализирована методом кластеризации. Результаты показали, что активность необученных культур остается стабильной на протяжении длительного времени, а внешняя электрическая стимуляция приводит к переключению между паттернами спонтанной активности.

Ключевые слова: нейрональные культуры, нейронные сети, обучение, спонтанная активность, кластерный анализ, анализ пачечной активности

Финансирование: работа выполнена при поддержке Российского научного фонда, грант № 15-11-30014.

✉ **Для корреспонденции:** Илья Сергеевич Соколов
117534, г. Москва, ул. Чертановская д. 49, к. 2, кв. 121; ilsersokolov@gmail.com

Статья поступила: 01.04.2016 **Статья принята к печати:** 07.04.2016

In medicine, brain-computer interfaces are used for the development of neuroprostheses comparable to healthy organs in their responsiveness to user's mental commands [1–3]. Data can also be transmitted in the reverse direction, from the computer to the brain; for example, lost sensory functions, such as auditory [4] and visual [5], can be recovered using electrical stimulation. However, what's more challenging for a researcher is transmission of information as such, i.e., knowledge and experience. It has been shown that using multi-input/multi-output non-linear dynamic model allows for transmitting a certain spatiotemporal pattern detected in the hippocampus of one rat to the hippocampus of another rat, which leads to the statistically reliable alterations in the behavior of the second animal [6].

It is known that neuronal networks that form a basis for cognitive activity do not have a distinct location in brain structures, but are distributed throughout them [7, 8]. From that, a need to reprogram neuronal networks ensues. Publications on the patterns patterns of neuronal network spontaneous activity *in vitro* and on the methods of its external modification [9–13] prove that networks of dissociated primary neuronal cultures of cortical and hippocampal cells on multi-electrode arrays (MEAs) can control external stimulation by changing their activity on the selected experimental electrode. Such neuronal network learning was first demonstrated by Shahaf and Marom [14] and was successfully reproduced by other researchers thereafter [15–18].

As the network is gradually developing from the dissociated neuronal culture, it starts to exhibit spontaneous bioelectrical activity recorded by array electrodes. Thus, in the absence of external stimulation in the first days of culture growth, only single action potentials are registered, but after a while they cluster into bursts [19]. In this work we hypothesize that spontaneous burst activity comes down to a small number of stereotypical patterns, and cluster analysis can help identify one or several dominating patterns. Since the external stimulation breaks the existing activation sequence, the network changes its activity pattern to switch off stimulation and go back to the typical pattern. Then, cluster analysis performed after the stimulation (training) can detect the resumption of the initial activity pattern.

METHODS

Cell cultures

Primary cell culture was prepared from the hippocampal tissue of newborn rats of C57BL/6 breed. Experimental animals used in the study were managed according to the guidelines specified in Order no. 267 of the Ministry of the Russian Federation, dated June 19, 2003, "On the approval of rules for good laboratory practice". The experiment was approved by the local Ethics Committee for Biomedical Research of the National Research Center "Kurchatov Institute" (protocol no. 1, dated July 9, 2015).

Cells were cultured on 60-channel multi-electrode arrays 60StimMEA200/30-ITO (Multichannel Systems, Germany). Prior to the experiment, plates were coated with poly-L-lysine for better cell adhesion. The initial culture density was 300,000 cells per mm^3. Their dissociation was achieved by using 0.25 % trypsin (Invitrogen 25200-056, USA). Neuronal viability was maintained in NeurobasalTM culture medium (Invitrogen 21103-049) in the complex with the bioactive additive B27 (Invitrogen 17504-044), glutamin (Invitrogen 25030-024) and penicillin-streptomycin (Life Technologies 15140122, USA) in GALAXY 170S incubator (New Brunswick Scientific, USA) under stable conditions: temperature of 37 °C, humidity of 100 % and 5 % CO_2 air concentration. Glial cell growth was not inhibited, because glial cells were necessary to ensure long-term culture viability *in vitro*. Half of the medium volume was replaced every three days.

Bioelectrical cell activity was recorded with MEA1060-Up-BC-Standard system (Multichannel Systems). For data acquisition, the bundled software was used.

Dynamics of spontaneous burst activity were observed in two cultures. Recording was performed from the 4^{th} day *in vitro* (DIV) until culture death. For further processing, we used data obtained in the interval between the onset and offset of burst activity. For training, one 24-DIV culture was used.

Protocol of neuronal culture training *in vitro*

1) 1-hour background recording of culture bioelectrical activity .

2) Stimulation by single bipolar rectangular pulses of ± 300 mV on each electrode (one at a time) to select the electrode that evoked the most intense culture response.

3) 5 stimulation cycles on the electrode selected in step 2. Every cycle consisted of a 5-minute series of rectangular pulses with 2-minute breaks. In every experiment, the pause between the pulses was adjusted so that every pulse could induce burst activity. Based on stimulation results, a recording electrode was chosen, for which electrical activity within 30–80 ms after the signal was the lowest.

4) 1-hour recording of culture spontaneous bioelectrical activity.

5) 20 training cycles. Training was considered successful if a twofold increase in the probability to record spike activity within the preset time interval on the electrode chosen in step 3 was observed. Training consisted of stimulation described in paragraph 3, given that as soon as the success criterion had been reached, stimulation was discontinued and a 2-minute break was provided.

6) 1-hour recording of culture spontaneous bioelectrical activity.

Detection of spikes and burst events

The initial signal was digitally processed by a second-order high-pass Butterworth filter with a passband of over 200 Hz, which allowed for the exclusion of low-frequency noise. Action potentials were detected if signal amplitude exceeded 4 standard deviations. In that case, the maximum amplitude was considered time of spike onset.

A burst event (burst) occurs on one electrode and is characterized by a short-term explosion-like impulse generation (0.1–3.0 s depending on culture age and its stocking density), and is usually accompanied by the low-frequency (1–5 Hz) signal component. Detection of bursts was based on the identification of the low-frequency component in a given interval and on spike detection in the vicinity of the component. Time when the first and the last spikes were generated was considered the burst onset and offset, respectively.

Population burst events are bursts that are observed simultaneously (with small delays of about 0.002–0.05 s) on more than a half of all active electrodes. The onset of the population burst is time of the first burst event onset.

Pattern analysis

As a feature V_k of a burst event, activation pattern was used [10]. Vector V_k dimensionality is equal to the number of active electrodes, i.e., electrodes on which at least one burst was observed:

$$V_k = \{t_k(i) - t^k_{start}\}^N_{i=0} = (c_{k0}\ldots c_{kN}), \quad (1)$$

where $t_k(i)$ represents activity onset on the ith electrode, and t^k_{start} represents time of population burst event onset. If no activity was recorded on the electrode during a given burst, but it was present during other bursts, the corresponding vector component takes the averaged value of other vector components.

As a metric, Pearson correlation coefficient was used. For cluster analysis, the weighted pair-group method with arithmetic averaging was used [20].

To obtain clusters, distances between neighboring vectors in the ordered feature vector sequence were found; then, based on the obtained distances, threshold value *th* was computed. Neighboring vectors, the distances between which were less than the threshold value, formed clusters.

Threshold value *th* was computed as follows. We built the graph representing the dependence of the maximum distance *(D)* between clusters on the number of clusters *(n)* in the order of increasing. Thus,

$$th = D(argmax(\frac{d^2D}{dn^2})+2), \quad (2)$$

where *argmax* is a function that computes the maximum value.

RESULTS

Cluster analysis of spontaneous burst activity in two neuronal cultures of 10…30 DIV (fig. 1) showed that in both cases over 50 % burst activation patterns belonged to the same dominating cluster (cluster 7 in fig. 1, A and cluster 5 in fig. 1, B). The majority of other population bursts (40 %) were distributed in two clusters that were equal in size, namely, clusters 6 and 9 (fig. 1, A) and clusters 4 and 6 (fig. 1, B). Dominating patterns of neuronal bursts were stable, despite of external factors related to medium replacements and to moving culture from the incubator to the recording device and back

In the neuronal network training experiment, electrode 22 was chosen for stimulation (see paragraph 2 of the training protocol); stimulation was terminated on electrode 12 (see paragraph 3 of the training protocol). A prerequisite for terminated stimulation was detection of 5 or more spikes in the interval of 50–80 ms after stimulation was applied.

Results of cluster analysis of spontaneous burst activity recorded at stages 1, 4 and 6 of the training protocol are presented in figure 2. Before stimulation was applied to the culture, population bursts were formed by two big clusters, namely, 15 and 18. After stimulation with no feedback (stage 4), the number of bursts decreased in clusters 15 and 18 and increased in clusters 2 and 4. After stimulation with feedback (stage 6), the number of bursts in dominating clusters 15 and 18 remained on the intermediate level. The rest of the activity shifted to cluster 3 from clusters 2 and 4.

The patterns of the dominating spontaneous burst activity registered before and after stimulation were different (fig. 3). In that respect, clusters 3 and 4 were alike, but both differed from clusters 15 and 18, which overlapped to a great extent. Cluster 2 combined features of both sets of clusters.

DISCUSSION

According to our hypothesis, spontaneous burst activity of neuronal networks *in vitro* must be characterized by self-organization and repetitive activity patterns. Our experiment and results obtained by other researchers [13, 21, 22] confirm

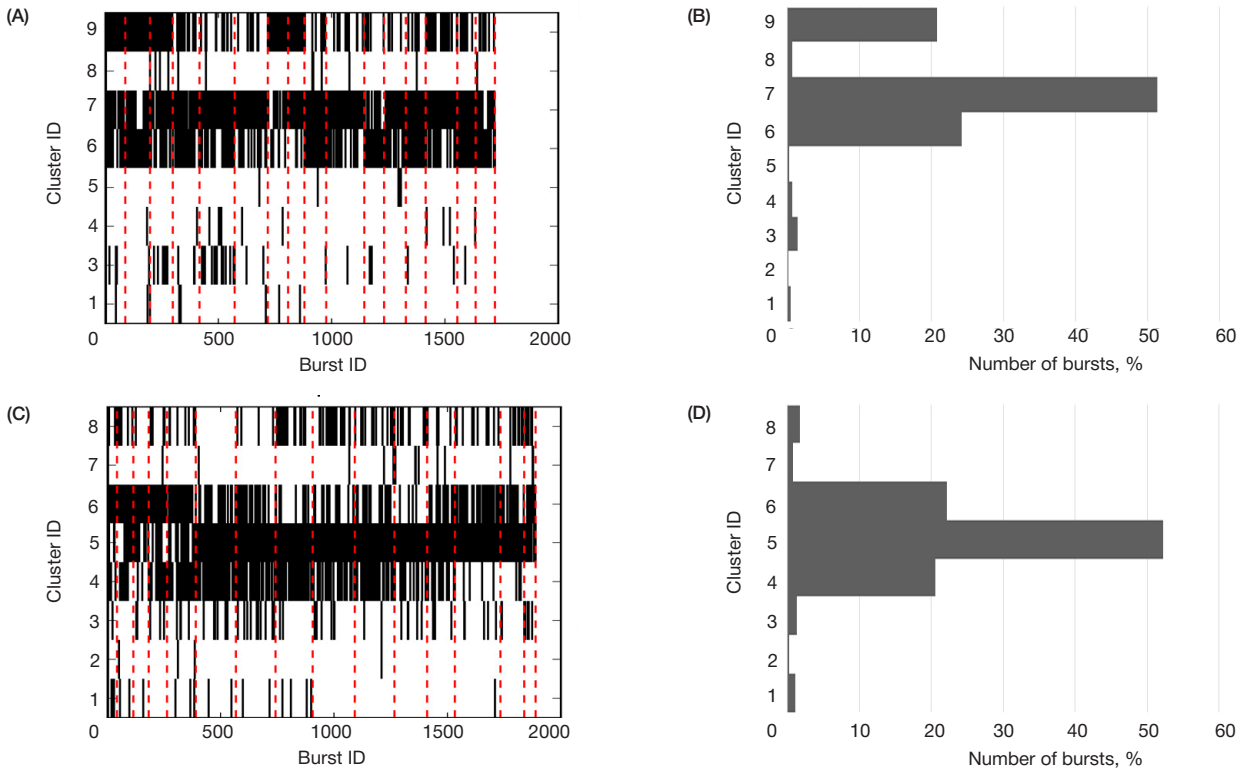

Fig. 1. Clustering of spontaneous burst activity of two neuronal cultures *in vitro* with the following IDs: 3035 **(A)** and 3040 **(C)**; percentage of bursts in clusters with the following IDs: 3035 **(B)** and 3040 **(D)**. Bursts are presented as they appeared. Red dotted lines represent days of culture development

that with culture growth, self-organization of neurons results in the emergence of the limited number of dynamic modes; each of those modes is characterized by its own activity pattern, i.e., an attractor. Thus, neurons *in vitro* can produce and maintain some activation sequence, which is necessary for memory trace retention.

We also made a supposition that patterns of spontaneous burst activity are resistant to external impact, including external electrical stimulation. Results of our study demonstrate that patterns do not depend on the presence of feedback during stimulation; what changes is the frequency of their occurrence. It allows us to make an assumption that in live neuronal networks, learning can be a result of variations of existing patterns with subsequent selection of a template used to solve the "problem". In the protocol used in this study, the "problem" was identified by means of external stimulation that can be switched off to provide a solution.

CONCLUSIONS

Study of spontaneous burst activity of neuronal networks *in vitro* showed that dynamics of network activity come down to a small number of attractors. Changes in burst activity registered after applying external stimulation showed that the dominating attractor of spontaneous activity does not disintegrate, but the variety of patterns increases. We can assume that learning is mediated by switching between the existing dynamic attractors of neuronal activity.

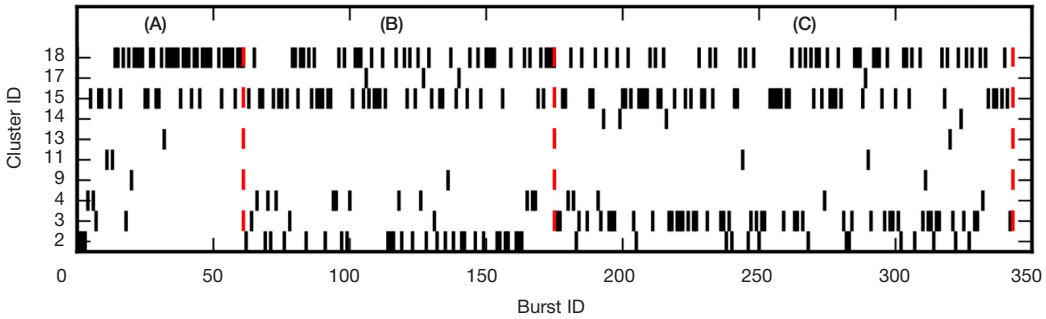

Fig. 2. Switching of activity patterns after stimulation without feedback and with feedback. **(A)** Before stimulation. **(B)** After stimulation without feedback. **(C)** After stimulation with feedback

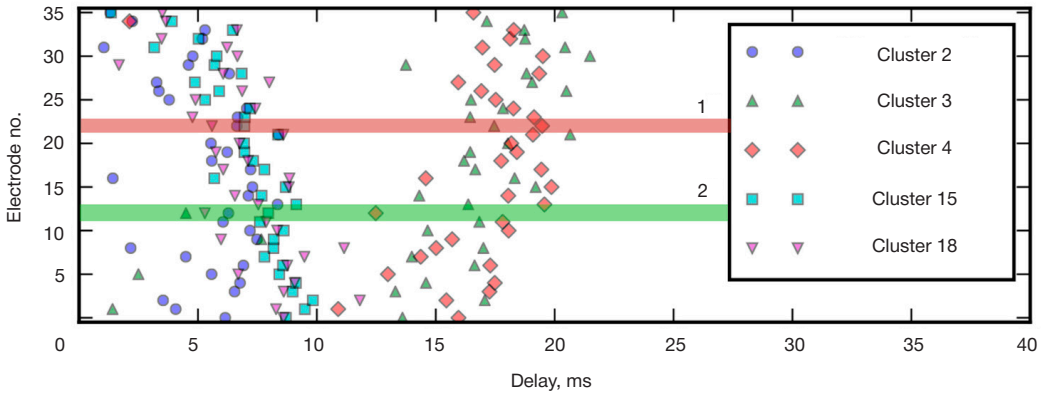

Fig. 3. Averaged burst feature vectors for clusters containing at least 5 % of all events shown in fig. 2. Green line (1) represents electrode 12, on which the culture was trained. Red line represents electrode 22, on which stimulation was performed

References

1. Velliste M, Perel S, Spalding MC, Whitford AS, Schwartz AB. Cortical control of a prosthetic arm for self-feeding. Nature. 2008 Jun 19; 453 (7198): 1098–101.
2. Wessberg J, Stambaugh CR, Kralik JD, Beck PD, Laubach M, Chapin JK, et al. Real-time prediction of hand trajectory by ensembles of cortical neurons in primates. Nature. 2000 Nov 16; 408 (6810): 361–5.
3. Serruya MD, Hatsopoulos NG, Paninski L, Fellows MR, Donoghue JP. Instant neural control of a movement signal. Nature. 2002 Mar 14; 416 (6877): 141–2.
4. Shannon RV. Advances in auditory prostheses. Curr Opin Neurol. 2012 Feb; 25 (1): 61–6.
5. Fernandes RA, Diniz B, Ribeiro R, Humayun M. Artificial vision through neuronal stimulation. Neurosci Lett. 2012 Jun 25; 519 (2): 122–8.
6. Hampson RE, Song D, Chan RH, Sweatt AJ, Riley MR, Gerhardt GA, et al. A nonlinear model for hippocampal cognitive prosthesis: memory facilitation by hippocampal ensemble stimulation. IEEE Trans Neural Syst Rehabil Eng. 2012 Mar; 20 (2): 184–97.
7. Josselyn SA, Kohler S, Frankland PW. Finding the engram. Nat Rev Neurosci. 2015 Sep; 16 (9): 521–34.
8. Quiroga RQ, Mukamel R, Isham EA, Malach R, Fried I. Human single-neuron responses at the threshold of conscious recognition. Proc Natl Acad Sci U S A. 2008 Mar 4; 105 (9): 3599–604.
9. Kermany E, Gal A, Lyakhov V, Meir R, Marom S, Eytan D. Tradeoffs and constraints on neural representation in networks of cortical neurons. J Neurosci. 2010 Jul 14; 30 (28): 9588–96.
10. Raichman N, Ben-Jacob E. Identifying repeating motifs in the activation of synchronized bursts in cultured neuronal networks. J Neurosci Methods. 2008 May 15; 170 (1): 96–110.
11. Shahaf G, Eytan D, Gal A, Kermany E, Lyakhov V, Zrenner C,

et al. Order-based representation in random networks of cortical neurons. PLoS Comput Biol. 2008 Nov; 4 (11): e1000228.
12. Xydas D, Downes JH, Spencer MC, Hammond MW, Nasuto SJ, Whalley BJ, et al. Revealing ensemble state transition patterns in multi-electrode neuronal recordings using hidden Markov models. IEEE Trans Neural Syst Rehabil Eng. 2011 Aug; 19 (4): 345–55.
13. Pimashkin A, Kastalskiy I, Simonov A, Koryagina E, Mukhina I, Kazantsev V. Spiking signatures of spontaneous activity bursts in hippocampal cultures. Front Comput Neurosci. 2011; 5: 46.
14. Shahaf G, Marom S. Learning in networks of cortical neurons. J Neurosci. 2001 Nov 15; 21 (22): 8782–8.
15. Marom S, Shahaf G. Development, learning and memory in large random networks of cortical neurons: lessons beyond anatomy. Q Rev Biophys. 2002 Feb; 35 (1): 63–87.
16. Li Y, Zhou W, Li X, Zeng S, Luo Q. Dynamics of learning in cultured neuronal networks with antagonists of glutamate receptors. Biophys J. 2007 Dec 15; 93 (12): 4151–8.
17. Stegenga J, Le Feber J, Marani E, Rutten WL. The effect of learning on bursting. IEEE Trans Biomed Eng. 2009 Apr; 56 (4): 1220–7.
18. le Feber J, Stegenga J, Rutten WL. The effect of slow electrical stimuli to achieve learning in cultured networks of rat cortical neurons. PloS One. 2010; 5 (1): e8871.
19. Wagenaar DA, Pine J, Potter SM. An extremely rich repertoire of bursting patterns during the development of cortical cultures. BMC Neurosci. 2006; 7: 11.
20. Sokal R, Michener C. A statistical method for evaluating systematic relationships. University of Kansas Science Bulletin. 1958; 38 (22): 1409–38.
21. Lebedev RD, Burtsev MS. Klasterizatsiya pachek spontannoy aktivnosti neyronal'noy kul'tury. In: Sbornik nauchnykh trudov Vserossiyskoy nauchno-tekhnicheskoy konferentsii «Neyroinformatika 2010» v 2-kh chastyakh. P. 1. Moscow: MEPhI; 2010. p. 296–303. Russian
22. Burtsev MS, Lebedev RD. Evolution of bursts onsets during the development of cortical cultures. FENS Abstr, vol. 5, 130.12, 2010.

Литература

1. Velliste M, Perel S, Spalding MC, Whitford AS, Schwartz AB. Cortical control of a prosthetic arm for self-feeding. Nature. 2008 Jun 19; 453 (7198): 1098–101.
2. Wessberg J, Stambaugh CR, Kralik JD, Beck PD, Laubach M, Chapin JK, et al. Real-time prediction of hand trajectory by ensembles of cortical neurons in primates. Nature. 2000 Nov 16; 408 (6810): 361–5.
3. Serruya MD, Hatsopoulos NG, Paninski L, Fellows MR, Donoghue JP. Instant neural control of a movement signal. Nature. 2002 Mar 14; 416 (6877): 141–2.
4. Shannon RV. Advances in auditory prostheses. Curr Opin Neurol. 2012 Feb; 25 (1): 61–6.
5. Fernandes RA, Diniz B, Ribeiro R, Humayun M. Artificial vision through neuronal stimulation. Neurosci Lett. 2012 Jun 25; 519 (2): 122–8.
6. Hampson RE, Song D, Chan RH, Sweatt AJ, Riley MR, Gerhardt GA, et al. A nonlinear model for hippocampal cognitive prosthesis: memory facilitation by hippocampal ensemble stimulation. IEEE Trans Neural Syst Rehabil Eng. 2012 Mar; 20 (2): 184–97.
7. Josselyn SA, Kohler S, Frankland PW. Finding the engram. Nat Rev Neurosci. 2015 Sep; 16 (9): 521–34.
8. Quiroga RQ, Mukamel R, Isham EA, Malach R, Fried I. Human single-neuron responses at the threshold of conscious recognition. Proc Natl Acad Sci U S A. 2008 Mar 4; 105 (9): 3599–604.
9. Kermany E, Gal A, Lyakhov V, Meir R, Marom S, Eytan D. Tradeoffs and constraints on neural representation in networks of cortical neurons. J Neurosci. 2010 Jul 14; 30 (28): 9588–96.
10. Raichman N, Ben-Jacob E. Identifying repeating motifs in the activation of synchronized bursts in cultured neuronal networks. J Neurosci Methods. 2008 May 15; 170 (1): 96–110.
11. Shahaf G, Eytan D, Gal A, Kermany E, Lyakhov V, Zrenner C, et al. Order-based representation in random networks of cortical neurons. PLoS Comput Biol. 2008 Nov; 4 (11): e1000228.
12. Xydas D, Downes JH, Spencer MC, Hammond MW, Nasuto SJ, Whalley BJ, et al. Revealing ensemble state transition patterns in multi-electrode neuronal recordings using hidden Markov models. IEEE Trans Neural Syst Rehabil Eng. 2011 Aug; 19 (4): 345–55.
13. Pimashkin A, Kastalskiy I, Simonov A, Koryagina E, Mukhina I, Kazantsev V. Spiking signatures of spontaneous activity bursts in hippocampal cultures. Front Comput Neurosci. 2011; 5: 46.
14. Shahaf G, Marom S. Learning in networks of cortical neurons. J Neurosci. 2001 Nov 15; 21 (22): 8782–8.
15. Marom S, Shahaf G. Development, learning and memory in large random networks of cortical neurons: lessons beyond anatomy. Q Rev Biophys. 2002 Feb; 35 (1): 63–87.
16. Li Y, Zhou W, Li X, Zeng S, Luo Q. Dynamics of learning in cultured neuronal networks with antagonists of glutamate receptors. Biophys J. 2007 Dec 15; 93 (12): 4151–8.
17. Stegenga J, Le Feber J, Marani E, Rutten WL. The effect of learning on bursting. IEEE Trans Biomed Eng. 2009 Apr; 56 (4): 1220–7.
18. le Feber J, Stegenga J, Rutten WL. The effect of slow electrical stimuli to achieve learning in cultured networks of rat cortical neurons. PloS One. 2010; 5 (1): e8871.
19. Wagenaar DA, Pine J, Potter SM. An extremely rich repertoire of bursting patterns during the development of cortical cultures. BMC Neurosci. 2006; 7: 11.
20. Sokal R, Michener C. A statistical method for evaluating systematic relationships. University of Kansas Science Bulletin. 1958; 38 (22): 1409–38.
21. Лебедев Р. Д., Бурцев М. С. Кластеризация пачек спонтанной активности нейрональной культуры. В сборнике: Сборник научных трудов Всероссийской научно-технической конференции «Нейроинформатика 2010» в 2-х частях. ч. 1. М.: НИЯУ МИФИ; 2010. с. 296–303.
22. Burtsev MS, Lebedev RD. Evolution of bursts onsets during the development of cortical cultures. FENS Abstr, vol. 5, 130.12, 2010.

STUDY OF ABLATED SURFACE SMOOTHNESS AND THERMAL PROCESSES IN RABBIT CORNEA TREATED WITH MICROSCAN-VISUM AND MICROSCAN-PIC EXCIMER LASER SYSTEMS

Kachalina GF, Takhchidi NCh ✉

Department for Clinical Research in Ophthalmology,
Clinical Research Center for Otorhinolaryngology, Moscow, Russia

In ophthalmology, excimer lasers are used for treating different refractive disorders. The performance of an excimer laser station can be assessed by a number of criteria, such as cornea surface smoothness after the ablation, differences between the diameter of the postoperative optical zone that received full correction and the diameter of the programmed optical zone, and cornea heating during the surgery. The article presents the results of the assessment of three Russian excimer laser systems: MicroScan-PIC 100 Hz, MicroScan-Visum 300 Hz and MicroScan-Visum 500 Hz (Optosystems Ltd.). The smoothness of the ablated surface was measured by New View – 5000 Zygo interferometer (Zygo Corporation, USA). Using PMMA plates, the ablated surface was formed tenfold with each laser as an imitation of the 3.0 D myopia surgical correction, with the optical zone diameter of 6 mm and the transition zone diameters of 2.3 mm for MicroScan-PIC 100 Hz and of 1.9 mm for MicroScan-Visum 300 Hz and MicroScan-Visum 500 Hz. Thermal processes in the cornea were studied in 15 grey chinchillas over 1 year old with a weight of 2–3 kg. With each of the laser systems, phototherapeutic keratectomy was performed on 5 eyes. The smoothest ablated surfaces were formed by MicroScan-Visum 500 Hz. Cornea temperature was the highest here (+ 3.95 °C by the end of treatment), but still within the range of values acceptable for modern scanning type lasers.

Keywords: excimer laser system, MicroScan-PIC 100 Hz, MicroScan-Visum 300 Hz, MicroScan-Visum 500 Hz, ablation, cornea, error of refraction

✉ **Correspondence should be addressed:** Nika Takhchidi
Volokolamskoe shosse, d. 30, str. 2, Moscow, Russia, 123182; nika-th@ya.ru

Received: 11.04.2016 **Accepted:** 14.04.2016

ИССЛЕДОВАНИЕ ГЛАДКОСТИ АБЛЯЦИОННОЙ ПОВЕРХНОСТИ И ТЕРМИЧЕСКИХ ПРОЦЕССОВ В РОГОВИЦЕ КРОЛИКА ПРИ РАБОТЕ ЭКСИМЕРЛАЗЕРНЫХ УСТАНОВОК «МИКРОСКАН-ВИЗУМ» И «МИКРОСКАН-ЦФП»

Г. Ф. Качалина, Н. Х. Тахчиди ✉

Научно-клинический отдел офтальмологии,
Научно-клинический центр оториноларингологии, Москва

Эксимерные лазеры используют в офтальмологии для лечения различных аномалий рефракции. Качество работы эксимерлазерной установки можно оценить по нескольким критериям: гладкости формируемой ею абляционной поверхности роговицы, соответствию диаметра полученной оптической зоны полной коррекции диаметру расчетной оптической зоны и нагреву роговицы в процессе операции. В статье представлены результаты оценки трех российских эксимерлазерных установок: «МикроСкан-ЦФП 100 Гц», «МикроСкан-Визум 300 Гц» и «МикроСкан-Визум 500 Гц» («Оптосистемы»). Гладкость абляционной поверхности, которую формировали десятикратно для каждого лазера на пластинах полиметилметакрилата, имитируя операцию коррекции миопии в 3,0 дптр и задавая диаметр оптической зоны в 6 мм и диаметр переходной зоны — в 2,3 мм для «МикроСкан-ЦФП 100 Гц» и в 1,9 мм для «МикроСкан-Визум 300 Гц» и «МикроСкан-Визум 500 Гц», измеряли с помощью интерферометра New View – 5000 Zygo (Zygo Corporation, США). Термические процессы в роговице изучали на 15 кроликах породы шиншилла серая в возрасте старше одного года и живой массой 2–3 кг. Каждым лазером проводили фототерапевтическую кератэктомию на 5 глазах. Установка «МикроСкан-Визум 500 Гц» формировала наиболее гладкие абляционные поверхности. Нагрев роговицы при ее использовании был наибольшим (+ 3,95 °С к концу операции), но находился в пределах значений, допустимых для современных лазеров сканирующего типа.

Ключевые слова: эксимерлазерная установка, МикроСкан-ЦФП 100 Гц, МикроСкан-Визум 300 Гц, МикроСкан-Визум 500 Гц, абляция, роговица, аномалия рефракции

✉ **Для корреспонденции:** Ника Христовна Тахчиди
123182, г. Москва, Волоколамское шоссе, д. 30, стр. 2; nika-th@ya.ru

Статья поступила: 11.04.2016 **Принята к печати:** 14.04.2016

According to the World Health Organization, the number of people with refractive errors has been steadily increasing in recent decades. Data obtained from various authors indicate that there is about 27 to 45 % prevalence of myopia and myopic astigmatism among people of working age in Russia, US and EU [1]. However, there has been an improvement both in the traditional (spectacle and contact lens correction) and in the surgical methods of correction of refractive errors.

Keratorefractive surgery with various lasers has improved rapidly [2–4].

In recent years, ophthalmologists from different countries have gained extensive clinical experience in the use of excimer laser for correction of refractive errors [3, 5–11]. In Russia, researchers are working to design excimer laser systems and introduce them into clinical practice. Since the late 1980s, Eye Microsurgery, an intersectoral research & technology complex, has created excimer lasers and deployed them into clinical practice. This complex has been doing this in cooperation with laser manufacturer – Physics Instrumentation Center of the General Physics Institute, Russian Academy of Sciences and Optosystems. Excimer laser system MicroScan-PIC was presented in 2000. Along with operations based on LASIK (laser in situ Keratomileusis) and TransPRK (transepithelial photorefractive keratectomy) standard technologies, the laser allows to perform personalized operations based on corneal topography and aberrometry data. Analysis of clinical and functional results of such operations showed that they are of high predictability, stability and safety [12].

Several criteria are used for objective assessment of the quality of excimer laser systems. One of them is the smoothness of corneal surface formed by the excimer laser. A smoother corneal surface facilitates normal course of corneal epithelialization after surgery and minimizes the likelihood of fibroplasia [13]. Quantitative characteristics of smoothness allow to obtain a measurement with interferometric microscopes from Zygo Corporation (USA). A number of investigators have shown that surface smoothness is higher in flying spot scanning lasers than in full-aperture lasers and lasers that use scanning slit and stopped down ablation formation system [14,15].

Another important criterion is the association of the diameter of the resulting optical zone of full correction with the computed optical zone diameter specified by the manufacturer in the computing program of the laser system. According to O'Donnel et al. [15], the ablation zone diameter obtained during excimer laser surgery using stopped down forming system is usually less than that indicated by the manufacturer. According to the researchers, the greater the optical and transition zone of influence, the better the functional outcome and the lesser the likelihood of regression of postoperative effect. A smaller optical zone can cause very unpleasant sensations in patients in lowered or increased illumination [16].

Another important indicator of the quality of excimer lasers is that there is no significant increase in corneal temperature during surgery. Despite the fact that excimer lasers are referred to as “cold”, they can break molecular bonds in cells and release energy that increases the corneal temperature [17,18]. The temperature increase cannot cause collagen denaturation but may affect the activity of keratocytes, postoperative healing and development of fibroplasia. Flying spot scanning lasers can significantly reduce possible heating of the cornea thanks to the small beam diameter and scanning algorithm in which the local areas of the corneal tissue, which are at a distance from each other, are ablated. Therefore, the cornea has no enough time to increase its temperature significantly [19, 20].

Efficiency in clinical practice is of course the main indicator of the quality of an excimer laser system. However, based on the criteria given above, the technical features and prospects for the use of the device at the pre-clinical study stage can be identified.

Next-generation device MicroScan-Visum is a modification of the MicroScan-PIC laser system and developed in two models — 300 and 500 Hz scanning frequencies. The aim of our study was to evaluate the surface ablation smoothness formed on polymeric materials and to investigate the thermal processes in a rabbit cornea treated with the studied laser systems during phototherapeutic keratectomy (PTK).

METHODS

An experiment to assess ablation surface smoothness was carried out using polymethylmethacrylate (PMMA) plates. In the control computer of each of the three test excimer lasers — MicroScan-PIC 100 Hz, MicroScan-Visum 300 Hz and MicroScan-Visum 500 Hz — myopia correction surgery was set in 3.0 diopter with the same optical zone diameter 6 mm but different transition zone diameters — 2.3 mm for MicroScan-PIC 100 Hz and 1.9 mm for MicroScan-Visum 300 Hz and MicroScan-Visum 500 Hz (this was due to different excimer laser light spot diameters — 1.15 and 0.95 mm respectively). Ten lenses for each of the lasers was formed on the plates, after which all the lenses were measured using interference microscope New View – 5000 Zygo. The following indicators characterizing the quality of the formed lens surface were identified:

RMS — root mean square deviation of the surface points relative to the average height across the study area;

PV — distance between the highest and lowest points of the study area;

Ra — average deviation of surface points from the middle surface.

Moreover, it was considered that the better the surface smoothness, the smaller the value of these indicators would be.

Thermographic analysis of corneal temperature changes was conducted in 15 gray chinchilla rabbits, more than one year old and with live weight of 2–3 kg. The experiment was approved by the Intercollegiate Ethics Committee (Minutes No 10–12 of 18 October 2012). Each of the three laser systems was used to operate on 5 eyes (one eye per animal). 15 min before the surgery, the rabbits were administered with 2 ml of relanium solution. The surgery was performed under local anesthesia (triple instillation of 1 % inokain solution). The estimated ablation depth during PTK was 52 microns.

Thermal imaging complex Thermo View Ti30 (Raytek, USA) was used to measure the corneal temperature. Imaging was carried out in a room with ambient temperature of 16.7 °C at a distance of 60–70 cm with frequency of 1 Hz and up to 0.1 °C accuracy. On the PC, thermal imager data were converted to thermographic map using a software tool supplied with the device, and the maximum and minimum corneal temperatures during the surgery were determined. Corneal emissivity was set at 0.93 (like water), i.e. it was considered that 0.93 of the total corneal radiation enters the device and the device adds 0.07 when calculating the temperature. For example, if the temperature is 37.3 °C for k = 0.93, then temperature will be equal to 36.1 °C for k = 1 for the same thermogram.

Data was statistically processed using software programs Statistica 6.0 (StatSoft, USA) and Excel 2003. Variation statistics methods were used. The results were presented as arithmetic mean (M) and standard deviation (σ). Student's t-test for independent cases was used to compare the means and evaluate the significance of differences ($p = 0.05$).

RESULTS

The results of comparative analysis of the quality of ablation surface of lens are presented in table 1. Laser system MicroScan-Visum 500 Hz yielded the best smoothness.

Table 1. Indicators of the ablation surface quality of lens formed on polymethylmethacrylate plates using radiation from MicroScan-PIC 100 Hz, MicroScan-Visum 300 Hz and MicroScan-Visum 500 Hz systems, nm (M ± δ, p <0.05)

Laser system	RMS	PV	Ra
MicroScan-PIC 100 Hz	392 ± 75	6454 ± 1752	311 ± 68
MicroScan-Visum 300 Hz	351 ± 35	2754 ± 298	282 ± 25
MicroScan-Visum 500 Hz	338 ± 25	2960 ± 51	268 ± 20

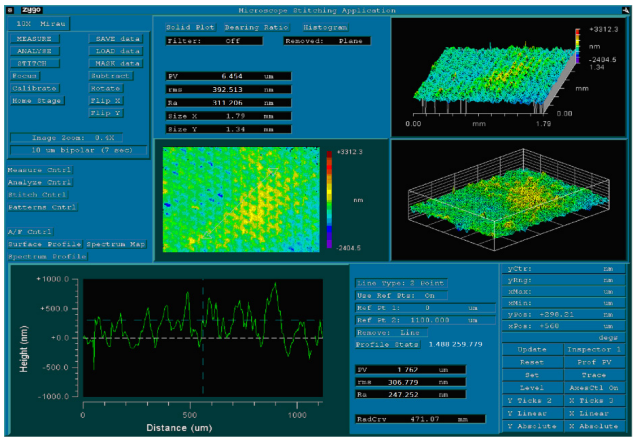

Fig. 1. Example of measurement of the smoothness of the ablation surface formed using MicroScan-PIC 100 Hz by interferometer New View – 5000 Zygo (Ra = 311 nm)

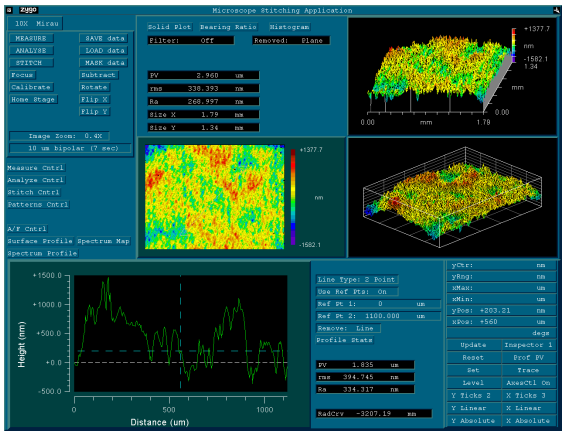

Fig. 2. Example of measurement of the smoothness of the ablation surface formed using MicroScan-Visum 500 Hz by interferometer New View – 5000 Zygo (Ra = 268 nm)

Fig. 1 and 2 show examples of measurement for MicroScan-PIC 100 Hz and MicroScan-Visum 500 Hz systems.

An example thermal map obtained during excimer laser ablation on MicroScan-PIC 100 Hz is shown in fig. 3, while the results of measurement of the transverse temperature profile for all the laser systems studied are presented in fig. 4.

For MicroScan-PIC 100 Hz, the average corneal temperature prior to laser exposure was 31.04 ± 0.63 °C, the maximum temperature at the end of surgery was 32.21 ± 0.68 °C, while the temperature change was 1.17 ± 0.05 °C (table 2). For MicroScan-Visum 300 Hz and MicroScan-Visum 500 Hz laser systems, the figures were 31.82 ± 0.87, 33.24 ± 1.21 and 1.42 ± 0.34 °C, and 31.02 ± 0.47, 34.97 ± 1.36 and 3.95 ± 0.89 °C, respectively.

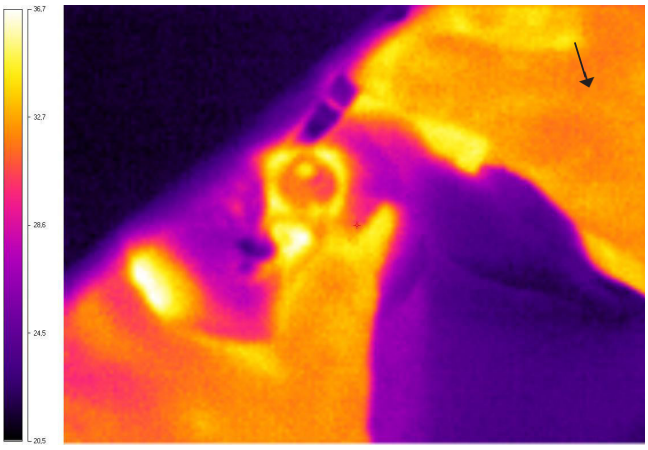

Fig. 3. Example of thermographic map during phototherapeutic keratectomy using MicroScan-PIC 100 Hz (rabbit cornea is marked by an arrow)

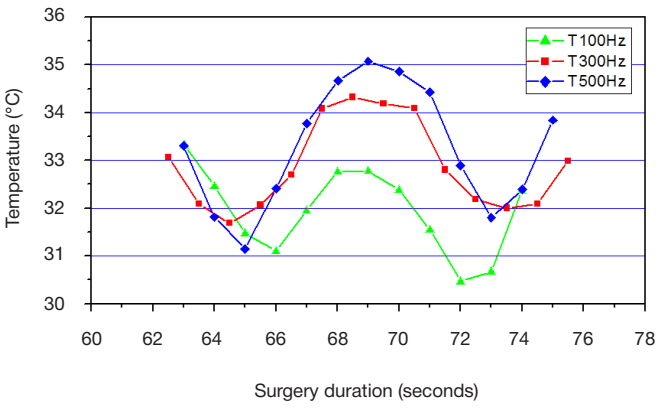

Fig. 4. Transverse temperature profiles for excimer laser systems MicroScan-PIC 100 Hz (green curve), MicroScan-Visum 300 Hz (red curve) and MicroScan-Visum 500 Hz (blue curve)

DISCUSSION

Laser system MicroScan-Visum 500 Hz yielded the smoothest ablative surfaces. Although corneal heating obtained with this laser was the highest (+3.95 °C by the end of surgery), the value was within acceptable range. For example, during LASIK surgery for treatment of high myopia Sph -9,25D using popular laser Schwind AMARIS 500 Hz (SCHWIND eye-tech-solutions, Germany), the corneal temperature increased by 3.73 °C [21].

CONCLUSIONS

All the three laser systems studied can create a high-quality ablation surface. However, the MicroScan-Visum 500 Hz system gave the best result. The laser yielded the highest corneal heating during phototherapeutic keratectomy in rabbits, but the value did not exceed the permissible values. After the study, MicroScan-Visum 500 Hz was recommended for clinical research.

Table 2. Dynamics of thermal processes in a rabbit cornea during phototherapeutic keratectomy using laser systems MicroScan-PIC 100 Hz, MicroScan-Visum 300 Hz and MicroScan-Visum 500 Hz, °C (M ± δ, p<0.05)

Laser system	Initial corneal temp.	Maximum corneal temp. at the end of surgery	Increase in temp.
MicroScan-PIC 100 Hz	31,04 ± 0,63	32,21 ± 0.68	1,17 ± 0,05
MicroScan-Visum 300 Hz	31,82 ± 0,87	33,24 ± 1,21	1,42 ± 0,34
MicroScan-Visum 500 Hz	31,02 ± 0,47	34,97 ± 1,36	3,95 ± 0,89

References

1. Libman ES, Shakhova EV. Slepota, slabovidenie i invalidnost' po zreniyu v rossiyskoy federatsii. In: Likvidatsiya ustranimoy slepoty: Vsemirnaya initsiativa VOZ: Materialy Rossiyskogo mezhregional'nogo simpoziuma; 2013 Apr 22–; Ufa, Russia. p. 38–42.
2. Avetisov SE, Mamikonyan VR. Keratorefraktsionnaya khirurgiya. Moscow: IPO "Poligran"; 1993. 120 p.
3. Balashevich LI. Tekhnika eksimerlazernoy keratektomii. Refraktsionnaya khirurgiya. 2002; 93–4.
4. Fedorov SN, Semenov AD, Kharizov AA, et al. Opyt ispol'zovaniya eksimernogo lazera v refraktsionnoy khirurgii blizorukosti. In: Tezisy dokladov Mezhdunarodnogo simpoziuma po refraktsionnoy khirurgii, implantatsii IOL; 1991; Moscow. p. 12.
5. Alisov IA. Eksimernyy lazer "Profil'-500" v korrektsii slozhnogo miopicheskogo astigmatizma [dissertation]. Moscow; 2002.
6. Kachalina GF. Khirurgicheskaya tekhnologiya transepitelial'noy fotorefraktivnoy keratektomii pri miopii na eksimerlazernoy ustanovke "Profil'-500" [dissertation]. Moscow: IRTC Eye Microsurgery; 2000.
7. Kishkin YuI. Eksimernyy lazer v korrektsii ostatochnoy blizorukosti posle radial'noy keratotomii [dissertation]. Moscow: IRTC Eye Microsurgery; 1998.
8. Kurenkov VV. Fotorefraktsionnaya keratektomiya i intrastromal'naya keratektomiya: Rukovodstvo po eksimerlazernoy khirurgii rogovitsy. Moscow: Izdatel'stvo RAMN; 2002. p. 197–200.
9. Tarutta EP, Smirnova TS, Khodzhabekyan NV. Dvukhletniy opyt FRK s pomoshch'yu eksimernogo lazera MEL-60. In: Materialy VII S"ezda oftal'mologov Rossii; 2000 May 16–20; Moscow. p. 298–9.
10. Esquenazi S, Mendoza A. Two-year follow-up of LASIK for hyperopia. J Refract Surg. 1999; 15 (6): 648–52.
11. Knorz M, Wiesinger B, Liermann A, Seiberth, Liesenhoff H. Laser in situ keratomileusis for moderate and high myopia and myopic astigmatism. Ophthalmology. 1998; 105 (5): 932–40.
12. Doga AV. Eksimerlazernaya refraktsionnaya mikrokhirurgiya rogovitsy na baze skaniruyushchey ustanovki «Mikroskan» [dissertation]. Moscow: IRTC Eye Microsurgery; 2004.
13. Liang FQ, Geasey SD, del Cerro M, Aquavella JV. A new procedure for evaluating smoothness of corneal surface following 193-nm excimer laser ablation. Corneal Surg. 1992; 8 (6): 459–65.
14. Argento C, Valenzuela G, Huck H, Cremona G, Cosentino MJ, Gale MF. Smoothness of ablation on acrylic by four different excimer lasers. J Refract Surg. 2001; 17 (1): 43–5.
15. O´Donnel F., Tang F., Han X., Chen D., Hwang M. PRK ablation zone anatomy. In: Book of abstract American Society of Cataract and Refractive Surgery Meeting; 1995 Apr 1–5; San Diego, USA.
16. O´Brart D, Corbett M, Verma S, et al. An investigation to determine the effects of ablation diameter, depth and profile on the outcome of excimer laser photorefractive keratectomy Invest. Ophthalmol Vis Sci. 1995; 36 (Suppl): S1063.
17. Bende T, Seiler T, Wollensak J. Side effects in excimer corneal surgery: corneal thermal gradients. Graefes Arch Clin Exp Ophthalmol. 1988; 226 (3): 277–80.
18. Berns MW, Liaw LH, Oliva A, Andrews JJ, Rasmussen RE, Kimel S. An acute light and electron microscopic study of ultraviolet 193-nm excimer laser corneal incisions. Ophthalmology. 1988; 95 (10): 1422–33.
19. Kornilovskiy IM, Dorri AM, Pavlenko VV. Izmeneniya temperatury rogovitsy pri FRK i lokal'noy gipotermii. In: Materialy IV mezhdunarodnoy konferentsii «Klinicheskie rezul'taty primeneniya eksimernogo lazera EC-5000 (NIDEK)». 1999; Moscow. p. 8.
20. Chatterjee A, Shah S, Bonshek R, et al. Relationship of histological change to corneal temperature change following PRK. J Refract Corneal Surg. 1997; 13 (Suppl): S462–3.
21. Schwind Press Release. Thermodynamic measurements confirm high safety of the SCHWIND AMARIS' intelligent thermal effect control. Kleinostheim, Germany; 2010 Apr. Available from: http://www.eye-tech-solutions.com/en/home/information-centre/press-centre.

Литература

1. Либман Е. С., Шахова Е. В. Слепота, слабовидение и инвалидность по зрению в российской федерации. В сборнике: Ликвидация устранимой слепоты: Всемирная инициатива ВОЗ: Материалы Российского межрегионального симпозиума; 22–23 апреля 2003 г.; Уфа. с. 38–42.
2. Аветисов С. Э., Мамиконян В. Р. Кераторефракционная хирургия. М.: ИПО «Полигран»; 1993. 120 с.
3. Балашевич Л. И. Техника эксимерлазерной кератэктомии. Рефракционная хирургия. 2002; 93–4.
4. Федоров С. Н., Семенов А. Д., Харизов А. А. и др. Опыт использования эксимерного лазера в рефракционной хирургии близорукости. В сборнике: Тезисы докладов Международного симпозиума по рефракционной хирургии, имплантации ИОЛ; 1991; Москва. с. 12.
5. Алисов И. А. Эксимерный лазер «Профиль-500» в коррекции сложного миопического астигматизма [диссертация]. Москва; 2002.
6. Качалина Г. Ф. Хирургическая технология трансэпителиальной фоторефрактивной кератэктомии при миопии на эксимерлазерной установке «Профиль-500» [диссертация]. Москва: Межотраслевой научно-технический комплекс «Микрохирургия глаза»; 2000.
7. Кишкин Ю. И. Эксимерный лазер в коррекции остаточной близорукости после радиальной кератотомии [диссертация]. Москва: Межотраслевой научно-технический комплекс «Микрохирургия глаза»; 1998.
8. Куренков В. В. Фоторефракционная кератэктомия и интрастромальная кератэктомия: Руководство по эксимерлазерной хирургии роговицы. М.: Издательство РАМН; 2002. с. 197–200.
9. Тарутта Е. П., Смирнова Т. С., Ходжабекян Н. В. Двухлетний опыт ФРК с помощью эксимерного лазера MEL-60. В сборнике: Материалы VII Съезда офтальмологов России; 16–20 мая 2000 г.; Москва. с. 298–9.
10. Esquenazi S, Mendoza A. Two-year follow-up of LASIK for hyperopia. J Refract Surg. 1999; 15 (6): 648–52.
11. Knorz M, Wiesinger B, Liermann A, Seiberth, Liesenhoff H. Laser in situ keratomileusis for moderate and high myopia and myopic astigmatism. Ophthalmology. 1998; 105 (5): 932–40.
12. Дога А. В. Эксимерлазерная рефракционная микрохирургия роговицы на базе сканирующей установки «Микроскан» [диссертация]. Москва: Межотраслевой научно-технический комплекс «Микрохирургия глаза»; 2004.
13. Liang FQ, Geasey SD, del Cerro M, Aquavella JV. A new procedure

for evaluating smoothness of corneal surface following 193-nm excimer laser ablation. Corneal Surg. 1992; 8 (6): 459–65.
14. Argento C, Valenzuela G, Huck H, Cremona G, Cosentino MJ, Gale MF. Smoothness of ablation on acrylic by four different excimer lasers. J Refract Surg. 2001; 17 (1): 43–5.
15. O´Donnel F., Tang F., Han X., Chen D., Hwang M. PRK ablation zone anatomy. In: Book of abstract American Society of Cataract and Refractive Surgery Meeting; 1995 Apr 1–5; San Diego, USA.
16. O´Brart D, Corbett M, Verma S, et al. An investigation to determine the effects of ablation diameter, depth and profile on the outcome of excimer laser photorefractive keratectomy Invest. Ophthalmol Vis Sci. 1995; 36 (Suppl): S1063.
17. Bende T, Seiler T, Wollensak J. Side effects in excimer corneal surgery: corneal thermal gradients. Graefes Arch Clin Exp Ophthalmol. 1988; 226 (3): 277–80.
18. Berns MW, Liaw LH, Oliva A, Andrews JJ, Rasmussen RE, Kimel S. An acute light and electron microscopic study of ultraviolet 193-nm excimer laser corneal incisions. Ophthalmology. 1988; 95 (10): 1422–33.
19. Корниловский И. М., Дорри А. М., Павленко В. В. Изменения температуры роговицы при ФРК и локальной гипотермии. В сборнике: Материалы IV международной конференции «Клинические результаты применения эксимерного лазера EC-5000 (NIDEK)». 1999; Москва. с. 8.
20. Chatterjee A, Shah S, Bonshek R, et al. Relationship of histological change to corneal temperature change following PRK. J Refract Corneal Surg. 1997; 13 (Suppl): S462–3.
21. Schwind Press Release. Thermodynamic measurements confirm high safety of the SCHWIND AMARIS' intelligent thermal effect contro. Kleinostheim, Germany; 2010 Apr. Доступно по ссылке: http://www.eye-tech-solutions.com/en/home/information-centre/press-centre.

LAPAROSCOPIC RESECTION OF THE HORSESHOE KIDNEY FOR RENAL CELL CARCINOMA

Muradyan AG[1,4] ✉, Vorobyev NV[2], Kostin AA[3,4], Tolkachev AO[2], Volchenko NN[5], Popov SV[4], Mamontova IS[6]

[1] Department of Urology and Surgical Nephrology, Medical College, Peoples' Friendship University of Russia, Moscow, Russia

[2] Oncourology Department, Hertzen Moscow Cancer Research Institute, a branch of the Medical Radiological Research Centre, Moscow, Russia

[3] Department of Urology, Oncology and Radiology, Faculty of advanced training for health workers, Peoples' Friendship University of Russia, Moscow, Russia

[4] Medical Radiological Research Centre, Moscow, Russia

[5] Department of Oncourology, Hertzen Moscow Cancer Research Institute, a branch of the Medical Radiological Research Centre, Moscow, Russia

[6] Department of radiology, Hertzen Moscow Cancer Research Institute, a branch of the Medical Radiological Research Centre, Moscow, Russia

Renal fusion is one of the most common kidney anomalies. The most frequent is horseshoe kidney, characterized by a fusion of the poles (typically the lower poles) of the kidneys. We described a clinical case of a malignant tumor in the right half of the horseshoe kidney (stage 1 cancer, CT1aN0M0) in a man aged 65 years, who underwent laparoscopic resection. It was shown that laparoscopy is no less efficient than open surgery. However, in planning the operation, it is necessary to use spiral computed tomography for three-dimensional reconstruction of the organ and identification of its anatomical features caused by aberrant blood supply to horseshoe kidney.

Keywords: horseshoe kidney, renal cell carcinoma, laparoscopic resection, laparoscopy

✉ **Correspondence should be addressed:** Avetik Muradyan
ul. Miklukho-Maklaya, d. 8, Moscow, Russia, 117997; mdmuradyan@gmail.com

Received: 29.02. 2016 **Accepted:** 04.04.2016

ЛАПАРОСКОПИЧЕСКАЯ РЕЗЕКЦИЯ ПОДКОВООБРАЗНОЙ ПОЧКИ ПО ПОВОДУ ПОЧЕЧНОКЛЕТОЧНОГО РАКА

А. Г. Мурадян[1,4] ✉, Н. В. Воробьев[2], А .А. Костин[3,4], А. О. Толкачев[2], Н. Н. Волченко[5], С. В. Попов[4], И. С. Мамонтова[6]

[1] Кафедра урологии и оперативной нефрологии, медицинский институт, Российский университет дружбы народов, Москва

[2] Отделение онкоурологии, Московский научно-исследовательский онкологический институт имени П. А. Герцена – филиал Национального медицинского исследовательского радиологического центра, Москва

[3] Кафедра урологии, онкологии, радиологии, факультет повышения квалификации медицинских работников, Российский университет дружбы народов, Москва

[4] Национальный медицинский исследовательский радиологический центр, Москва

[5] Отделение онкоцитологии, Московский научно-исследовательский онкологический институт имени П. А. Герцена – филиал Национального медицинского исследовательского радиологического центра, Москва

[6] Отделение рентгенодиагностики, Московский научно-исследовательский онкологический институт имени П. А. Герцена – филиал Национального медицинского исследовательского радиологического центра, Москва

Сращение почек — одна из наиболее распространенных почечных аномалий. Чаще всего встречается подковообразная почка, которая характеризуется сращением полюсов органа, как правило — нижних. Нами описан клинический случай злокачественной опухоли в правой половине подковообразной почки (рак I стадии cT1aN0M0) у мужчины 65 лет, которому была выполнена лапароскопическая резекция. Было показано, что лапароскопия является не менее эффективным методом, чем открытое хирургическое вмешательство. Однако при планировании операции необходимо использовать спиральную компьютерную томографию для трехмерной реконструкции органа и выявления его анатомических особенностей, вызванных аберрантным кровоснабжением подковообразной почки.

Ключевые слова: подковообразная почка, почечноклеточный рак, лапароскопическая резекция, лапароскопия

✉ **Для корреспонденции:** Аветик Гагикович Мурадян
117997, г. Москва, ул. Миклухо-Маклая, д. 8; mdmuradyan@gmail.com

Статья поступила: 29.02.2016 **Статья принята к печати:** 04.04.2016

The incidence of renal cell cancer has been rising over the decades. In Russia, kidney cancer (most commonly renal cell carcinoma, RCC) accounts for 3.9 % of all malignant tumors. The country recorded 8,430 deaths from the disease in 2014 and 22,234 new kidney cancer patients were revealed [1]. If RCC is diagnosed at clinical stage T1 [2], then partial nephrectomy — the gold standard of treatment for renal tumors smaller than 4 cm in diameter — can be effectively performed. It should be noted that recent years have witnessed an increase in the number of laparoscopic and robotic surgeries in this group of patients in recent years.

Congenital anomalies of the kidney and urinary tract are common in about 3.3–11 % of the population [3]. According to autopsy data, renal fusion accounts for 16.5 % of all kidney anomalies — 1 in every 425–700 people. The number of men with such anomalies is twice higher than women. The most common and clinically significant type of renal fusion is the horseshoe kidney, which is characterized by the fusion of the lower poles (in about 90 % of cases) and rarely of the upper poles, causing the joined kidneys to take a U-shape form, resembling a horseshoe. In addition, each kidney has its own ureter emptying into the bladder and supply vessels [4].

Diagnosing renal anomalies of shape at the present stage is not difficult since ultrasound imaging can identify the presence and type of abnormal fusion. Intravenous contrast-enhanced computed tomography scan provides more complete information about the state of the renal parenchyma, blood supply, urinary tract, and relationship with neighboring organs. So, according to studies, horseshoe kidney has abnormal blood flow in 70–84.3 % of cases [5].

Description of clinical case

Patient V., 65 years old, came to the Hertzen Moscow Cancer Research Institute (HMCRS) with previously identified space-occupying lesions of the right kidney.

From the patient's history, it was known that the patient had been feeling sick since August 2015 when he experienced increased body temperature of up to 38.5–40 °C and was hospitalized at the infectious department of a medical unit in Chelyabinsk. Ultrasound imaging was used to examine the abdominal cavity, which identified a tumor in the right kidney. Afterwards, the patient decided to visit HMCRS for treatment.

The patient has a hereditary burden: the father suffered from lung cancer. Among the comorbidities are stage II hypertension, type 2 diabetes (decompensation stage), cirrhosis of the liver caused by toxins (class B according to Child-Pugh score), portal hypertension, esophageal varices complicated by bleeding for which endoscopic ligation was performed in 2014.

A tumor of 34 x 35 x 35 mm in size without any signs of invasion into the pyelocaliceal system was found through ultrasound imaging and spiral computed tomography scan of the abdomen and retroperitoneal space at the border of the upper and lower third of the right kidney on the front surface. Besides, renal fusion in the lower pole region was identified. The defect detected was a medical finding since it had no clinical manifestations in the patient. The RENAL nephrometry score was 4a (fig. 1, 2).

No regional and distant metastasis were found by assessment of the prevalence of tumoral process. Diagnosis: tumor in the right half of horseshoe kidney, stage I, cT1aN0M0.

Laparoscopic resection of the right half of the horseshoe kidney was performed in October 19, 2015. After pneumoperitoneum was created using a Veress needle, three trocars were inserted by a standard technique [6]. During inspection on the border of the upper and middle third of the right half of the horseshoe kidney along the lateral surface, a tumor mass, 4 cm maximum size, was identified. The renal hilum was mobilized, and a clamp was imposed on it through a counteropening. A cold scissors was used to resect the tumor within healthy tissues. Kidney wound was cut down by atraumatic suture using non-absorbable clips Absolok (Ethicon, Belgium, USA) (fig. 3). During the operation, we used tools and devices from endoscope manufacturer Karl Storz (Germany).

The surgery lasted for 160 minutes, anoxia period lasted for 20 minutes, and there was 400 ml of blood lost. The postoperative period was uneventful. Glomerular filtration rate at the preoperative stage was 87 mL/min, at the 4th day — 59 mL/min, and 8th day — 67 mL/min. The patient was discharged on the 9th day in a satisfactory condition.

Morphological study revealed a clear-cell renal cell carcinoma G1, without extension to the perirenal fat and with no tumor cells on the resection edge (R0) (fig. 4).

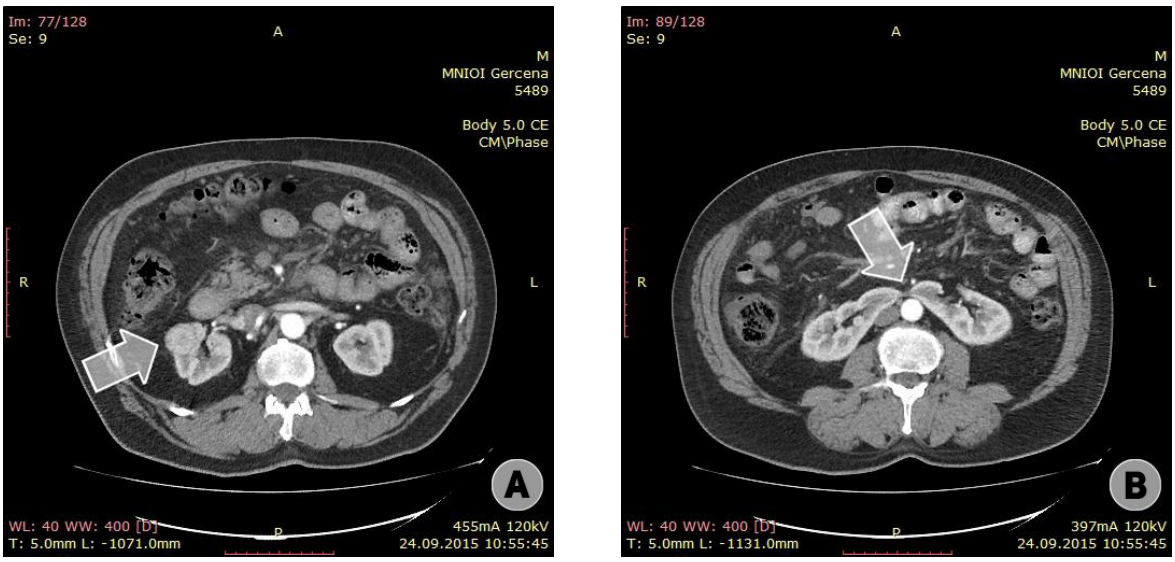

Fig. 1. Sections of the arterial phase of spiral CT scan of the abdominal cavity. **(A)** Tumor in the right half of the horseshoe kidney (arrow) on the border between the upper and middle third. **(B)** Isthmus of the horseshoe kidney (arrow) at L_{II} level

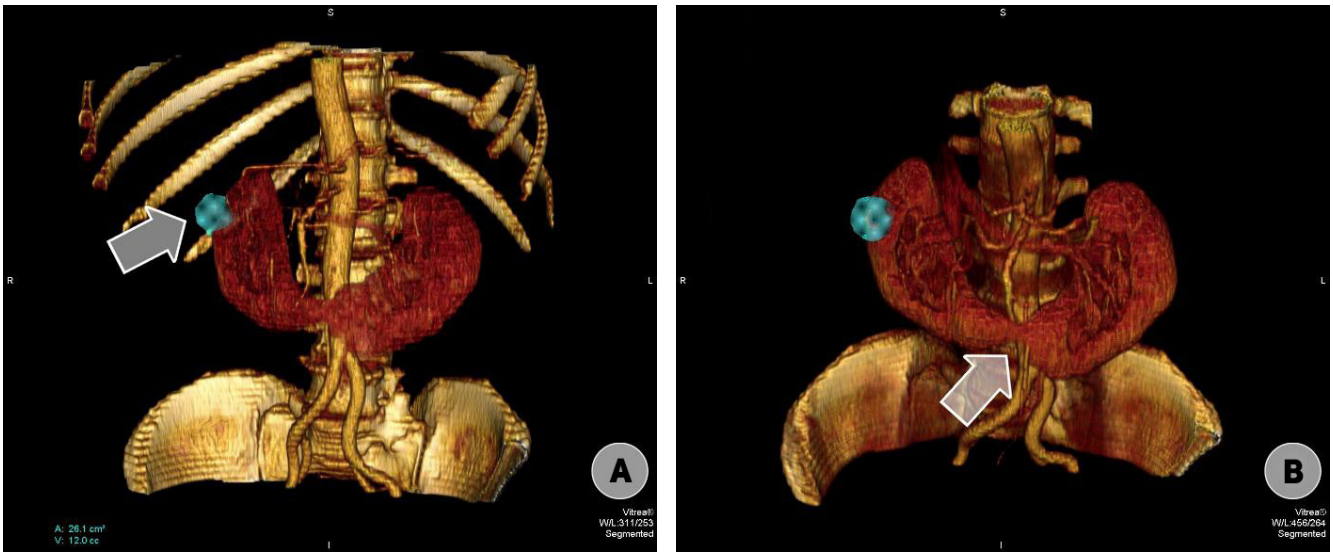

Fig. 2. Three-dimensional reconstruction of the kidneys and great vessels using spiral computed tomography scan. **(A)** Tumor in the right half of the horseshoe kidney (arrow). **(B)** Isthmus of the horseshoe kidney (arrow)

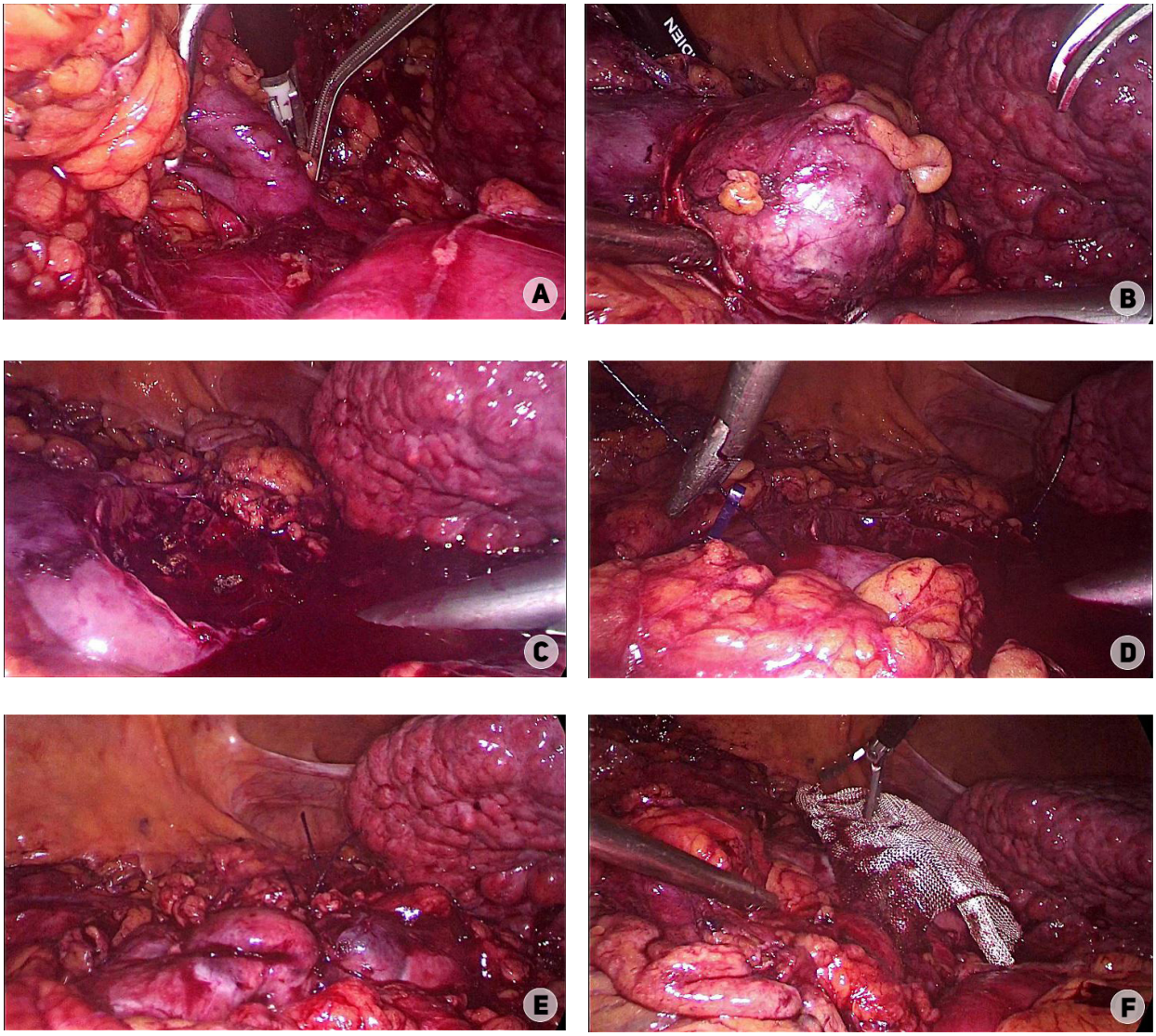

Fig. 3. Surgery stages. **(A)** Imposition of clamp in the renal blood vessels. **(B)** Tumor in the right half of the horseshoe kidney. **(C)** Site of the removed tumor. **(D)** Sealing of kidney injury. **(E)** Appearance of resected kidney. **(F)** Covering of the kidney injury with hemostatic mesh

Discussion of clinical case

Horseshoe kidney was first described by da Carpi in 1522 and in more details by Morgagni in 1761 [7]. Despite the fact that such abnormality often has no clinical manifestations, in some cases it goes with UPJ strictures and urolithiasis [8, 9]. Horseshoe kidney is found in 20 % of Down's syndrome cases and 60 % of Turner syndrome cases, as well as in Patau, Gardner and Edwards syndromes [10, 11]. According to Glenn, horseshoe kidney is found in 78.9 % of stillborn fetuses, 28.5 % of newborns and 3.5 % of adult patients [12].

Surgical treatment of horseshoe kidney tumor is based on the same principles as those applied in non-tumor surgical procedures. Wells first reported the feasibility of partial nephrectomy in 1884, while Vermooten in 1950 described and substantiated indications for organ operations in renal cell carcinoma [13, 14].

Transperitoneal laparoscopic approach is the most commonly used method for separation of the isthmus (isthmotomy), for pyeloplasty, for resection or heminephrectomy. Currently, it has been ascertained that laparoscopic surgery for tumor in a horseshoe kidney is as effective as open surgery [15]. However, open surgery is often necessary when complex vasculature and rotation are involved [16]. Due to aberrant blood supply during surgery planning, especially concerning tumor formations, it is necessary to use a CT scan to determine the vascular architectonics and exact location of the pelvicalyceal system [17–19].

It should be noted that laparoscopic surgery for tumor in a horseshoe kidney is still rare and we were able to find descriptions of only three cases of laparoscopic resection of a horseshoe kidney [7, 13, 20]. The details are presented in the table.

CONCLUSIONS

Laparoscopic partial nephrectomy in patients with renal tumors smaller than 4 cm in diameter is the standard surgical treatment. Nevertheless, in view of aberrant blood supply to the horseshoe kidney, it requires special diagnostic approach to manage patients with this anomaly. From our experience, contrast-enhanced spiral CT scan allows to assess the anatomical features of the patient's kidneys and consequently apply modern minimally invasive surgery procedures. Laparoscopic approach for conservation treatment of renal cell carcinoma in a horseshoe kidney can be an alternative treatment for this abnormality.

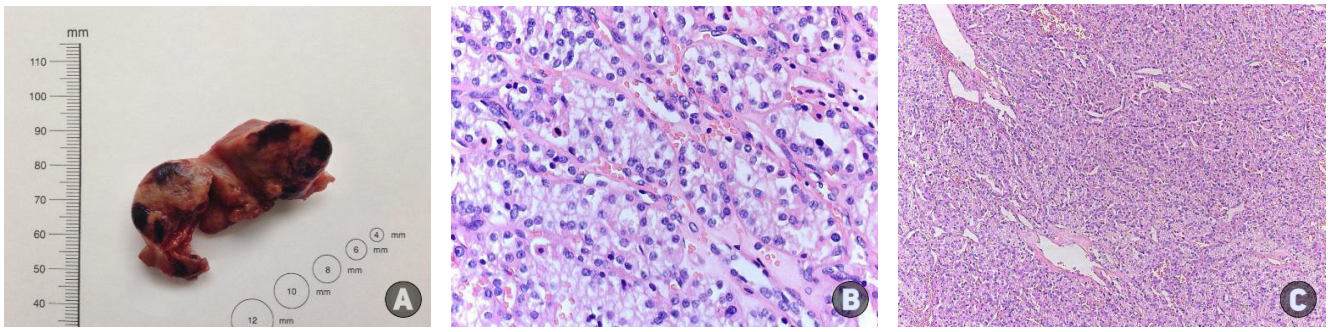

Fig. 4. **(A)** Macropreparation on a section. **(B)** Micropreparation with hematoxylin staining, x10. **(C)** Micropreparation with eosin staining, x40

Brief description of clinical cases of laparoscopic resection of a horseshoe kidney for renal cell carcinoma (according to scholarly literature)

Research	Age/sex	Side	Tumor location	Tumor size, mm	Surgery	Surgery duration, min	Warm ischemia duration	Blood loss	Morphological diagnosis
Tsivian et al., 2006 [20]	62/F	Right	Lower front surface of the right side of the isthmus	20	Laparoscopic	210	–	70	RCC
Tkocz et al.,2012 [13]	72/F	–	Lower pole	40	Retroperitoneoscopic	–	–	–	RCC, G3
Benidir et al., 2014 [7]	58/M	Right	Upper pole	40	Laparoscopic	180	25	200	RCC, G1

References

1. Kaprin AD, Starinskiy VV, Petrova GV, editors. Zlokachestvennye novoobrazovaniya v Rossii v 2014 godu. Moscow: MNIOI im. P. A. Gertsena – filial FGBU «NMIRTs» Minzdrava Rossii; 2016. 250 p. Russian.
2. Kane CJ, Mallin K, Ritchey J, Cooperberg MR, Carroll PR. Renal cell cancer stage migration: analysis of the National Cancer Data Base. Cancer. 2008 Jul 1; 113 (1): 78–83.
3. Barakat AJ, Drougas JG. Occurrence of congenital abnormalities of kidney and urinary tract in 13,775 autopsies. Urology. 1991 Oct; 38 (4): 347–50.
4. Lopatkin NA, editor. Rukovodstvo po urologii. 3 volumes. Vol. 2. Moscow: Meditsina; 1998. 768 p. Russian.
5. Lopatkin NA, editor. Urologiya: Natsional'noe rukovodstvo. Moscow: GEOTAR-Media; 2009. 1024 p. Russian.
6. Hinman F. Operativnaya urologiya: Atlas. Moscow: GEOTAR-Media; 2007. 1192 p. Russian.
7. Benidir T, Coelho de Castilho TJ, Cherubini GR, de Almeida Luz M. Laparoscopic partial nephrectomy for renal cell carcinoma in a horseshoe kidney. Can Urol Assoc J. 2014 Nov; 8 (11–12): E918-20.
8. Natsis K, Piagkou M, Skotsimara A, Protogerou V, Tsitouridis I, Skandalakis P. Horseshoe kidney: a review of anatomy and pathology. Surg Radiol Anat. 2014 Aug; 36 (6): 517–26.
9. Hohenfellner M, Schultz-Lampel D, Lampel A, Steinbach F,

Cramer BM, Thüroff JW. Tumor in the horseshoe kidney: clinical implications and review of embryogenesis. J Urol. 1992 Apr; 147 (4): 1098–102.
10. Araki K, Matsumoto K, Shiraishi T, Ogura H, Kurashige T, Kitamura I. Turner's syndrome with agenesis of the corpus callosum, Hashimoto's thyroiditis and horseshoe kidney. ActaPaediatrJpn, 1987 Aug; 29 (4): 622–6.
11. Herrera L, Kakati S, Gibas L, Pietrzak E, Sandberg A. Brief clinical report: Gardner syndrome in a man with an interstitial deletion of 5q. Am J Med Genet. 1986 Nov; 25 (3):473–6.
12. Glenn JF. Analysis of 51 patients with horseshoe kidney. N Engl J Med. 1959 Oct 1; 261: 684–7.
13. Tkocz M, Kupajski M. Tumour in horseshoe kidney — different surgical treatment shown in five example cases. Contemp Oncol (Pozn). 2012; 16 (3): 254–7.
14. Herr HW. Surgical management of renal tumors: a historical perspective. Urol Clin North Am. 2008 Nov; 35 (4): 543–9.
15. Pitts WR Jr., Muecke EC. Horseshoe kidneys: a 40-year experience. J Urol. 1975 Jun; 113 (6): 743–6.
16. Greene GF, Bissada NK, Madi R. Renal cell carcinoma with caval thrombus extending to the right atrium in a horseshoe kidney: a unique surgical challenge. Can Urol Assoc J. 2009 Oct; 3 (5): 55–7.
17. Jabbour ME, Goldfischer ER, Stravodimos KG, Klima WJ, Smith AD. Endopyelotomy for horseshoe and ectopic kidneys. J Urol. 1998 Sep; 160 (3 Pt 1): 694–7.
18. Yohannes P, Smith AD. The endourological management of complications associated with horseshoe kidney. J Urol. 2002 Jul; 168 (1): 5–8.
19. Patankar S, Dobhada S, Bhansali M. Case report: laparoscopic heminephrectomy in a horseshoe kidney using bipolar energy. J Endourol. 2006 Sep; 20 (9): 639–41.
20. Tsivian A, Shtricker A, Benjamin S, Sidi AA. Laparoscopic partial nephrectomy for tumour excision in a horseshoe kidney. Eur Urol. 2007 Apr; 51 (4):1132–3. Epub 2006 Nov 3.

Литература

1. Каприн А. Д., Старинский В. В., Петрова Г. В., редакторы. Злокачественные новообразования в России в 2014 году. М.: МНИОИ им. П. А. Герцена – филиал ФГБУ «НМИРЦ» Минздрава России; 2016. 250 с.
2. Kane CJ, Mallin K, Ritchey J, Cooperberg MR, Carroll PR. Renal cell cancer stage migration: analysis of the National Cancer Data Base. Cancer. 2008 Jul 1; 113 (1): 78–83.
3. Barakat AJ, Drougas JG. Occurrence of congenital abnormalities of kidney and urinary tract in 13,775 autopsies. Urology. 1991 Oct; 38 (4): 347–50.
4. Лопаткин Н. А., редактор. Руководство по урологии. В 3-х томах. Т. 2. М.: Медицина; 1998. 768 с.
5. Лопаткин Н. А., редактор. Урология: Национальное руководство. М.: ГЭОТАР-Медиа; 2009. 1024 с.
6. Хинман Ф.. Оперативная урология: Атлас. М.: ГЭОТАР-Медиа; 2007. 1192 с.
7. Benidir T, Coelho de Castilho TJ, Cherubini GR, de Almeida Luz M. Laparoscopic partial nephrectomy for renal cell carcinoma in a horseshoe kidney. Can Urol Assoc J. 2014 Nov; 8 (11–12): E918-20.
8. Natsis K, Piagkou M, Skotsimara A, Protogerou V, Tsitouridis I, Skandalakis P. Horseshoe kidney: a review of anatomy and pathology. Surg Radiol Anat. 2014 Aug; 36 (6): 517–26.
9. Hohenfellner M, Schultz-Lampel D, Lampel A, Steinbach F, Cramer BM, Thüroff JW. Tumor in the horseshoe kidney: clinical implications and review of embryogenesis. J Urol. 1992 Apr; 147 (4): 1098–102.
10. Araki K, Matsumoto K, Shiraishi T, Ogura H, Kurashige T, Kitamura I. Turner's syndrome with agenesis of the corpus callosum, Hashimoto's thyroiditis and horseshoe kidney. ActaPaediatrJpn, 1987 Aug; 29 (4): 622–6.
11. Herrera L, Kakati S, Gibas L, Pietrzak E, Sandberg A. Brief clinical report: Gardner syndrome in a man with an interstitial deletion of 5q. Am J Med Genet. 1986 Nov; 25 (3): 473–6.
12. Glenn JF. Analysis of 51 patients with horseshoe kidney. N Engl J Med. 1959 Oct 1; 261: 684–7.
13. Tkocz M, Kupajski M. Tumour in horseshoe kidney — different surgical treatment shown in five example cases. Contemp Oncol (Pozn). 2012; 16 (3): 254–7.
14. Herr HW. Surgical management of renal tumors: a historical perspective. Urol Clin North Am. 2008 Nov; 35 (4): 543–9.
15. Pitts WR Jr., Muecke EC. Horseshoe kidneys: a 40-year experience. J Urol. 1975 Jun; 113 (6): 743–6.
16. Greene GF, Bissada NK, Madi R. Renal cell carcinoma with caval thrombus extending to the right atrium in a horseshoe kidney: a unique surgical challenge. Can Urol Assoc J. 2009 Oct; 3 (5): 55–7.
17. Jabbour ME, Goldfischer ER, Stravodimos KG, Klima WJ, Smith AD. Endopyelotomy for horseshoe and ectopic kidneys. J Urol. 1998 Sep; 160 (3 Pt 1): 694–7.
18. Yohannes P, Smith AD. The endourological management of complications associated with horseshoe kidney. J Urol. 2002 Jul; 168 (1): 5–8.
19. Patankar S, Dobhada S, Bhansali M. Case report: laparoscopic heminephrectomy in a horseshoe kidney using bipolar energy. J Endourol. 2006 Sep; 20 (9): 639–41.
20. Tsivian A, Shtricker A, Benjamin S, Sidi AA. Laparoscopic partial nephrectomy for tumour excision in a horseshoe kidney. Eur Urol. 2007 Apr; 51 (4):1132–3. Epub 2006 Nov 3.

MFTS AND AQSA SCALES VALIDATION IN PATIENTS WITH MULTIPLE AND CONCOMITANT FOOT FRACTURES

Korolev MA ✉, Yarmak DO, Miroschnikova CA, Korobushkin GV

Department of Traumatology, Orthopedics and Field Surgery, Faculty of Pediatrics
Pirogov Russian National Research Medical University, Moscow, Russia

To assess the effectiveness of treatment in traumatology, different scales and assessment questionnaires are used. This work presents the results of the validity test of the two scales designed by the authors, namely, Moscow Foot Trauma Scale (MFTS) and Abbreviated Questionnaire of Subjective Assessment (AQSA). The study enrolled 79 patients (59 male and 20 female individuals with a mean age of 42) with multiple or concomitant foot fractures. For the scales, coefficients of reliability, stability, constancy, internal consistency (Cronbach's alpha), split-half correlation (Guttman's lambda) and intraclass correlation were calculated. SF-36 (Short Form 36) and AOFAS (American Orthopaedic Foot and Ankle Society Score) were used as reference scales. The study revealed a high reproducibility of the new scales: stability coefficient was 0.85–0.96 for MFTS and up to 0.93 for AQSA. Their reliability and internal consistency were established.

Keywords: MFTS, AQSA, SF-36, AOFAS, rating scale, validity, convergent validity, internal consistency coefficient, split-half correlation coefficient, intraclass correlation coefficient, foot fractures, multiple injury

✉ **Correspondence should be addressed:** Maksim Korolev
Leninskiy prospect, d. 10, korp. 7, Moscow, Russia, 117049; doctorkoroleff@mail.ru

Recieved: 30.03.2016 **Accepted:** 07.04.2016

ВАЛИДИЗАЦИЯ ШКАЛ MFTS И AQSA У БОЛЬНЫХ С ПЕРЕЛОМАМИ КОСТЕЙ СТОПЫ В СОСТАВЕ МНОЖЕСТВЕННОЙ И СОЧЕТАННОЙ ТРАВМЫ

М. А. Королёв✉, Д. О. Ярмак, Е. А. Мирошникова, Г. В. Коробушкин

Кафедра травматологии, ортопедии и военно-полевой хирургии, педиатрический факультет,
Российский национальный исследовательский медицинский университет имени Н. И. Пирогова, Москва

Для оценки эффективности лечения в травматологии применяют различные шкалы и оценочные опросники. В работе представлены данные проверки валидности двух шкал, разработанных авторами: Moscow Foot Trauma Scale, MFTS (московская шкала оценки функции стопы после травмы) и Abbreviated Questionnaire of Subjective Assessment, AQSA (сокращенный опросник субъективной оценки). В исследовании участвовали 79 пациентов (59 мужчин, 20 женщин; средний возраст — 42 года) с переломами костей стопы в составе сочетанной и множественной травмы. Для шкал рассчитывали коэффициенты надежности, стабильности, константности, внутренней согласованности (альфа Кронбаха), раздельной корреляции (лямбда Гутмана) и внутригрупповой корреляции. В качестве шкал-эталонов использовали SF-36 (Short Form 36) и AOFAS (American Orthopaedic Foot and Ankle Society Score). Исследование выявило высокую воспроизводимость новых шкал: коэффициент стабильности был равен 0,85-0,96 для MFTS и до 0,93 для AQSA. Была отмечена их надежность и внутренняя согласованность.

Ключевые слова: MFTS, AQSA, SF-36, AOFAS, шкала оценки, валидность, конвергентная валидность, коэффициент внутренней согласованности, коэффициент раздельной корреляции, коэффициент внутригрупповой корреляции, переломы костей стопы, множественная травма

✉ **Для корреспонденции:** Максим Александрович Королёв
117049, г. Москва, Ленинский пр-т, д. 10, корп. 7; doctorkoroleff@mail.ru

Статья получена: 30.03.2016 **Статья принята в печать:** 07.04.2016

Modern requirements on provision of medical care to patients with severe injuries are now compelling physicians to focus not just on early diagnosis, active treatment and subsequent rehabilitation of the patient, but also on the cost-effectiveness of procedures, reduction of treatment and rehabilitation duration and reduction in disability. In addition to objective difficulties, such as short duration of stay by the patient at the hospital, lack of medical history data and general serious condition, diagnosis and treatment of concomitant and multiple injuries carry considerable financial and material costs for clinics and health insurance funds. This underlines the importance of objective evaluation of efficacy of treatment using rating scales.

There are so many scales and assessment questionnaires. There are non-specific scales (general assessment: VAS, NRS, SF-36, etc.) and specific scales (for a certain anomaly: AOFAS, FFI, DASH, etc.), which can be characterized by validity, compliance (friendliness), reliability, reproducibility of results in subsequent studies, and sensitivity to objective changes in indicators. A particular assessment tool for a specific group of patients is chosen based on these parameters [1–3].

However, the existing scales are imperfect. There is need to create new questionnaires for assessment of treatment results and correctly interpret the results; validation of these questionnaires is also required [4–7]. We developed two new

scales at the Department of Traumatology, Orthopedics and Field Surgery, Faculty of Pediatrics, Pirogov Russian National Research Medical University.

Moscow Foot Trauma Scale (MFTS) is a specific scale for evaluation of treatment outcome after foot injury. It consists of subjective and objective parts, each of which includes 3 multiple-choice questions (fig. 1). At the end of the scale are keys indicating the number of points for each answer. Possible score ranges from 0 to 90. Possible treatment effectiveness assessment results: 90–61 p — excellent; 60–41 p — good; 40–21 p — satisfactory; 20–11 p — bad; 10–0 p — very bad.

Abbreviated Questionnaire of Subjective Assessment (AQSA) is a non-specific scale that can be used to assess whether a patient has limited activity, whether he needs special orthopedic shoes or additional support, whether his pain syndrome needs to be relieved using analgesics, and to assess the change in the nature of work performed. The Questionnaire includes 6 questions (fig. 2). At the end of the scale are keys that indicate the number of points for each answer. The possible score ranges from 0 to 30. The higher the score, the worse the result: 0–10 p — good; 11–20 p — satisfactory, above 20 p — bad.

Before using the newly developed scale, it is necessary to confirm its theoretical and pragmatic validity in the conditions of use. Confirmation of theoretical validity enables to establish whether this scale indeed assesses the indicator needed by us, while confirmation of pragmatic validity allows to determine how well does the scale perform its function in practice when dealing with patients. Validity is interpreted in different ways, depending on the task. Validity usually refers to the degree of confidence at which a test, measurement or experiment actually performs the function for which it is intended [8].

Checking the validity of the new assessment tool is quite a challenging task. In traumatology, the SF-36 (Short Form 36) and AOFAS (American Orthopaedic Foot and Ankle Society Score) scales are most commonly used to verify theoretical validity. These scales have confirmed their stability in population-based studies on large and relatively homogeneous samples [9–13].

During analysis, correlation between the attributes assessed by the scale and similar attributes of the reference scale should be revealed, and there should be no correlation with symptoms that have other theoretical grounds. Meeting these conditions means that the scope of the scale has been chosen correctly.

Pragmatic validity was evaluated by an external attribute, which should be relevant (i.e. correspond to the test attribute by meaning), free from interference (this is usually ensured by formation of a fairly homogeneous sample) and reliable [14].

Before validity checking, it is required to establish the level of system reliability. Reliability is a relative constancy, stability, consistency of test results in initial and repeated use on the same group of patients. Gurevich recommends interpreting reliability as: 1) reliability of the measuring instrument itself; 2) stability of the test attribute; 3) constancy, i.e., relative independence of results from the experimenter's identity.

To be completed by the doctor

Objective part

1) Function (range of motions)
1.1) Active motions
- A) Full — 100 %
- B) Moderately disabled — over 50 %
- C) Strongly limited — less than 50 %

1.2) Passive movements
- A) Full — 100 %
- B) Moderately limited — over 50 %
- C) Strongly limited — less than 50 %

2) Use of additional support and orthopedic products
- A) No
- B) Sometimes
- C) Constantly

3) Extremity support ability
- A) Full
- B) Moderate
- C) Low

To be completed by the patient

Subjective part

4) Pain
- A) None
- B) Moderate
- C) Severe
- D) Very severe
- E) Unbearable

5) Socialization
- A) Previous work without limitations
- B) Previous work with limitations
- C) Changed to an easier work
- D) I don't work because of a foot injury
- E) I don't work for other reasons

6) Satisfaction with outcome
- A) Excellent
- B) Good
- C) Satisfactory
- D) Bad
- E) Very bad

Keys (in points)

1.1) A 20, B 10, C 0
1.2) A 3, B 2, C 0
2) A 2, B 1, C 0
3) A 4, B 1, C 0
4) A 15, B 10, C 5, D 1, E 0
5) A 40, B 30, C 20, D 10, E 0
6) A 6, B 3, C 2, D 1, E 0

Interpretation of results

90–61 p — excellent; 60–41 p — good; 40–21 p — satisfactory; 20–11 p — bad; 10–0 p — very bad.

Fig. 1. Questionnaire for assessing the effectiveness of treatment of foot fractures using the Moscow Foot Trauma Scale (MFTS)

Question

1) Are you working now?
- A) Yes
- B) No

2) What kind of work?
- A) Previous
- B) Lightweight
- C) Disability

3) Do you take painkillers?
- A) Yes
- B) No

4) Do you have any physical disability?
- A) Yes
- B) No

5) Do you use additional means of support?
- A) Yes
- B) No

6) What kind of shoes do you wear?
- A) Regular
- B) Orthopedic
- C) Insoles

Keys (in points)

1) A 0, B 5
2) A 0, B 3, C 5
3) A 5, B 0
4) A 5, B 0
5) A 5, B 0
6) A 0, B 5, C 3

Interpretation of results

0–10 p — good; 11–20 p — satisfactory, above 20 p — bad.

Fig. 2. The questionnaire for assessing the effectiveness of treatment of foot fractures using the Abbreviated Questionnaire of Subjective Assessment (AQSA)

He proposes calculating three corresponding coefficients: reliability, stability and constancy [15].

Reliability coefficient was calculated by split-half reliability method, in which the test was divided into equal parts and the correlation between their values calculated. The technique is considered reliable if the correlation coefficient is above 0.75.

The stability coefficient of the attribute under study is determined through test-retest. Its meaning lies in the re-testing of the group being investigated using the methodology under study. The correlation coefficient between the initial and repeated test characterizes the stability of the attribute.

Constancy is checked by the testing of one test group based on one technique but by different researchers. The correlation coefficient should be greater than 0.80 provided the same conditions apply.

Apart from calculation of these coefficients, it is possible to assess the reliability of the system by equivalent-form technique, which requires creation of similar forms of one test and testing that test on a large group of patients with correlation calculated. We didn't use it due to large labor input and relatively small sample involved.

In addition to calculating the above indicators, the coefficient of internal consistency (Cronbach's alpha, αK), split-half correlation coefficient (Guttman's lambda, ʎG) and Kuder–Richardson coefficient (KR20) should be calculated [16–18].

The aim of the study was to test the validity of the MFTS and AQSA scales for patients with multiple and concomitant foot fractures.

METHODS

The study included 79 patients (59 men and 20 women; mean age – 42 years) at the trauma unit of Pirogov City Clinical Hospital No 1. The patients were treated for multiple and concomitant foot fractures in 2007-2016. Surgical treatment was carried out in 32 patients, conservative treatment in 47. The study was approved by the Ethics Committee of Pirogov Russian National Research Medical University (Minutes No 139 of 10 November 2014). All the patients gave informed consent to participate in the study.

By localization, right foot fractures occurred more frequently (n = 39) than left foot fractures (n = 27) and were bilateral in 13 patients. Initial examination revealed 69 fractures, which is 54.3 % of the total number of fractures. Subsequent examinations by traumatologists and other specialists detected other 24 fractures (26 %). Another 28 fractures were late-diagnosed and 12 of these cases needed surgical treatment. The more severe a patient's condition was, the higher the likelihood of diagnosing the fractures late. In severe condition assessed on the ISS scale (Injury Severity Score), 11 and 17 fractures were undiagnosed for scores less than 16 p and above 16 p respectively. Before injury, 55 people were able to work fully. After treatment, 37 patients retained their working ability.

After multiple-stage or single-stage treatment, the patients were discharged from the hospital and observed at an injury care center near where they lived. When necessary, the patients were sent to major hospitals for consultations.

The patients were divided into two groups: group of patients with retrospective observation (n = 36) and group with prospective observation (n = 43). The treatment results were evaluated 1, 3, 6 and 12 months after injury or the treatment was repeated using the developed scales MFTS and AQSA and scales SF-36 and AOFAS. The coefficients of reliability, stability, constancy, αK, ʎG and the intraclass correlation coefficient were calculated for all the scales. The Kuder–Richardson coefficient was not calculated due to the non-dichotomous nature of all the scales. While using the test-retest approach, repeated testing was performed after 11 ± 3.2 days.

These numerical values of treatment results for patients with foot fractures showed the importance of careful attention to diagnosis and treatment of foot bones, as well as timely and thorough examination of the patient with further treatment tactics.

The Statistica 10.0 software (StatSoft, USA) was used for statistical data analysis. With a relatively small sample, a significance level of $p \leq 0.05$ was taken. For data analysis, non-parametric statistics methods were used due to the presence of data distribution in most cases that is different from normal distribution.

RESULTS

Table 1 presents the treatment effectiveness assessment results after 12 months using reference scales and the studied scales as an example of the use of scales. Like assessment using the SF-36 and AOFAS scales, the MFTS and AQSA assessments confirmed a pattern: the later the fractures are diagnosed, the lower the treatment effectiveness.

The MFTS scale recorded the highest Cronbach's coefficient that indicates the internal consistency of a scale, while the physical component summary of the SF-36 scale yielded the biggest Guttman coefficient (PCS) (tab. 2). The ʎG value was also high in MFTS.

For the MFTS scale, in different periods of testing, the values of the constancy coefficient ranged from 0.81 to 0.93, for the AQSA scale — from 0.57 to 0.69.

The intraclass correlation coefficient defined through the test-retest approach was equal to 0.85–0.96 for MFTS and 0.76–0.93 for AQSA. For both scales, $p \leq 0.05$. This result indicates there is high dependency of indicators within the MFTS and AQSA scales.

Table 3 shows convergent correlations between the reference scales and studied scales for both groups of patients. As can be seen, they have low level of significance. Correlation between MFTS and AOFAS and correlation between MFTS and the physical component summary of the SF-36 scale were identified, which is logical, given the one-way specialization of these questionnaires. However, all the values had a low level of significance. Therefore, the existence of a real relationship between the scales can only be assumed.

In view of its low specificity, AQSA correlated with both physical and mental components of the SF-36 scale. It correlated negatively with AOFAS.

DISCUSSION

The high Cronbach's coefficient recorded in the MFTS scale indicates there is optimal construction of questions in the scale. With the help of the Statistica 10.0 software, the need to exclude similar questions was assessed. For the MFTS scale, it was recommended to remove 2 questions (in order to reduce the value of αK). For the AOFAS and AQSA scales, it was recommended to add from 1 to 3 questions to improve the internal consistency of the evaluating tool.

Guttman coefficient confirmed the effectiveness of assessment with the use of physical component summary

Table 1. Treatment effectiveness assessment (12 months) using the SF-36, AOFAS, MFTS and AQSA scales

Scale	Foot fractures		
	Diagnosed early	Diagnosed late	Undiagnosed
SF-36 (PCS/MCS)	51/47	38/46	34/28
AOFAS	54	43	31
MFTS	45	22	15
AQSA	7	18	16

Note: PCS — Physical Component Summary of the SF-36 scale, MCS — Mental Component Summary of the SF-36 scale. The results are presented as arithmetic mean.

Table 2. Clinical and metric properties of the SF-36, AOFAS, MFTS and AQSA scales

Scale	SF 36		AOFAS	MFTS	AQSA
	PCS	MCS			
Number of questions	21	15	9	6	6
Cronbach's coefficient (αK)	0.982	0.957	0.989	0.993	0.99
Guttman coefficient (ʎG)	0.986	0.951	0.983	0.985	0.981
Intraclass correlation coefficient	0.896	0.769	0.93	0.961	0.936

Note: PCS — Physical Component Summary of the SF-36 scale, MCS — Mental Component Summary of the SF-36 scale.

of the SF-36 scale (0.986). The high values of the test-retest indicator — 0.85–0.96 for MFTS and up to 0.93 for AQSA — reflected the good reproducibility of these scales.

The data obtained indicate there is a fairly high level of individual validity of the MFTS and AQSA scales. However, the convergent validity values were lower than those of the reference scales. One cannot tell exactly what will be the correlation between the indicators under the conditions of another experiment, but it is important that a relationship is still there. Perhaps in future studies involving different groups of patients, we will be able to confirm that there is a relationship.

CONCLUSIONS

Statistical data analysis confirmed that the MFTS scale has a high validity and compliance for the doctor, and high sensitivity and reliability. The disadvantages are average reproducibility and low compliance for the patient. The AQSA scale showed high reliability, reproducibility and compliance for the doctor and patient, but low validity and sensitivity. The convergent validity values of these scales with the SF-36 and AOFAS scales showed there is a weak correlation between the scales.

The MFTS and AQSA scales can be used to assess the effectiveness of treatment of patients with multiple and concomitant foot fractures. In this case, the peculiarities indicated for them should be taken into account.

Table 3. Convergent validity values for the SF-36, AOFAS, MFTS and AQSA scales

Scale		SF-36 PCS		SF-36 MCS		AOFAS	
		R	P	R	P	R	P
MFTS	R	0.183	–	-0.206	–	0.22	–
	P	–	0.215	–	-0.719	–	0.104
AQSA	R	0.227	–	0.170	–	-0.301	–
	P	–	0.378	–	0.351	–	-0.292

Note: PCS — Physical Component Summary of the SF-36 scale, MCS – Mental Component Summary of the SF-36 scale; R — group of patients with retrospective observation, P — group of patients with prospective observation; p ≤0.05.

References

1. Viskarra ME, Zimina EV, Gurina SA, Yarygin NV. Validizatsiya shkal i voprosnikov dlya otsenki funktsional'nogo sostoyaniya i kachestva zhizni patsientov s perelomovyvikhami golenostopnogo sustava. Rossiyskie meditsinskie vesti. 2011; 16 (2): 61–71. Russian.
2. Novik AA, Ionova TI. Rukovodstvo po issledovaniyu kachestva zhizni v meditsine. Moscow: Izd-vo "OLMA Media Grupp"; 2007. 313 p. Russian.
3. Knop C, Oeser M, Bastian L. Development and validation of the visual analogue scale (VAS) spine score. Unfallchirurg. 2001; 104 (6): 488–97. German.
4. Evsina OV. The quality of life in medicine — an important andicator pf patient health status (review). Lichnost' v menjajushhemsja mire: zdorov'e, adaptacija, razvitie. 2013; (1): 119–33. Russian.
5. Viskarra ME, Yarygin NV, Zimina EV. Analiz faktorov, vliyayushchikh na kachestvo zhizni i funktsional'noe sostoyanie patsientov s perelomovyvikhami golenostopnogo sustava. Problemy standartizatsii v zdravookhranenii. 2011; (3-4): 9–15. Russian.
6. Viskarra ME. Izuchenie kachestva zhizni i funktsional'nogo sostoyaniya patsientov s perelomovyvikhami golenostopnogo sustava s pomoshch'yu shkal i oprosnikov [dissertation]. Moscow: M. I. Evdokimov Moscow State University of Medicine and Dentistry; 2011. Russian.
7. Glantz S. Mediko-biologicheskaya statistika. Moscow: Izd-vo "Praktika"; 1998. 459 c.
8. Golovin SYu. Slovar' prakticheskogo psihologa. Minsk: Izd-vo "Kharvest"; 1998. 800 p.
9. Amirdzhanova VN, Goryachev DV, Korshunov NI, Rebrov AP, Sorotskaya VN. SF-36 questionnaire population quality of life indices. Nauchno-prakticheskaya revmatologiya. 2008; (1): 36–48.
10. Jenkinson C, Coulter A, Wright L. Short form 36 (SF-36) health survey questionnaire: normative data for adults of working age. BMJ. 1993; 306 (6890): 1437–40.
11. Kitaoka HB, Alexander U, Adelaar RS, et al. Clinical rating systems for the ankle hindfoot, midfoot, hallux and lesser toes. Foot Ankle Int.1994. 15: 349–53.
12. SooHoo NF, Shuler M, Fleming LL; American Orthopaedic Foot and Ankle Society. Evaluation of the validity of the AOFAS Clinical Rating Systems by correlation to the SF-36. Foot Ankle Int. 2003 Jan; 24 (1): 50–5.
13. Ware JE, Sherbourne CD. The MOS 36-item short-form health survey (SF-36). I. Conceptual framework and item selection. Med Care. 1992 Jun; 30 (6): 473–83.
14. Schuh A, Hausel M. Difficlties in evaluating follow-up outcome in calcaneus fracture managed with plate osteosinthesis. Is there a reliable score? Unfallchirurg. 2000; 103 (4): 295–300. German.
15. Gurevich KM, Borisova EM. Psihologicheskaja diagnostika. Moscow: Izd-vo "URAO"; 1997. 304 p. Russian.
16. Cronbach LJ. Coefficient alpha and the internal structure of tests.

Psychometrika. 1951; 16: 297–334.
17. Kline P. A handbook of test construction (psychology revivals): introduction to psychometric design. Abingdon, UK: Routledge; 2015. 274 p.
18. Schmitt N. Uses and abuses of coefficient alpha. Psychological Assessment. 1996; 8 (4): 350–3.

Литература

1. Вискарра М. Э., Зимина Э. В., Гурина С. А., Ярыгин Н. В. Валидизация шкал и вопросников для оценки функционального состояния и качества жизни пациентов с переломовывихами голеностопного сустава. Российские медицинские вести. 2011; 16 (2): 61–71.
2. Новик А. А., Ионова Т. И. Руководство по исследованию качества жизни в медицине. М.: Изд-во «ОЛМА Медиа Групп»; 2007. 313 с.
3. Knop C, Oeser M, Bastian L. Development and validation of the visual analogue scale (VAS) spine score. Unfallchirurg. 2001; 104 (6): 488–97. German.
4. Евсина О. В. Качество жизни в медицине — важный показатель здоровья пациента (обзор литературы). Личность в меняющемся мире: здоровье, адаптация, развитие. 2013; (1): 119–33.
5. Вискарра М. Э., Ярыгин Н. В., Зимина Э. В. Анализ факторов, влияющих на качество жизни и функциональное состояние пациентов с переломовывихами голеностопного сустава. Проблемы стандартизации в здравоохранении. 2011; (3-4): 9–15.
6. Вискарра М. Э. Изучение качества жизни и функционального состояния пациентов с переломовывихами голеностопного сустава с помощью шкал и опросников [диссертация]. М.: Московский государственный медико-стоматологический университет имени М. А. Евдокимова; 2011.
7. Гланц С. Медико-биологическая статистика. М.: Изд-во «Практика»; 1998. 459 с.
8. Головин С. Ю. Словарь практического психолога. Минск: Изд-во «Харвест»; 1998. 800 с.
9. Амирджанова В. Н., Горячев Д. В., Коршунов Н. И., Ребров А. П., Сороцкая В. Н. Популяционные показатели качества жизни по опроснику SF-36 (результаты многоцентрового исследования качества жизни «МИРАЖ»). Научно-практическая ревматология. 2008; (1): 36–48.
10. Jenkinson C, Coulter A, Wright L. Short form 36 (SF-36) health survey questionnaire: normative data for adults of working age. BMJ. 1993; 306 (6890): 1437–40.
11. Kitaoka HB, Alexander U, Adelaar RS, et al. Clinical rating systems for the ankle hindfoot, midfoot, hallux and lesser toes. Foot Ankle Int.1994. 15: 349–53.
12. SooHoo NF, Shuler M, Fleming LL; American Orthopaedic Foot and Ankle Society. Evaluation of the validity of the AOFAS Clinical Rating Systems by correlation to the SF-36. Foot Ankle Int. 2003 Jan; 24 (1): 50–5.
13. Ware JE, Sherbourne CD. The MOS 36-item short-form health survey (SF-36). I. Conceptual framework and item selection. Med Care. 1992 Jun; 30 (6): 473–83.
14. Schuh A, Hausel M. Difficlties in evaluating follow-up outcome in calcaneus fracture managed with plate osteosinthesis. Is there a reliable score? Unfallchirurg. 2000; 103 (4): 295–300. German.
15. Гуревич К. М., Борисова Е. М. Психологическая диагностика. М: Изд-во «УРАО»; 1997. 304 с.
16. Cronbach LJ. Coefficient alpha and the internal structure of tests. Psychometrika. 1951; 16: 297–334.
17. Kline P. A handbook of test construction (psychology revivals): introduction to psychometric design. Abingdon, UK: Routledge; 2015. 274 p.
18. Schmitt N. Uses and abuses of coefficient alpha. Psychological Assessment. 1996; 8 (4): 350–3.

CHEMILUMINESCENT DETERMINATION OF TOTAL ANTIOXIDANT CAPACITY IN MEDICINAL PLANT MATERIAL

Vladimirov GK[1]✉, Sergunova EV[2], Izmaylov DYu[1], Vladimirov YuA[1]

[1] Department of Medical Biophysics, Faculty of Fundamental Medicine, Lomonosov Moscow State University, Moscow, Russia

[2] Department of Pharmacognosy, Faculty of Pharmacy, The First Sechenov Moscow State Medical University, Moscow, Russia

Medicinal plant material is one of the sources of antioxidants for the human body. Chemiluminescence analysis is one of the common methods of determining the content of antioxidants in plant materials. In our work, chemiluminescence analysis was used to determine the total antioxidant capacity (TAC) of fruit decoctions of mountain-ash, rose and hawthorn, as well as raspberry fruit infusion. Experiments established the kinetics of the chemiluminescence of a system consisting of horseradish peroxidase, hydrogen peroxide and luminol. Concentrations and volumes of components of the system were chosen such that strong antioxidants (ascorbic acid) and antioxidants of average force (quercetin) were completely oxidized during measurement (10 minutes). A method for TAC calculation based on changes in chemiluminescence light sum in the presence of plant samples was proposed and substantiated. Analysis of chemiluminescence kinetics showed that antioxidants of average force dominate in the objects studied, including flavonoids and weak antioxidants (tocopherol and others). Comparison of the calculated TAC values for the objects under study and their chemical analysis data showed that products containing the same amount of antioxidants with different ratios of antioxidants by types might vary in their ability to protect the body against the harmful effects of free radicals. The technique described is a promising one for the study of plant objects containing a mixture of different types of antioxidants.

Keywords: free radical, antioxidant, antioxidant activity, total antioxidant capacity, chemiluminescence, luminol

Funding: this work was supported by the Russian Science Foundation, grant no. 14-15-00375.

Acknowledgments: authors thank Andrey Alekseev from Lomonosov Moscow State University for his assistance in conducting the experiment.

✉ **Correspondence should be addressed:** Georgiy Vladimirov
Lomonosovskiy prospekt, d. 31, k. 5, Moscow, Russia, 119192; ura-vladimirov@yandex.ru

Received: 10.03.2016 **Accepted:** 18.03.2016

ХЕМИЛЮМИНЕСЦЕНТНАЯ МЕТОДИКА ОПРЕДЕЛЕНИЯ ОБЩЕЙ АНТИОКСИДАНТНОЙ ЕМКОСТИ В ЛЕКАРСТВЕННОМ РАСТИТЕЛЬНОМ СЫРЬЕ

Г. К. Владимиров[1]✉, Е. В. Сергунова[2], Д. Ю. Измайлов[1], Ю. А. Владимиров[1]

[1] Кафедра медицинской биофизики, факультет фундаментальной медицины, Московский государственный университет имени М. В. Ломоносова, Москва

[2] Кафедра фармакогнозии, фармацевтический факультет, Первый Московский государственный медицинский университет имени И. М. Сеченова, Москва

Лекарственное растительное сырье является одним из источников антиоксидантов для организма человека. Среди методов определения содержания антиоксидантов в растительных объектах распространен метод хемилюминесцентного анализа. В настоящей работе он был использован для оценки общей антиоксидантной емкости (ОАЕ) отваров плодов рябины, шиповника и боярышника и настоя плодов малины. В опыте регистрировали кинетику хемилюминесценции в системе, состоящей из пероксидазы хрена, перекиси водорода и люминола. Концентрации и объем компонентов системы в пробе были подобраны так, чтобы сильные антиоксиданты (аскорбиновая кислота) и антиоксиданты средней силы (кверцетин) полностью окислялись за время измерения (10 мин). Предложен и обоснован способ расчета ОАЕ на основе изменения светосуммы хемилюминесценции в присутствии растительных образцов. Анализ кинетики хемилюминесценции показал, что в изученных объектах преобладают антиоксиданты средней силы, в том числе флавоноиды, и слабые антиоксиданты (токоферол и др.). Сопоставление рассчитанных значений ОАЕ для изучаемых объектов и данных их химического анализа показало, что продукты, содержащие одно и то же количество антиоксидантов с разным их соотношением по типам, могут различаться по способности защищать организм от вредного воздействия свободных радикалов. Описанная методика перспективна для изучения растительных объектов, содержащих смесь антиоксидантов различных типов.

Ключевые слова: свободный радикал, антиоксидант, антиоксидантная активность, общая антиоксидантная емкость, хемилюминесценция, люминол

Финансирование: работа выполнена при поддержке Российского научного фонда, грант № 14-15-00375.

Благодарности: авторы благодарят Андрея Алексеева из Московского государственного университета имени М. В. Ломоносова за помощь в проведении эксперимента.

✉ **Для корреспонденции:** Георгий Константинович Владимиров
119192, г. Москва, Ломоносовский пр-т, д. 31, к. 5; ura-vladimirov@yandex.ru

Статья получена: 10.03.2016 **Статья принята в печать:** 18.03.2016

Free radicals generated in the body causes damage to the cell membranes, which in turn triggers various diseases [1]. The destructive oxidative effects of radicals are checked by the body's antioxidant defense system, in which low-molecular compounds — radical interceptors (traps) — play an important role. Medicinal plant material and herbal preparations are one of the sources of antioxidants [2]. Understanding the antioxidant capacity of these plant materials and preparations helps to enhance their preventive and therapeutic actions.

The main techniques used to identify antioxidants are considered in [3–8]. However, identifying antioxidants as chemical compounds does not provide a complete picture of the protective properties of the object being studied: they are caused not only by the amount of a particular antioxidant but also by the activity of each of them. Antioxidant activity (AOA) is the constant (k_{InH}) of the reaction rate of a free radical and antioxidant. The chemiluminescence technique (CL) is used to determine the total number of radicals that react with antioxidants in a sample (total antioxidant capacity, TAC); when mathematical modeling of CL kinetics is used, the technique enables to also determine the rate of formation and reaction of radicals with antioxidants, i.e. AOA [9–11].

The most common modification of the chemiluminescent technique of determining the total antioxidant capacity is based on the use of luminol as a chemiluminescence activator [12–15]. The sample is placed in a chemiluminometer cuvette with addition of luminol, hydrogen peroxide and compounds capable of forming radicals by spontaneous decay (thermolysis), for example 2,2'-Azobis(2-amidinopropane) dihydrochloride (AAPH):

$$AAPH \rightarrow 2R\bullet.$$

In the presence of molecular oxygen, alkyl radical R• forms peroxyl radical ROO•:

$$R\bullet + O_2 \rightarrow ROO\bullet.$$

Next, the peroxyl radical oxidizes luminol-based chemiluminescent probe (LH2) to form a radical luminol (LH•):

$$ROO\bullet + LH_2 \rightarrow ROOH + LH\bullet.$$

Through formation of intermediate compounds (luminol hydroperoxide and luminol endoperoxide), LH• forms the molecule of the final product of luminol oxidation (aminophthalic acid) in an electronically excited state, which highlights photon and as a result, chemiluminescence is observed [9]. CL intensity is proportional to the rate of formation of photons, which in turn is proportional to stationary concentration of LH• in the system. While interacting with radicals, antioxidants interrupt the above-described transformation chain and prevent photon formation.

Compounds subject to thermolysis are not the only possible source of radicals in analysis of the antioxidant capacity of a sample by chemiluminescence method. Alternatives include horseradish peroxidase/hydrogen peroxide compound [13, 16], hemin-hydrogen peroxide [8], cytochrome *c*/cardiolipin/hydrogen peroxide [11], and others. The mechanism of peroxidation of luminol is considered in Cormier et al. [17].

CL kinetic curves for these systems reflect two reaction stages: step of increase in CL intensity and the stage of plateau or gradual recession of luminescence when CL intensity is either constant or decreases slowly. Authors in [15] described two approaches to measuring the total antioxidant capacity, taking into account this curve feature. TRAP (Total Reactive Antioxidant Potential) method is based on measurement of CL latency τ and can be used to determine such antioxidants as Trolox and ascorbic acid — they are characterized by high constant of the rate of radical reaction, and for this reason can be called powerful antioxidants [11]. They are completely oxidized during the latent period. The TAR (Total Antioxidant Reactivity) technique is used to measure the degree of suppression of chemiluminescence q on the plateau or at the maximum chemiluminescence curve:

$$q = \frac{(I - I_1)}{I},$$

where I is CL intensity without an antioxidant, while I_1 is CL intensity in the presence of an antioxidant. This method is used if the system contains predominantly weak antioxidants with low constants of rate of interaction with radicals — much lower than the luminol constant [11].

The action of antioxidants is characterized not only by indicators τ and q. As can be seen from [8, 11], the action of such antioxidants as uric acid in gemin/H_2O_2/luminol or tocopherol, rutin and quercetin in cytochrome *c*/cardiolipin/H_2O_2/luminol system is characterized by a change in the maximum rate of CL rise (v_{max}). As shown by results of mathematical modeling of kinetics, the constants of the constants of the reaction rate of such antioxidants with radicals are close to luminol constant. Therefore, such antioxidants may be regarded as medium-strength antioxidants [11].

If the test material, particularly plant materials, contained only one type of antioxidants, their content would have been characterized by one of the above three indicators (τ, q or v_{max}). But a plant material contains a mixture of antioxidants of different strength. To address this problem, some authors [8, 18–20] used chemiluminescence light sum change ΔS over a specific time calculated by the formula:

$$\Delta S = \Delta S_0 - \Delta S_s,$$

where ΔS_0 and ΔS_s are CL light sums for a predetermined time t in the control and test samples respectively. The time should be sufficient to oxidize all the antioxidants in the system, i.e. for the CL curve of the test sample to reach the level of the CL curve of the control sample. The latter suggests that researchers should not only establish the luminescence light sum, but also record the CL kinetics curve within quite a long time. However, this is not always done.

Since all measurable indicators depend on the instrument and measurement conditions, the antioxidant effect of a substance in a system is usually compared with the effect of an antioxidant taken as the standard, for example Trolox [8, 21].

Many authors have used the horseradish peroxidase/hydrogen peroxide system to analyze the total antioxidant capacity of plant material. In [22, 23], CL latency (TRAP method) was used to estimate the amount of antioxidants in samples, while in [18–20], the area under the CL curve was used. However, these studies did not provide a clear justification of the choice of a particular indicator for TAC assessment. The aim of the study was to determine how the ratio of different types of antioxidants affects TAC and to modify the chemiluminescence method in such a way as to be able to more accurately estimate TAC in a plant material. To this end, we set a number of tasks. First, to compare the CL kinetics of the test objects with the kinetics of the standard three types of antioxidants (strong, medium and weak) in order to understand what type of antioxidants contributes most to the TAC of the test objects. Secondly, to calculate the TAC of the test objects by measuring the reduction in CL light sum under the influence of these objects in comparison with the effect of an antioxidant that contributes most to the TAC.

METHODS

The test objects were industrial samples of the fruits of hawthorn, mountain-ash and wild rose produced by herbal

company Krasnogorskleksredstva (Russia), as well as naturally grown raspberry fruits collected by the authors in Moscow Oblast and dried at a temperature of 60–80 °C until they had no juice left in them and were deformed under pressure.

The reagents used for analysis of antioxidant capacity by chemiluminescent method were: KH_2PO_4, 20 mM buffer solution (pH 7.4); horseradish peroxidase (activity 112 U/mg, M = 44173.9), 1 mM aqueous solution; Luminol (5-amino-1,2,3,4-tetrahydro-1,4-phthalazinedione, 3-Aminophthalic acid hydrazide, M = 177.11), 1 mM aqueous solution; hydrogen peroxide (H2O2, M = 34.01), 1 mM aqueous solution; antioxidant solutions (ascorbic acid, quercetin, tocopherol). All reagents were produced by Sigma Aldrich, USA.

Hawthorn, mountain-ash and wild rose fruit decoctions and raspberry fruit infusion were prepared according to the procedure of the State Pharmacopoeia of the USSR set out in the general pharmacopoeial article “Infusions and decoctions” [24].

The total antioxidant capacity was determined through chemiluminescence on chemiluminometer Lum-100 (DISoft, Russia) using PowerGraph 3.3 software. To determine the TAC in the plant material, 40 µl of luminol at a concentration of 1 mM, 40 µl of horseradish peroxidase at a concentration of 0.1 µm, 10 to 50 µl of decoction or infusion (depending on concentration) and phosphate buffer in the quantity necessary to bring the total sample volume to 1 ml were placed in the cuvette of the device. The cuvette was mounted on the device and CL was recorded, observing the background signal. After 48 s of observing the background signal, 100 µl of H_2O_2 at 1 mM concentration was added into the cuvette and CL observation continued for 10 minutes. Four samples with different concentrations of each of the plant objects were prepared. CL was also observed for solutions of ascorbic acid, quercetin and tocopherol at five different concentrations for each of the antioxidants. Later, the TAC of the samples of decoctions and infusions were recalculated to quercetin.

Concentrations of luminol, horseradish peroxidase and hydrogen peroxide were selected such that it was possible to determine the antioxidant capacity of aqueous extracts of medicinal plants in a reasonable time (no more than 10 min). Within this time, the chemiluminescence curves for the antioxidants ascorbic acid and flavonoid quercetin (the main antioxidants of plant materials) reached a plateau, indicating complete destruction of antioxidants in the system. Dilutions of the test samples and concentration of solutions of standard antioxidants (indicated in the captions of the figures) were selected such that all the CL kinetic curves were measured with the same device sensitivity.

The antioxidant capacity was calculated from the change in area (ΔS) under chemiluminescence kinetic curve (light sum) by adding a substance containing an antioxidant. To this end, S_0 was calculated for the system without an antioxidant and the area S_S (characterizing the system in which the antioxidant was added) subtracted therefrom. The value of ΔS depends on chemiluminometer sensitivity and measurement conditions. The ratio $\Delta S/C \cdot V$ (where C is the concentration of the test biological material in the cuvette, in g/l, and V — the volume of the cuvette in liters) expresses the antioxidant capacity of 1 g of the test plant material.

Similarly, antioxidant capacity ΔS_A of the standard antioxidant solution, e.g. quercetin, placed in the same reaction mixture volume, was calculated. The ratio $\Delta S_A/C_A \cdot V$ (where C_A is the weight concentration of the antioxidant in the cuvette, g/l) expresses the antioxidant capacity of 1 g of the antioxidant.

For each of the standard antioxidants, a signal from the solutions of several concentrations were observed to make sure that calculations were performed within linear dependence, and results obtained are reproducible. Indeed, a linear dependence ($\Delta S_A = k_A \cdot C_A$) of the signal on the concentration at which stoichiometric ratio k_A was calculated was obtained. According to Fisher’s exact test, the k_A values obtained for standard antioxidants are statistically significant with a 0.975 probability. Then, a signal from four concentrations for each of the four plant samples was observed. A linear dependence of the signal on the concentration ($\Delta S = k \cdot C$) at which stoichiometric coefficient k was calculated was obtained for all the samples. With a probability of 0.975 (Fisher’s exact test), the k values obtained for the plant samples are statistically significant. Total antioxidant capacity of the plant material in terms of the weight of a standard antioxidant (mg%) was calculated using the formula

$$TAC = \frac{k}{k_a} \cdot 10^5.$$

The values were presented as the arithmetic mean ± standard deviation (M ± δ) at $p < 0.05$.

RESULTS

The study of chemiluminescence kinetics in the presence of sodium ascorbate (fig. 1) showed that this antioxidant is characterized by latency when CL is almost completely suppressed. Its duration is proportional to the amount of the antioxidant in the system. In this case, neither the slope of the CL curves nor the CL intensity at the plateau changes. This is due to the fact that ascorbic acid is a strong antioxidant that intercepts all radicals formed in the system, including luminol radicals and CL does not develop until the entire ascorbate is oxidized.

The action of tocopherol (fig. 2) was manifested in the form of a decrease in the CL plateau intensity, which is characteristic of weak antioxidants, though tocopherol is considered to be one of the most powerful antioxidants. Possibly, this discrepancy is due to the fact that in our experiment, the free radicals were in aqueous solution, whereas the effect of tocopherol is typically studied in non-polar media. Tocopherol had medium-strength antioxidant properties in [11], where the cytochrome *c*/cardiolipin complex was used as the source of radicals; reaction with luminol proceeded within this complex.

After studying the effect of different concentrations of quercetin on our system (fig. 3) and comparing the kinetic curves for it and sodium ascorbate and tocopherol, it was observed that the main effect of quercetin manifested in the form of a change in the slope angle of curves, i.e. the speed of CL development, which is typical for medium-strength antioxidants.

The CL curves for all the decoctions studied (fig. 4) resemble the curves for quercetin with a slight decrease in CL intensity at the end, i.e. at the exit to the plateau. As shown in [11], such behavior is characteristic of medium-strength antioxidants, which, in our case, can include polyphenols – flavonoids and tannins. For raspberry fruit infusion (fig. 4, D), decrease in chemiluminescence at the plateau level is noticeable, which is characteristic of weak antioxidants [11] such as tocopherol in this case. In terms of quercetin and tocopherol, raspberry fruit infusion contains 4.7 ± 0.9 mmol/g quercetin and 11.9 ± 0.8 mmol/g of tocopherol.

Comparing the chemiluminescence curves obtained for different concentrations of the four investigated aqueous water extracts from plant materials showed that the contribution of medium-strength and weak antioxidants in the total antioxidant

capacity of the sample decreased in series: raspberry fruit infusion, rosehip decoction (fig 4, C), mountain-ash fruit decoction (fig. 4, A), hawthorn fruit decoction (fig. 4, B). The values of ΔS based on concentration C of the test substance in the cuvette and the total antioxidant capacity values expressed in terms of quercetin are shown in the table.

DISCUSSION

Data obtained in the course of experiments and TAC values (calculated based on the data) of the test objects were compared with their content of main antioxidants identified by chemical analysis methods [25–29]. Despite the fact that there is undeniable positive correlation between the total amount of antioxidants and TAC in different objects, there are still notable differences between these indicators. For example, the total content of flavonoids, tannins, and ascorbic acid is greater than the TAC calculated for all the test objects, except hawthorn fruit decoction (see table).

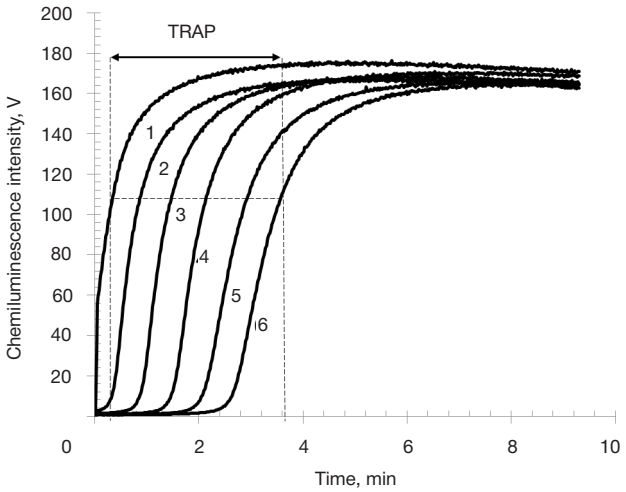

Fig. 1. Effect of sodium ascorbate on chemiluminescence kinetics

Concentrations of components of the system: luminol — 40 μm, horseradish peroxidase — 4 nM, hydrogen peroxide — 100 μm. Curves: 1 — control sample; 2 — 0.05 μm; 3 — 0.10 μm; 4 — 0.15 μm; 5 — 0.2 μm; 6 — 0.25 μmM sodium ascorbate.

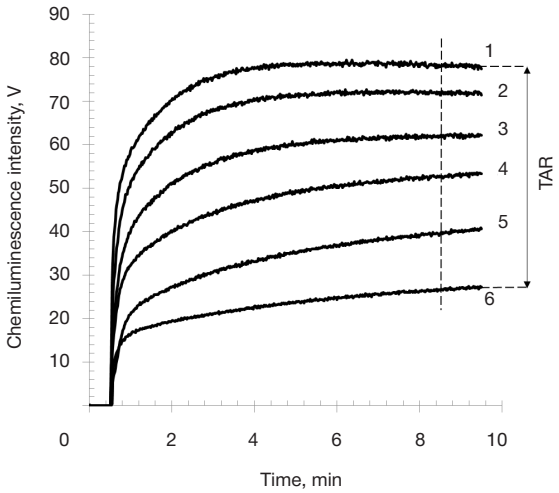

Fig. 2. Effect of tocopherol on chemiluminescence kinetics

Concentrations of components of the system: luminol — 40 μm, horseradish peroxidase — 4 nM, hydrogen peroxide — 100 μm. Curves: 1 — control sample; 2 — 0.01 μm; 3 — 0.025 μm; 4 — 0.06 μm; 5 — 0.1 μm; 6 — 0.2 μm of tocopherol.

Other researchers have also shown that chemical analysis results and TAC value determined by chemiluminescent do not coincide often. In [19], the total antioxidant capacity determined in a peroxidase/luminol/hydrogen peroxide system correlated with the content of triterpene compounds. However, in another study [18] conducted by the same authors where another plant was used as the test object, no correlation was found between TAC and the content of a group of substances, including flavonoids.

Such differences are related to at least three factors. First, antioxidant activity matters, i.e. the rate of reaction of antioxidants with radicals, which is different for different antioxidants included in the plant sample. According to Izmailov [11], the rate constant for the corresponding reactions for mexidol, tocopherol and quercetin correspond as 0.04 : 2 : 60. Secondly, each antioxidant molecule entering into a chemical reaction can intercept different numbers of radicals. According to [8], quercetin, uric and ascorbic acid intercepted 3.6 ± 0.1, 1.4 ± 0.1 and 0.5 ± 0.2 radicals per reacting antioxidant molecule respectively (hemin/H_2O_2/luminol system was used). Thirdly, the results of the study could have been affected by the presence of peroxidase activity in the plant samples, as in [23], as well as by the presence of calcium in the samples, which, as shown in [30], can, under certain conditions, enhance the activity of peroxidase horseradish. This usually results in higher CL intensity on the plateau than on the control curves, which, however, we didn't observe.

The first factor severely limits the use of such indicator as a change in light sum because chemiluminescence measurement time should be more than the time of expenditure of all antioxidants in the sample. You know when this moment arrives only by measuring the chemiluminescence kinetics. Furthermore, the contribution of weak antioxidants in TAC is sharply undervalued since the time of their complete oxidation is by far higher than the acceptable measurement duration (10–20 min).

Stoichiometric coefficient of the antioxidant is even greater in value. The number of radicals n intercepted by them is equal to

$$n = \rho \cdot \Delta m,$$

where ρ is the stoichiometric coefficient, and Δm is the change in antioxidant concentration during measurement — in this

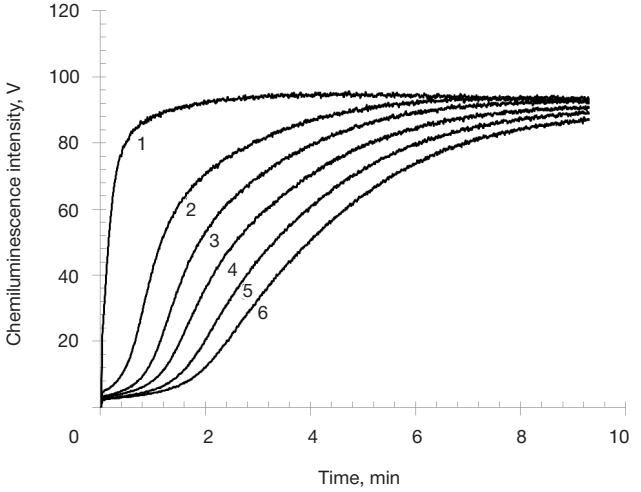

Fig. 3. Effect of quercetin on chemiluminescence kinetics

Concentrations of components of the system: luminol — 40 μm, horseradish peroxidase — 4 nM, hydrogen peroxide — 100 μm. Curves: 1 — control sample; 2 — 0.02 μm; 3 — 0.03 μm; 4 — 0.04 μm; 5 — 0.05 μm; 6 — 0.06 μm of quercetin.

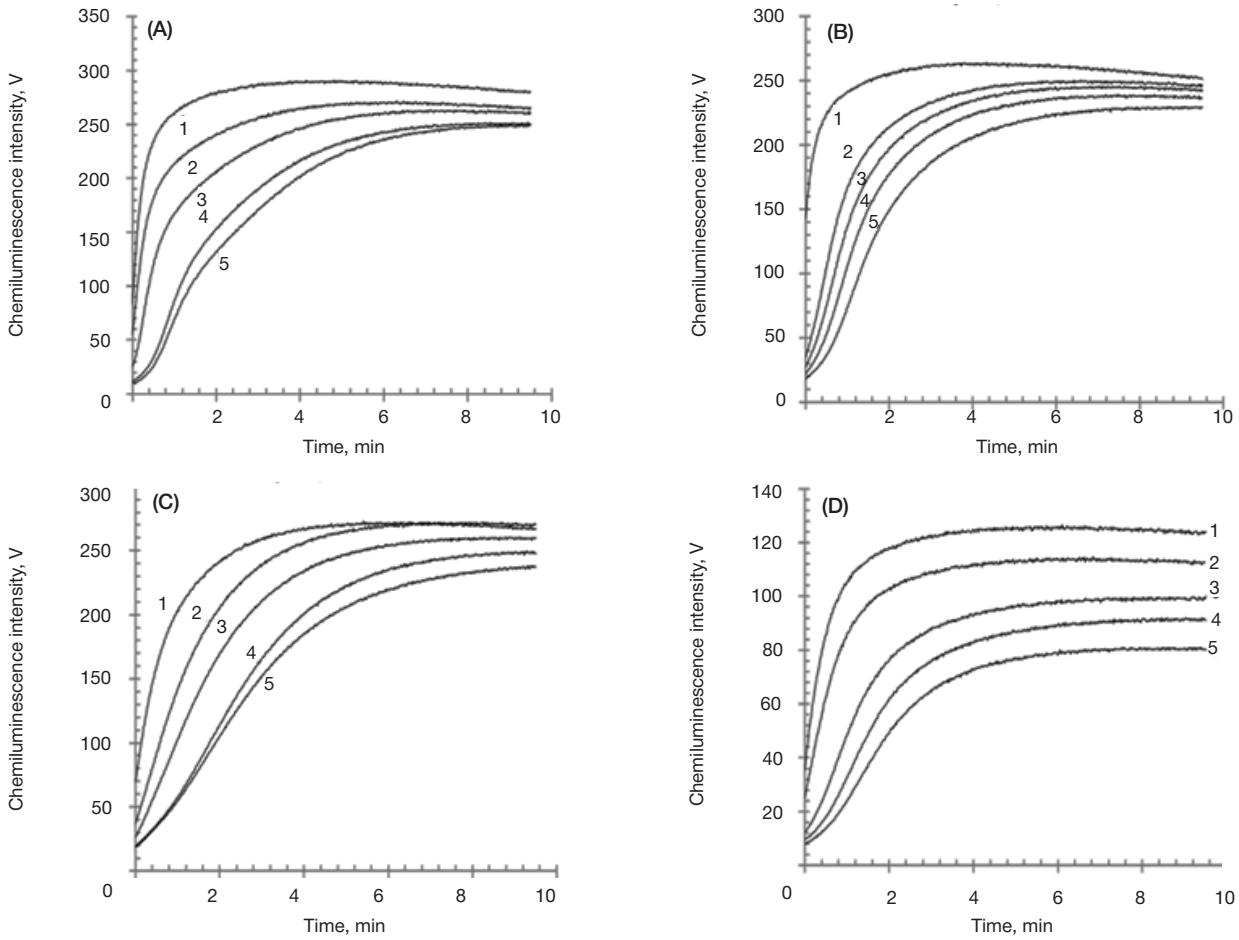

Fig. 4. Effect of fruit decoctions of mountain-ash (A), hawthorn (B), rose (C), and raspberry fruit infusion (D) on chemiluminescence kinetics

Concentrations of components of the system: luminol — 40 μm, horseradish peroxidase — 4 nM, hydrogen peroxide — 100 μm. **(A)** Curves: 1 — control sample; 2 — 0.002 g/L; 3 — 0.004 g/L; 4 — 0.006 g/L; 5 — 0.008 g/L of mountain-ash fruit decoction. **(B)** Curves: 1 — control sample; 2 — 0.005 g/L; 3 — 0.0075 g/L; 4 — 0.01 g/L; 5 — 0.0125 g/L of hawthorn fruit decoction. **(C)** Curves: 1 — control sample; 2 — 0.001 g/L; 3 — 0.0015 g/L; 4 — 0.002 g/L; 5 — 0.0025 g/L of rosehip decoction. **(D)** Curves: 1 — control sample; 2 — 0.001 g/L; 3 — 0.003 g/L; 4 — 0.004 g/L; 5 — 0.005 g/L of raspberry fruit infusion.

Content of antioxidants in the plant material according to chemical analysis and the total antioxidant capacity of the same objects, M ± δ

Test object	Flavonoids, mg%*	Tannins, mg%*	Ascorbic acid, mg%*	$\Delta S/C \cdot 10\text{-}8$, standard unit	TAC, mg% quercetin
Mountain-ash fruit decoction	8.87 ± 0.01	210.00 ± 10.00	0.67 ± 0.02	7.13 ± 0.96	56.53 ± 7.61
Rosehip fruit decoction	4.66 ± 0.04	850.00 ± 20.00	3.70 ± 0.12	16.60 ± 3.40	131.63 ± 27.26
Hawthorn fruit decoction	3.01 ± 0.06	12.00 ± 3.00	0.23 ± 0.002	3.18 ± 0.29	25.20 ± 2.32
Dried raspberry fruit infusion	90.00 ± 4.00	40.00 ± 20.00	3.91 ± 0.08	6.65 ± 1.21	52.69 ± 9.56

Note: * — literature data, [25-29]. ΔS — change in light sum for the sample, relative unit, C — sample concentration in the cuvette, g/L. The calculated values are significant at $p < 0.05$.

case it is the initial concentration of the test substance in the test sample.

The difference in the light sum of the luminescence in the absence and presence of an antioxidant is proportional to n. The total number of intercepted radicals is equal to

$$n = \Sigma p_i \cdot m_i,$$

where p_i is the stoichiometric coefficient of a particular antioxidant, and m_i is its concentration during measurement. The total number of intercepted radicals is obviously not equal to the total amount of antioxidants since p_i coefficients are not equal to one and also differ significantly for different antioxidants.

$$S = k \cdot n,$$

where k is the coefficient, constant under the same measurement conditions.

The method considered in this paper allows to determine the total antioxidant capacity, whereas chemical analysis allows to determine the total content of antioxidants in a product. Therefore, chemiluminescence method is more informative than chemical analyses.

CONCLUSIONS

The conditions selected by us for evaluation of the total antioxidant capacity of plant materials by observing chemiluminescence kinetics in a system consisting of horseradish peroxidase, hydrogen peroxide and luminol (concentration of the components are 4 nM, 100 μm and 40 μm, respectively; 20 mM phosphate buffer, pH 7.4) ensured oxidation of strong antioxidants (ascorbic acid) and medium-

strength antioxidants (quercetin) within 10 minutes. Such duration of measurement is convenient and provides the required measurement quality.

Analysis of chemiluminescence kinetics showed that in the test objects (fruit decoctions of mountain-ash, rosehips, hawthorn and raspberry fruit infusion), the main antioxidants were medium-strength antioxidants, including flavonoids, as well as weak antioxidants (tocopherol and others). Based on reduction in the chemiluminescence light sum, the total antioxidant capacity of the test objects was calculated. Comparison of TAC values obtained with chemical analysis results showed that products containing the same amount of antioxidants in different ratios may differ by their ability to effectively protect the body against the harmful effects of free radicals. The technique described is a promising one for the study of plant materials that contain a mixture of different antioxidants. In addition, the technique is simple and not expensive. A combination of measurement of chemiluminescence kinetics with mathematical modeling of reactions will allow not only to automate the process of determining the total antioxidant capacity but also to determine the contribution of individual groups of antioxidants in the indicator.

References

1. Proskurnina EV, Vladimirov YuA. Svobodnye radikaly kak uchastniki regulyatornykh i patologicheskikh protsessov. In: Grigor'ev AI, Vladimirov YuA, editors. Fundamental'nye nauki — meditsine. Biofizicheskie meditsinskie tekhnologii. Moscow: MAKS Press; 2015. v. 1. p. 38–71. Russian.
2. Chanda S, Dave R. In vitro models for antioxidant activity evaluation and some medicinal plants possessing antioxidant properties: An overview. Afr J Microbiol Res. 2009 Dec; 3 (13): 981–96.
3. Khasanov VV, Ryzhova GL, Mal'tseva EV. Metody issledovaniya antioksidantov. Khimija Rastitel'nogo Syr'ja. 2004; (3): 63–75. Russian.
4. Vasil'ev RF, K"ncheva VD, Fedorova GF, B"tovska DI, Trofimov AV. Antioksidantnaya aktivnost' khalkonov. Khemilyuminestsentnoe opredelenie reaktsionnoi sposobnosti i kvantovo-khimicheskii raschet energii i stroeniya reagentov i intermediatov. Kinetics and catalysis. 2010; 51 (4): 533–41. Russian.
5. Slavova-Kazakova AK, Angelova SE, Veprintsev TL, Denev P, Fabbri D, Dettori MA, et al. Antioxidant potential of curcumin-related compounds studied by chemiluminescence kinetics, chain-breaking efficiencies, scavenging activity (ORAC) and DFT calculations. Beilstein J Org Chem. 2015 Aug 11; 11: 1398–411.
6. Fedorova GF, Trofimov AV, Vasil'ev RF, Veprintsev TL. Peroxy-radical-mediated chemiluminescence: mechanistic diversity and fundamentals for antioxidant assay. Arkivoc. 2007; 8: 163–215.
7. Fedorova GF, Menshov VA, Trofimov AV, Vasil'ev RF. Facile chemiluminescence assay for antioxidative properties of vegetable lipids: fundamentals and illustrative examples. Analyst. 2009 Oct; 134 (10): 2128–34.
8. Bastos EL, Romoff P, Eckert CR, Baader WJ. Evaluation of antiradical capacity by H2O2-hemin-induced luminol chemiluminescence. J Agric Food Chem. 2003 Dec 3; 51 (25): 7481–8.
9. Vladimirov YuA, Proskurnina EV. Svobodnye radikaly i kletochnaya khemilyuminestsentsiya. Usp Biol Khim. 2009; 49: 341–88. Russian.
10. Vladimirov YuA, Proskurnina EV, Izmailov DYu. Kineticheskaya khemilyuminestsentsiya kak metod izucheniya reaktsii svobodnykh radikalov. Biophysics. 2011; 56 (6): 1081–90. Russian.
11. Izmailov DYu, Demin EM, Vladimirov YuA. Opredelenie aktivnosti antioksidantov metodom izmereniya kinetiki khemilyuminestsen-tsii. Fotobiologiya i fotomeditsina. 2011; 7 (2): 70–6. Russian.
12. Lissi EA, Pascual C, Del Castillo MD. Luminol luminescence induced by 2,2'-Azo-bis(2-amidinopropane) thermolysis. Free Radic Res Commun. 1992; 17 (5): 299–311.
13. Lissi EA, Pascual C, Del Castillo MD. On the use of the quenching of luminol luminescence to evaluate SOD activity. Free Radic Biol Med. 1994 Jun; 16 (6): 833–7.
14. Lissi EA, Escobar J, Pascual C, Del Castillo MD, Schmitt TH, Di Mascio P. Visible chemiluminescence associated with the reaction between methemoglobin or oxyhemoglobin with hydrogen peroxide. Photochem Photobiol. 1994 Nov; 60 (5): 405–11.
15. Lissi EA, Salim-Hanna M, Pascual C, Del Castillo MD. Evaluation of total antioxidant potential (TRAP) and total antioxidant reactivity from luminol-enhanced chemiluminescence measurements. Free Radic Biol Med. 1995 Feb; 18 (2): 153–8.
16. Landi-Librandi AP, de Oliveira CA, Azzolini AE, Kabeya LM, Del Ciampo JO, Bentley MV, et al. In vitro evaluation of the antioxidant activity of liposomal flavonols by the HRP-H2O2-luminol system. J Microencapsul. 2011; 28 (4): 258–67.
17. Cormier MJ, Prichard PM. An investigation of the mechanism of the luminescent peroxidation of luminol by stopped flow techniques. J Biol Chem. 1968 Sep 25; 243 (18): 4706–14.
18. Chang CL, Lin CS, Lai GH. Phytochemical characteristics, free radical scavenging activities, and neuroprotection of five medicinal plant extracts. Evid Based Complement Alternat Med. 2012; 2012: 984295. doi: 10.1155/2012/984295. Epub 2011 Aug 10.
19. Chang CL, Lin CS. Phytochemical composition, antioxidant activity, and neuroprotective effect of Terminalia chebula Retzius extracts. Evid Based Complement Alternat Med. 2012; 2012: 125247. doi: 10.1155/2012/125247. Epub 2011 Jul 5.
20. Georgetti SR, Casagrande R, Di Mambro VM, Azzolini AE, Fonseca MJ. Evaluation of the antioxidant activity of different flavonoids by the chemiluminescence method. AAPS PharmSci. 2003; 5 (2): 111–5.
21. Alekseev AV, Proskurnina EV, Vladimirov YuA. Opredelenie antioksidantov metodom aktivirovannoi khemilyuminestsentsii s ispol'zovaniem 2,2'-azo-bis(2-amidinopropana). Moscow University Chemistry Bulletin. 2012; 53 (3): 187–93. Russian.
22. Pogačnik L, Ulrih NP. Application of optimized chemiluminescence assay for determination of the antioxidant capacity of herbal extracts. Luminescence. 2012 Nov–Dec; 27 (6): 505–10.
23. Saleh L, Plieth C. Total low-molecular-weight antioxidants as a summary parameter, quantified in biological samples by a chemiluminescence inhibition assay. Nat Protoc. 2010 Sep; 5 (10): 1627–34.
24. Ministerstvo zdravookhraneniya SSSR. Gosudarsvennaya farmakopeya SSSR. 11th ed. Iss. 2. "Obshchie metody analiza. Lekarstvennoe rastitel'noe syr'e". Moscow: Meditsina; 1987. p. 147–8. Russian.
25. Sergunova EV, Sorokina AA, Kornyushina MA. Izuchenie ekstraktsionnykh preparatov shipovnika. Pharmacy. 2012; (2): 14–6. Russian.
26. Sergunova EV, Sorokina AA, Avrach AS. Izuchenie plodov boyaryshnika razlichnykh sposobov konservatsii i vodnykh izvlechenii. Farmatsiya. 2010; (5): 16–8. Russian.
27. Avrach AS, Sergunova EV, Kuksova YaV. Biologicheski aktivnye veshchestva plodov i vodnykh izvlechenii maliny obyknovennoi. Farmatsiya. 2014; (1): 8–10. Russian.
28. Avrach AS, Samylina IA, Sergunova EV. Izuchenie biologicheski aktivnykh veshchestv plodov boyaryshnika — syr'ya dlya prigotovleniya nastoek gomeopaticheskikh matrichnykh. Proceedings of the 14th Moscow International Homeopathic Conference "Razvitie gomeopaticheskogo metoda v sovremennoi meditsine"; 2014 Jan 24–25; Moscow. M.; 2014. p. 146–7. Russian.
29. Sergunova EV, Sorokina AA. Izuchenie sostava biologicheski aktivnykh veshchestv v lekarstvennom rastitel'nom syr'e razlichnykh sposobov konservatsii. Proceedings of the 20th Russian National Congress "Chelovek i lekarstvo"; 2013 Apr 15–19; Moscow. Moscow: EkOOnis; 2013. p. 184–90. Russian.

30. Aleksandrova EYu, Orlova MA, Neiman PL. Izuchenie peroksidaznoi aktivnosti v ekstraktakh iz kornevishcha i kornei khrena i ee stabil'nosti k razlichnym vozdeistviyam. Moscow University Chemistry Bulletin. 2006; 47 (5): 350–2. Russian.

Литература

1. Проскурнина Е. В., Владимиров Ю. А. Свободные радикалы как участники регуляторных и патологических процессов. В сб.: Григорьев А. И., Владимиров Ю. А., редакторы. Фундаментальные науки — медицине. Биофиз. мед. технол. М.: МАКС Пресс; 2015. т. 1. с. 38–71.
2. Chanda S, Dave R. In vitro models for antioxidant activity evaluation and some medicinal plants possessing antioxidant properties: An overview. Afr J Microbiol Res. 2009 Dec; 3 (13): 981–96.
3. Хасанов В. В., Рыжова Г. Л., Мальцева Е. В. Методы исследования антиоксидантов. Хим. раст. сырья. 2004; (3): 63–75.
4. Васильев Р. Ф., Кънчева В. Д., Федорова Г. Ф., Бътовска Д. И., Трофимов А. В. Антиоксидантная активность халконов. Хемилюминесцентное определение реакционной способности и квантово-химический расчет энергий и строения реагентов и интермедиатов. Кинетика и катализ. 2010; 51 (4): 533–41.
5. Slavova-Kazakova AK, Angelova SE, Veprintsev TL, Denev P, Fabbri D, Dettori MA, et al. Antioxidant potential of curcumin-related compounds studied by chemiluminescence kinetics, chain-breaking efficiencies, scavenging activity (ORAC) and DFT calculations. Beilstein J Org Chem. 2015 Aug 11; 11: 1398–411.
6. Fedorova GF, Trofimov AV, Vasil'ev RF, Veprintsev TL. Peroxy-radical-mediated chemiluminescence: mechanistic diversity and fundamentals for antioxidant assay. Arkivoc. 2007; 8: 163–215.
7. Fedorova GF, Menshov VA, Trofimov AV, Vasil'ev RF. Facile chemiluminescence assay for antioxidative properties of vegetable lipids: fundamentals and illustrative examples. Analyst. 2009 Oct; 134 (10): 2128–34.
8. Bastos EL, Romoff P, Eckert CR, Baader WJ. Evaluation of antiradical capacity by H2O2-hemin-induced luminol chemiluminescence. J Agric Food Chem. 2003 Dec 3; 51 (25): 7481–8.
9. Владимиров Ю. А., Проскурнина Е. В. Свободные радикалы и клеточная хемилюминесценция. Успехи биол. хим. 2009; 49: 341–88.
10. Владимиров Ю. А., Проскурнина Е. В., Измайлов Д. Ю. Кинетическая хемилюминесценция как метод изучения реакций свободных радикалов. Биофизика. 2011; 56 (6): 1081–90.
11. Измайлов Д. Ю., Демин Е. М., Владимиров Ю. А. Определение активности антиоксидантов методом измерения кинетики хемилюминесценции. Фотобиология и фотомедицина. 2011; 7 (2): 70–6.
12. Lissi EA, Pascual C, Del Castillo MD. Luminol luminescence induced by 2,2'-Azo-bis(2-amidinopropane) thermolysis. Free Radic Res Commun. 1992; 17 (5): 299–311.
13. Lissi EA, Pascual C, Del Castillo MD. On the use of the quenching of luminol luminescence to evaluate SOD activity. Free Radic Biol Med. 1994 Jun; 16 (6): 833–7.
14. Lissi EA, Escobar J, Pascual C, Del Castillo MD, Schmitt TH, Di Mascio P. Visible chemiluminescence associated with the reaction between methemoglobin or oxyhemoglobin with hydrogen peroxide. Photochem Photobiol. 1994 Nov; 60 (5): 405–11.
15. Lissi EA, Salim-Hanna M, Pascual C, Del Castillo MD. Evaluation of total antioxidant potential (TRAP) and total antioxidant reactivity from luminol-enhanced chemiluminescence measurements. Free Radic Biol Med. 1995 Feb; 18 (2): 153–8.
16. Landi-Librandi AP, de Oliveira CA, Azzolini AE, Kabeya LM, Del Ciampo JO, Bentley MV, et al. In vitro evaluation of the antioxidant activity of liposomal flavonols by the HRP-H2O2-luminol system. J Microencapsul. 2011; 28 (4): 258–67.
17. Cormier MJ, Prichard PM. An investigation of the mechanism of the luminescent peroxidation of luminol by stopped flow techniques. J Biol Chem. 1968 Sep 25; 243 (18): 4706–14.
18. Chang CL, Lin CS, Lai GH. Phytochemical characteristics, free radical scavenging activities, and neuroprotection of five medicinal plant extracts. Evid Based Complement Alternat Med. 2012; 2012: 984295. doi: 10.1155/2012/984295. Epub 2011 Aug 10.
19. Chang CL, Lin CS. Phytochemical composition, antioxidant activity, and neuroprotective effect of Terminalia chebula Retzius extracts. Evid Based Complement Alternat Med. 2012; 2012: 125247. doi: 10.1155/2012/125247. Epub 2011 Jul 5.
20. Georgetti SR, Casagrande R, Di Mambro VM, Azzolini AE, Fonseca MJ. Evaluation of the antioxidant activity of different flavonoids by the chemiluminescence method. AAPS PharmSci. 2003; 5 (2): 111–5.
21. Алексеев А. В., Проскурнина Е. В., Владимиров Ю. А. Определение антиоксидантов методом активированной хемилюминесценции с использованием 2,2′-азо-бис(2-амидинопропана). Вестн. МГУ. Сер. 2. Хим. 2012; 53 (3): 187–93.
22. Pogačnik L, Ulrih NP. Application of optimized chemiluminescence assay for determination of the antioxidant capacity of herbal extracts. Luminescence. 2012 Nov–Dec; 27 (6): 505–10.
23. Saleh L, Plieth C. Total low-molecular-weight antioxidants as a summary parameter, quantified in biological samples by a chemiluminescence inhibition assay. Nat Protoc. 2010 Sep; 5 (10): 1627–34.
24. Министерство здравоохранения СССР. Государсвенная фармакопея СССР. XI изд. Вып. 2 «Общие методы анализа. Лекарственное растительное сырье». М.: Медицина; 1987. с. 147–8.
25. Сергунова Е. В., Сорокина А. А., Корнюшина М. А. Изучение экстракционных препаратов шиповника. Фармация. 2012; (2): 14–6.
26. Сергунова Е. В., Сорокина А. А., Аврач А. С. Изучение плодов боярышника различных способов консервации и водных извлечений. Фармация. 2010; (5): 16–8.
27. Аврач А. С., Сергунова Е. В., Куксова Я. В. Биологически активные вещества плодов и водных извлечений малины обыкновенной. Фармация. 2014; (1): 8–10.
28. Аврач А. С., Самылина И. А., Сергунова Е. В. Изучение биологически активных веществ плодов боярышника — сырья для приготовления настоек гомеопатических матричных. В сб. науч. тр. по материалам XXIV Моск. междунар. гомеопат. конф. «Развитие гомеопатического метода в современной медицине»; 24–25 января 2014 г.; Москва. М.; 2014. с. 146–7.
29. Сергунова Е. В., Сорокина А. А. Изучение состава биологически активных веществ в лекарственном растительном сырье различных способов консервации. В сб. тезисов по материалам XX Росс. нац. конгр. «Человек и лекарство»; 15–19 апреля 2013 г.; Москва. М.: ЭкООнис; 2013. с. 184–90.
30. Александрова Е. Ю., Орлова М. А., Нейман П. Л. Изучение пероксидазной активности в экстрактах из корневища и корней хрена и ее стабильности к различным воздействиям. Вестн. МГУ. Сер. 2. Хим. 2006; 47 (5): 350–2.